DESIGN OF OPTIMALLY BALANCED PLANAR MECHANISMS WITH KINETOELASTODYNAMIC CONSIDERATIONS

A Thesis Submitted
In Partial Fulfilment of the Requirements
for the Degree of

DOCTOR OF PHILOSOPHY

By

MUNAWWAR ALI KHAN ZOBAIRI

to the

DEPARTMENT OF MECHANICAL ENGINEERING

INDIAN INSTITUTE OF TECHNOLOGY, KANPUR

DECEMBER, 1979

ME-1979-D-ZOB-DES

TO MY MOTHER

CERTIFICATE

This is to certify that the work presented in this thesis entitled "DESIGN OF OPTIMALLY BALANCED PLANAR MECHANISMS WITH KINETOELASTODYNAMIC CONSIDERATIONS" submitted in partial fulfilment of the requirements for the degree of Doctor of Philosophy by Mr. Munawwar Ali Khan Zobairi has been carried out under our supervision and that this has not been submitted elsewhere for the award of a degree.

B. SAHAY
Assistant Professor
Department of Mech. Engg.
I.I.T. Kanpur

S.S. Rao
Professor
Department of Mech. Engg.
I.I.T. Kanpur

December, 1979

ACKNOWLEDGEMENTS

It gives me great pleasure to express my deep sence of gratitude to my supervisors Professor S. S. Rao and Dr. B. Sahay for their erudite guidance and kind encouragement in all phases of preparation of this thesis without which it would not have come into existence. I am greatly indebted to their friendly attitude and extending the liberty to me with which I have encroached upon their valuable time at any hour of the day to discuss my difficulties.

I am also indebted to Professor J. Chakraborty who first introduced to me the subject of mechanism design through a course. I also express my sincere gratefulness to Professor M. P. Kapoor, Dr. B. P. Singh and Dr. B. D. Aggarwal for introducing me the related topics involved in this work.

I am specially grateful to Professor A. Ghosh and Dr. S. Dhande for their valuable discussions which I had with them at a number of times during the preparation of this work.

I wish to express my sense of appreciation and gratefulness to Professor B. L. Dhoopar, Professor M. M. Oberai, Professor V. Sundararajan and Professor V. K. Stokes for their valuable help in various administrative matters.

I am sincerely appreciative of the friendly cooperation from my co-research scholars at IITK, specially from Messrs S.Q.A. Naqvi, M. A. Sofi, Q.J.A. Khan, M. Saleem, Mehrajuddin, Kultar Singh and G. Srihari.

Thanks are due to Dr. P. K. Nath (Jalpaiguri Government Engineering College) who first diverted my attention towards the problem undertaken in this work.

I also wish to extend my appreciation and indebtedness to Professor J. A. Munir and Professor S. H. Mohsin (Z.H. Engineering College, A.M.U., Aligarh) for granting me leave and relieving me of my duties from the college.

Thanks are due to my colleagues in the Mechanical Engineering Department for their valuable help and cooperation in many ways. I wish to mention particularly, Messrs S. K. Ayyubi, S. S. Alvi, Nayar Alam, S. A. W. Usmani, S.M.H. Rizvi, Saghir Ahmad, Iqbal Ahmad and Kh. Zaheeruddin.

My special thanks go to my friends Messrs S. Tariq Jilani and Abdul Mughis (both from Mech. Engg. Dept., AMU Aligarh) for their constant support and encouragement rendered to me from time to time.

I wish to thank Mr. Irshad Ahmad for his valuable assistance given to me by drawing the figures and tables. My acknowledgement is also due to Mr. Nihal Ahmad for his excellent typing from an untidy manuscript.

My affectionate thanks go to Qaisar, my wife, without whose deep sense of understanding, full cooperation and patience the work would not have taken this shape. I am

aware of my negligence towards my family during the period of my stay here and hope to compensate it in the days to come. I also take this opportunity to thank my brothers and sisters, Messrs T. A. Khan, S. U. Zuberi, Izzat Ali, Mrs. Najma Sibgaht and Mrs. Salma Izzat for their sympathies and encouragement.

Munawwar Ali Khan Zobairi

CONTENTS

LIST OF FIGURES

LIST OF TABLES

NOMENCLATURE

A	-	Area of the cross-section of an element
A_s	-	Effective shear area of the cross-section of an element
B	-	Body force vector due to the distributed rigid body inertia forces within an element
C	-	Damping matrix of the system
C_i	-	Rigid body inertia couple of the i-th link
DXi	-	Rigid body inertia force acting on the centroid of the i-th link in the X direction of the system coordinates
DYi	-	Rigid body inertia force acting on the centroid of the i-th link in the Y direction of the system coordinates
E	-	Young's modulus of elasticity
F_A	-	Inertia forces and external forces at the master coordinates
F_C	-	Known forces at the slave coordinates
FS	-	Shaking force transmitted to the foundations
G	-	Shear modulus of elasticity
I	-	Second moment of area of the cross-section, also identity matrix
I_A, etc.	-	Mass moment of inertia of a counterweight at an end (A) of a link
I_i	-	Mass moment of inertia of the i-th link
K	-	Elastic stiffness matrix of the system
L_i	-	i-th equality constraint
M	-	Mass matrix of the system

MS - Shaking moment transmitted to the foundations

P - Load vector of the system, also coupler extension point

P_e - System load vector due to KED inertia of the links

P_j - j-th position of the rigid body

R - Rotation matrix

R_A, etc.- Radius of the counterweights

R_j - Position vector of the rigid body in j-th position

R_{ij} - The force exerted by the j-th link on the i-th link at a joint.

S_F - Shear force acting at a position x of a link

T - Rigid body displacement transformation matrix

T_C - Reaction force vector at the slave coordinates

T_{c1}, etc- Component of the reaction force vector T_C

T_1 - Torque at the crank input end

U - Displacement vector of the system

$\dot{U}$ - Velocity vector of the system

$\ddot{U}$ - Acceleration vector of the system

U_o - Initial displacement vector of the system

$\dot{U}_o$ - Initial velocity vector of the system

X - X-axis of the system coordinates, also a general vector

Y - Y-axis of the system coordinates

Z_1, etc.- Vectors representing links of a mechanism or position of a point on them

a - Shape function of an element

a_{Ax}, etc- Component of the absolute acceleration of an end (A) of a link in a coordinate direction (x)

aX_i, etc.- Component of the absolute acceleration of the centroid of the i-th link in a coordinate direction (X)

b - Element strain matrix

e_{xx} - Normal strain at any point within an element

e_{xy} - Shear strain at any point within an element

f - Objective function

g_i - i-th inequality constraint

$\bar{k}$ - Element stiffness matrix in element oriented coordinates

$\hat{k}$ - Element stiffness matrix in system oriented coordinates

l - Length of an element

l_i - Length of the i-th link

m_i - Mass of the i-th link

m_A, etc. - Mass of the counterweight attached to an end (A) of a link

$\bar{m}$ - Element mass matrix in element oriented coordinates

$\hat{m}$ - Element mass matrix in system oriented coordinates

n - Total number of constrained coordinates of the system

p_1, etc. - Component of the additional nodal forces due to rigid body inertia of the counterweights

p_{e_1}, etc.- Component of the additional nodal forces due to KED inertia of the counterweights

$\bar{p}$ - Element load vector in element oriented coordinates

$\hat{p}$ - Element load vector in system oriented coordinates

r - penalty parameter

r_A, etc. - Distance of the centroid of the counterweight attached to an end (A) of a link

r_i - Radial distance of the centroid of the i-th link from its one end

r_j - Displacement vector of the rigid body in j-th position

u - Internal displacement vector of the element in element oriented coordinates

u_x - Component of u in the x-direction

u_y - Component of u in the y-direction

u_x^b - Component of u_x due to the transverse forces

u_x^a - Component of u_x due to the axial forces

u_y^b - Component of u_y due to bending only

u_y^s - Component of u_y due to shear only

$\bar{u}$ - Element displacement vector in element oriented coordinates

$\bar{u}_1$, etc. - Elements of $\bar{u}$

u - Element displacement vector in system oriented coordinates

v - Volume of an element

w - Total number of the rigid body degrees of freedom

x - x-axis of the element oriented coordinates of the element (or link) along its axis

y - y-axis of the element oriented coordinates of an element (or link) along its transverse direction

α - Absolute angular acceleration of a link

δ - Small variation

$\frac{\partial}{\partial x}$ - Partial derivative with respect to x

Δ - Small finite variation

θ - Angular rotation of the input crank

θ_i - angle made by the i-th link with the X-axis

φ - A factor to account for the shear effect, also: modal matrix; angular finite rotation of the follower; minimizing function; angular position of the centroid of a link

ψ - Angular finite rotation of the coupler

η - Displacement vector in normal coordinates

ξ - Non-dimensionalized X-coordinate

ξ_i - Damping ratio corresponding to the i-th normal mode

ς - Non-dimensionalized Y-coordinates

ρ - Density of the material

σ - Internal stress vector of an element

σ_i - Stress in the i-th link

σ_{xx} - Normal stress at any point within an element

σ_{xy} - Shear stress at any point within an element

τ - Time

χ - A matrix relating the strains of an element with its stresses

ω - Natural frequency of the system, also angular velocity of a link

$\{\ \}$ - Column vector

$[\ ]$ - Matrix (or vector)

$(\dot{})$ - Differentiation with respect to time

$(\ddot{})$ - Double differentiation with respect to time.

SYNOPSIS

MUNAWWAR ALI KHAN ZOBAIRI
Department of Mechanical Engineering
Indian Institute of Technology Kanpur

DESIGN OF OPTIMALLY BALANCED PLANAR MECHANISMS WITH KINETOELASTODYNAMIC CONSIDERATIONS

a thesis submitted
in partial fulfilment of the requirements
for the degree of Doctor of Philosophy
December, 1979

The present study deals with the subject of optimal balancing of planar mechanisms when the contribution due to vibratory inertia forces of mechanisms with elastic links towards the shaking force and the shaking moment transmitted to the supports is taken into consideration along with the contribution due to the rigid body inertia forces. A reduction in the shaking force, the shaking moment and the input end torque fluctuations is obtained by an appropriate reduction in the total mechanism mass. This is achieved by allowing the cross sections of the links to vary and putting constraints on the stresses in the links and on the deflections of the strategic points on the mechanism. A procedure to obtain an optimum design of planar mechanisms is presented using different methods of achieving the balance in these mechanisms. For a specified aim, which the mechanism has to serve, the kinematic synthesis of the mechanism is

changed to arrive at an optimum design from the point of view of balance in the mechanism incorporating the aforementioned aspects. The effect of redistributing the link masses in order to reduce the shaking force and/or the shaking moment on the stresses in the links and on the contribution of vibratory inertia forces towards the shaking force and the shaking moment has been studied and an optimum design is obtained taking these effects into consideration.

The kinetoelastodynamic analysis of the mechanism is made to determine the stresses in the links and the vibratory inertia forces using the finite element approach of structural dynamics. Taking the combined effect of the rigid body inertia forces and the vibratory inertia forces the maximum shaking force and the maximum shaking moment during a complete motion cycle of the mechanism are determined using the dynamic force analysis.

The constrained minimization problem is first converted into an unconstrained problem using interior penalty function method, Davidson-Fletcher-Powell method is then used to solve it. Since the evaluation of the stresses in the links and the vibratory inertia forces at each design point during the optimization process is very time consuming, two approximate procedures have been adopted. Firstly, during one dimensional minimization the gradients of the maximum

link stresses, maximum shaking force and the maximum shaking moment are used to predict them at the neighboring design points. Secondly, during the calculation of the above mentioned gradients and the gradient of the penalty function by backward finite difference method, the kinetoelastodynamic analysis, to obtain the maximum stresses in the links, the maximum shaking force and the maximum shaking moment, is made for the complete cycle of mechanism motion only at the base point. When each design variable is perturbed by a small amount the kinetoelastodynamic analysis is, however, made only upto a certain small interval beyond the position at which either the maximum stress in the links or the maximum shaking force or the maximum shaking moment (whichever corresponds to maximum crank angle) has occurred at the base point. These approximations have been observed to be reasonably good and have reduced the computational time considerably.

The results obtained show that to achieve a balance in mechanism with elastic links in a real sense the contribution of vibratory inertia forces towards the shaking force and the shaking moment must be taken into consideration. Furthermore reducing the areas of the cross-sections of the links by putting constraints on the stresses in the links is very effective in minimizing the shaking force and the

shaking moment as well as the fluctuations in the input end torque. Thus, the present work represents a unified approach to the design of optimally balanced mechanisms with elastic links.

CHAPTER I

INTRODUCTION

Every machine is composed of one or more mechanisms performing different tasks. The successful operation of a machine depends on the extent the expected operating conditions are realized during the process of synthesis through various assumptions made at that stage. Kinematic criteria were the major considerations in the design of mechanisms in the long past. With the advent of machines moving at higher speeds the consideration of dynamic criteria for synthesis of mechanisms have become essential. The dynamic criteria for synthesis such as fluctuations in input speed, balance of mechanism, and stresses due to dynamic forces were based on the assumption of rigid links till recent past. However, during the last decade, research has shown that the results predicted with the assumption of rigid links are far from accurate due to the elasticity of the links, specially at high speeds or when the links are massive. Thus, there is a need to put the design techniques on more rigorous basis by developing new synthesis procedures that take into account the elastic properties of the mechanism. The present study is an attempt in this direction.

When a mechanism moves, occupying various positions in space, the velocity and acceleration of the links vary during a complete cycle of motion of the mechanism. Thus, there are varying forces and moments due to rigid body inertia of the links transmitted to the machine foundation which results in undesirable vibrations of the machine as well as its supports. As the speed of the mechanism increases these unbalance forces and moments transmitted to the foundation pose a much greater problem. Thus, it becomes necessary to reduce these forces and moments. Several methods are available for this purpose. However, in all these methods the consideration is limited to mechanisms with rigid links. In actual practice, specially at higher speeds, the links of a mechanism, due to their elasticity, vibrate about some mean position under the action of rigid body forces and external forces present on the mechanism. These vibrations give rise to an additional acceleration field besides the acceleration field produced by the gross rigid body motion of the links. The acceleration field resulting from the vibration of the links develops additional inertia forces which may be called as kineto-elastodynamic inertia forces (referred to as KED inertia forces hereafter). The order of magnitude of KED inertia forces depends upon the mass distribution of the links as well as the magnitude of the acceleration field resulting from the vibration of the links. If any of these two is large the resulting KED inertia forces will also be

high. As such, the varying forces and moments transmitted to the machine foundation due to the KED inertia forces will also be substantial. Therefore, while considering the problem of reducing or balancing the unbalance forces and/or moments transmitted to the machine foundation due to rigid body inertia, one should also take into account the effect of KED inertia. Furthermore, while attempting to reduce or balance the forces and moments transmitted to the foundations due to rigid body inertia, either by redistribution of the link masses or by changing kinematic synthesis, no effort has been made to observe the effect of these changes on the stress distribution in the links. Also no attempt has been made to reduce the unbalance forces and moments by a reduction in the total mechanism mass by reducing the areas of cross-sections of the links, which is not possible without the inclusion of the analysis of stresses in the links.

Thus, for the rational dynamical design of mechanisms with regard to minimization of the shaking force and/or the shaking moment one should also include the effect of KED inertia and keep the stresses in the links and the deflections of the vital points on the mechanism within prescribed limits. Moreover, efforts should be made to develop approximate methods to obtain the solution of such problems with reduced computer time without any significant loss of accuracy.

A brief survey of the publicatins relevant to this work is presented below.

1.1 A Survey of Past Works

1.1.1 Mechanism Balancing

The subject of dynamics of mechanisms deals with the motion of mechanisms under the action of actuating forces and torques and also the forces and the torques produced by the motion of the mechanism. Mechanism balancing involves the design or modification of a mechanism to control the force and the torque levels produced by its motion. The mechanism balancing falls under two major categories, namely, (i) input torque balancing and (ii) shaking force and shaking moment balancing.

1.1.1(a) Input Torque Balancing

Fluctuations in input speed and torque in a mechanism occur since the energy requirements vary during a complete cycle of motion of the mechanism. To reduce or minimize these fluctuations many researchers have put forward various procedures. Some important ones are briefly discussed below.

Sherwood [1] attempted to make the total kinetic energy of a mechanism constant (or approximately constant) during its entire cycle of motion. This resulted in constant input shaft speed or reduced variation in the input shaft

speed. Thus, for no load or constant output load the input end torque fluctuations were minimised. This 'iso-energetic' condition was achieved by the optimum distribution of link masses in the mechanism. For a four bar linkage a certain distribution of coupler mass made the total kinetic energy approximately constant. For a drag link mechanism the results were very good, whereas for a crank-rocker mechanism, the variation in the total kinetic energy was reduced to half only.

Sherwood and Hockey [2] presented a general method of optimization of the mass distribution in the links of a mechanism using dynamically similar system which minimised the fluctuation in the kinetic energy of the mechanism running at the constant angular input speed. Using the property that any link in plane motion might be represented by four variable point masses at four almost arbitrarily chosen points fixed in the link, the links of the mechanism were represented by the above mentioned dynamically equivalent set of point masses and an optimum mass distribution was worked out giving minimum fluctuation in the kinetic energy.

Skreiner [3] studied the fluctuation of the input torque and demonstrated that it could be reduced by the addition of a spring in the system of linkages. Assuming the links to be rigid he performed the dynamic motion analysis for the resulting one degree of freedom system.

Applying the principle of virtual work the equation of motion was established. He determined the variation in input speed and the pin forces in one case by varying the inertia of the input shaft and in another case by using a spring with different attachment points to the frame. He showed that it was possible to reduce fluctuation in the input speed without much increase in the pin force by the use of a suitable spring.

Hockey [4] presented an improved technique for obtaining the optimum mass distribution of the links to reduce the fluctuation of kinetic energy in planar mechanisms over their previous procedure [2] so as to place the concept on a more rigorous mathematical footing. He concluded that the fluctuation of kinetic energy of a mechanism could be efficiently reduced by proper distribution of link masses and it was claimed that his new method of determining this 'proper' distribution was superior to the previous method. He reported that this method of mass distribution was more efficient than the use of a flywheel at the input shaft. However, he pointed out that though this technique would reduce the fluctuations of kinetic energy and input speed but other dynamic effects such as force and moment unbalance might worsen.

Hockey [5] took up the problem of minimizing fluctuations of input torque resulting not only due to the inertia

of the moving links but also due to fluctuating external loads. The previous works, which were aimed at reducing the fluctuation of kinetic energy in a mechanism in the absence of external loads and friction, also resulted in the reduction in the fluctuation of torque required at the input shaft to maintain constant speed.. He developed a method of dynamic synthesis using system of variable point masses as outlined in his earlier work [4] to include mechanisms which had resisting loads on their links. The mass in the links of the mechanism was so distributed that the fluctuation of the torque required to overcome the external loads was counteracted by the fluctuation of torque required to overcome the effects of inertia. It was shown that the mechanism might be completely force balanced by using a method due to Berkof and Lowen [6] without affecting in any way the minimized fluctuation of input shaft torque.

1.1.1(b) Shaking Force and Shaking Moment Balancing

Lowen and Berkof [7] presented a detailed survey of the force and moment balancing literature for mechanisms with rigid link of constant mass. Eleven translations from the German and Russian literature in English were also included. Therefore in this survey, only references of relatively recent origin have been discussed.

Han [8] developed an analytical method for the optimal balancing of the shaking force and shaking moment of forces of a planar mechanism driven by a constant speed shaft. He used a single balance weight and determined its mass moment of inertia and phase angle which gave minimum disturbing action through a complete revolution of the driving shaft. He applied Legendre's principle of least squares of the compromised expression for the deviations of the shaking load on the machine supports produced by the resultant shaking force and shaking moment to obtain the optimum set of values for the balance weight. He also suggested an iterative procedure for determining the mass moment of inertia and phase angle of the balance weight when the input angular speed was not constant. However, his method was not suitable for application to every machine in general. Use of a single mass rotating at the crank speed is helpful only when the force vector is predominently the first harmonic. For other mechanisms, specially in which the center of mass of the parts is far from circles, ellipses and straight lines, balance masses rotating at constant speed is of not much use.

Berkof and Lowen [6] developed the "method of linearly independent vectors" to obtain the complete force balance in planar linkages. The position of the total mechanism center of mass was written in such a way that the coefficients of the time dependent terms could be equated to zero, thereby

making the total center of mass stationary. Thus the resultant of all dynamic forces reduced to zero for all positions of the mechanism. The relationships obtained by equating the co-efficients of the time dependent terms to zero were used to determine the necessary distribution of link masses. Using this method the shaking force was completely eliminated but it caused the bearing reactions, the shaking moment and the input torque variations to increase.

Later the same authors [9] presented a least squares optimization theory which minimised the shaking moment of a fully force balanced inline four bar linkage. Using the angular momentum principle an expression was derived for the shaking moment of a force balanced four bar linkage. Next, a periodic function of the same general type as the shaking moment was formulated. This periodic function was made to deviate least from zero in root-mean-square sense, to yield the optimum relationship between the coefficients of the periodic function. The coefficients of the moment expression depend only on the link mass distribution. The optimum coefficient ratios are functions of link lengths only.

Lowen and Berkof [10] demonstrated how their above-mentioned theory could be applied to obtain a linkage with an optimum shaking moment characteristic. According to these authors, the theory was applicable to most linkages,

but for practical reasons the field of application was restricted to standard linkage configurations which were generally used in practice. A matching procedure was developed to determine all these families of mechanisms for which the standard configurations represent the optimum mass distribution. This method required the construction of moment optimization graphs which were used to match the theoretical optimum coefficient ratios of the moment equation with the actual attainable ratios.

Kaufman and Sandor [11] extended the 'method of linearly independent vectors' [6] to spatial linkages and obtained the complete force balance of spatial linkages such as the RSSR and RSSP mechanisms.

Tepper and Lowen [12] gave a contour theorem that differentiated between mechanisms which could be fully force balanced and those which could not. In addition, the method of linearly independent vectors [6] has been generalized and it was shown that the 'apparent' minimum number of counterweights producing full force balancing by internal mass redistribution alone equals n/2 where n was the number of links in the mechanism.

Berkof [13] obtained the complete shaking moment balance of force-balanced inline four bar linkage using two circular masses moving in opposite directions to that of the crank and the follower, respectively, with the help of

gears. The moment of inertia of the masses were so chosen that the inertial torques produced by them balanced the contribution due to the crank and the follower assembly towards the shaking moment respectively. The contribution of the coupler link towards the shaking moment was made zero by making the coupler a physical pendulum. This procedure, however, resulted in increased bearing reactions and increase fluctuations in the input end torque.

Tepper and Lowen [14] presented a method, wherein the RMS shaking force of a general four bar linkage running at constant input shaft speed was optimized while the RMS ground bearing reaction were limited to lie between those corresponding to the unbalanced mechanism and those of the fully force-balanced mechanism. The optimization was done using a single counterweight as well as two counterweights. The authors claimed that the two-counterweights technique was capable of producing considerably lower bearing forces than the single-counterweight technique for comparable values of the RMS shaking force. However, the authors did not make any attempt to limit either the RMS input moment or the RMS shaking moment. The effect on coupler bearing forces was also not considered.

Conte, George, Mayne and Sadler [15] used nonlinear programming techniques to combine the kinematic synthesis and dynamic design of four-bar mechanisms. The arbitrary

parameters of kinematic synthesis were determined to satisfy the performance criteria related to dynamic force, as well as kinematics. In their examples, the authors obtained optimum crank-rocker path generating mechanisms with prescribed timing, using various objective functions such as shaking force, shaking moment, input torque fluctuation and bearing reactions for minimization. The optimization procedure resulted in a significant improvement in these dynamic characteristics. Minimizing the total mechanism mass, the authors demonstrated that instead of an improvement, all the dynamic performance properties became worse compared to that of the original linkage, thereby indicating that minimization of the total mechanism mass was not fruitful.

Wiederrich and Roth [16] determined condition for reducing the angular momentum fluctuations transmitted to the frame of a completely force-balanced four bar linkage. The authors claimed that their approach led to simple design equations for determining the inertial properties of the links for good momentum balance, as compared to the computer based search techniques required in earlier methods.

Elliott and Tesar [17] extended the "method of linearly independent vectors" of Berkof and Lowen [6] to shaking moment and driving torque functions. They defined four mass parameters for each link of the mechanism. These were the mass, the radius of gyration (or mass moment of inertia) and

the centroid coordinates. Thus, they considered twelve mass parameters in a four bar linkage and by adjusting as many of these parameters as possible they obtained a balanced device. For this purpose they described the shaking moment as the time rate of change of total momentum about the input crank pivot and finally put it into a form similar to that of the shaking force. By equating the coefficient of time dependent terms to zero a relationship between various parameters was obtained. But it required two rotary inertias to be negative, which was achieved by adding counter rotating masses to the system. Thus using their general approach they completely eliminated the shaking force and the shaking moment with the addition of physical negative mass for all the four-link mechanisms: the four bar, the slider crank, the inverted slider crank and the oscillating block mechanisms. From a similar formulation for driving torque it was possible to meet exactly specified values of driving torque upto three positions or in the least-square sense for the full cycle while maintaining shaking force balance.

Walker and Oldham [18] presented a procedure of force balancing multidegree of freedom multibar linkages. They derived three equations from which the force balance conditions were obtained. The linkage could have both revolute or prismatic joints. However, there were force balance restrictions with prismatic joints.

Carson and Stephens [19] extended the theory developed by Berkof and Lowen [9,10] to problem of force and RMS moment balancing by redistribution of masses when all links length ratios were specified. The criteria for distributing the link mass involved selecting numerical values for eight unknown mass parameters to satisfy three equations. Selection of five parameters arbitrarily and calculating the remaining three might result in physical impossibilities such as imaginary radius of gyration. To overcome this difficulty the authors developed feasible design spaces and monographs showing feasible parameter design spaces and parameter interrelationship.

Using the 'method of linearly independent vectors' Balasubramanian and Bagci [20] developed design equations for complete shaking force balancing of commonly used planar Stephenson's and Watt's type 6R 6-bar and 6-bar slider-crank regular force transmission mechanisms. It was aimed to provide counter-balancing masses only on the shafts supported by the fixed frame whenever possible to avoid the worsening of the unbalanced shaking moment.

Walker and Oldham [21] further extended their earlier work [18] and presented a method which indicated whether a linkage could be fully force-balanced using counterweights alone. A formula was given to determine the minimum number of counterweights needed for a full force-balance. A criterio

was presented to select an optimum counterweight set so that the increase in bearing reactions, driving torque and out of balance couples were checked.

Bagci [22] presented a method of complete force-balancing of planar mechanisms with force transmission irregularities by adding idler loops and using the method of linearly independent mass vectors. A mechanism containing a link or group of links that had connection to frame of the machine through pairs all permitting linear freedom was termed as irregular force transmission mechanism. The component of shaking force contributed by these links could not be balanced by means of distributing the masses of the existing links of the mechanism. However by the addition of idler loop consisting of a set of two binary links having all revolute pairs to the original mechanism it was made possible to completely force balance the mechanism.

1.1.2 Deflection and Stress Analysis

Erdman and Sandor [23] presented an excellent review of the work carried out on the deflection and stress analysis in the mechanisms due to elastic links till about 1971. A considerable progress has been made in this direction since then by various researchers. Therefore these latter works are briefly presented in this section.

Winfrey [24] used finite element method to determine the longitudinal, transverse and torsional displacements of a general mechanism. Each link was modelled to have six elastic and three rigid body coordinates. Using a connectivity matrix the element matrices were assembled into system matrices. Using conservation of momentum during the free vibration of the mechanism a transformation matrix was obtained for the elimination of the rigid body degrees of freedom. Use of this transformation matrix made the stiffness matrix non-singular and hence the eigenvalue problem in the transformed coordinates could be solved. With the help of the modal matrix thus obtained, and by assuming the damping matrix to be proportional to the mass matrix, a set of uncoupled differential equations in normal coordinates was obtained. The solution of these equations was determined and converted back into the original system coordinates from the normal coordinates by using first the modal matrix and then the transformation matrix. The final displacement and velocity determined at the end of current interval of time were used as initial conditions for the next interval.

Erdman, Sandor and Oakberg [25] used the flexibility approach of structural analysis to determine the elastic deflection of entire mechanism system. The effect of elastic accelerations was also included in determining the load vector. For this purpose a kineto-elastodynamic

stretch rotation operator was defined which was used to determine the total acceleration of the mechanism including elastic accelerations. Starting from these accelerations the inertia forces were determined and deflection analysis was made. The total accelerations were then again determined and compared with the old ones. If they were not within acceptable tolerance then above procedure was repeated. The crank was assumed as a cantilever beam which converted the mechanism into structure.

Erdman, Imam and Sandor [26] extended the above analysis and used the method of 'dynamic equivalence system' to take into account the elastic inertia forces. It was indicated that in certain cases the elastic accelerations were comparable with the rigid body accelerations.

Imam, Sandor and Kramer [27] analysed planar mechanisms with elastic links using stiffness approach of the finite element method. Permutation vector method was used to assemble the element matrices into system matrices. To reduce the computational time the rate of change of eigenvalues and eigenvectors was employed. The rotation at the support end was not included in the system coordinate thereby making the crank a cantilever beam and reducing the mechanism to a structure. Thus the true boundary conditions of the mechanism were not met during the analysis. To determine the stresses, using deflections obtained from

the above analysis, a polynomial expansion method based on the theory of strength of materials [28] was used.

Imam and Sandor [29] used these methods of kineto-elastodynamic design of elastic mechanisms to minimise the mass of the mechanism with constraints on stresses and deflections. The optimization problem was formulated in terms of stepwise linear programming. Simplex method was used to obtain a linkage with minimum mass with linearized constraints on deflection and stresses. To keep the error caused by linearization of constraints within limits the range of variation of design variable was restricted to a region about the initial design point by the help of side constraints. Later the authors [30] applied nonlinear programming technique to meet the same goal. Both quasi-static and rate of change of eigenvalues methods were used to determine the elastic deflections.

Sadler and Sandor [31] presented a lumped mass approach to analyse the vibration and stresses in a slider crank mechanism. They [32] further extended their method of analysis to a planar four-bar linkage with three elastic links. Applying d'Alembert's principle to each lumped mass the Euler's equation of elastic curve was obtained, which was then solved using finite difference method to obtain the transverse deflections. The additional relative normal and tangential accelerations were taken into account

and the pin forces were obtained applying force and moment balance to each link at their instantaneous positions. The additional rigid body motions of the coupler and the follower due to elastic deformations of the crank were also considered. The longitudinal deformations due to axial forces and the foreshortening of the links due to bending were neglected.

Alexander and Lawrence [33,34] were the first to obtain experimentally the strain histories of the coupler and rocker midpoints of a four bar linkage with elastic links. These results were compared with the analytical results obtained by using the stiffness method presented by Imam, Sandor and Khamer [27]. To represent the continuous displacements of the individual links in terms of their nodal displacements a two term sine series was assumed. Runge-Kutta method was used to solve the linear coupled equations. There was reasonable agreement between the experimental and analytical results.

Nath [35] used the basic concept of the finite element technique to analyse elastic mechanisms. He included many considerations which were not considered in the earlier works. The effect of subdividing the links on the solution accuracy was studied. To account for the dynamic behaviour of the rigid body inertia forces, the harmonic analysis of these forces was made and used for the vibration analysis. A novel method of making rigid body analysis by the use of

a transformation matrix was presented. The effect of additional acceleration terms and the rigid body axial forces on the dynamics of the mechanism was observed. A method to obtain steady state displacements for all configurations of the mechanism by means of a single expression was developed for a restricted class of mechanisms incorporating all the dynamic factors. However, the validity of this method was not well demonstrated.

Sutherland [36] adopted a different technique (unlike flexibility or stiffness approach of structural dynamics) by deriving the Euler-Lagrange equation of motion of a purely elastic four bar linkage using the assumed mode analysis approach [37]. The form of the solution for the member deflections was discussed and the governing non-dimensional parameters were identified. The results were determined in a non-dimensional form. These results were compared with the results of physical experimentation to establish the validity of the mathematical model.

Golebiewski and Sadler [38] compared analytical and experimental dynamic bending stresses in a elastic connecting rod of a slider-crank mechanism with a rigid crank. The differential equation including viscous damping was derived by way of lumped parameter approach using d'Alembert's principle and the Euler-Bernoulli beam theory, and solved numerically. Experimental data were obtained using strain gauges.

Thompson and Barr [30] applied variational procedure for setting up the equations describing the elastodynamic motion of planar linkages in which all the members were considered to be elastic. By permitting independent variations of stress, strain, displacement and velocity parameters for each link approximate equations of motion, boundary and compatibility conditions for the complete mechanism were systematically constructed. The procedure modelled the physical situation by allowing the simultaneous displacement of all the members from the rigid linked configuration, each displacement being the sum of rigid body and deformation components. The authors claimed that the following special features could be incorporated with this procedure. (i) The links might be made of different materials or even anisotropic materials. (ii) Linear or nonlinear strain displacement relationships could be taken. (iii) A particular link might be considered as rigid while the other members of the mechanism were flexible. (iv) The effect of viscous torque at each joint could be incorporated.

Jandarasits and Lowern [40] had analysed the transverse elastic behaviour of a counterweighted rocker link with an endmass. The crank and coupler were taken as rigid. The Hamilton's integral and method of Kantorovich were used to obtain the linearized decoupled Hill's equations,

which were solved to furnish the time portion of the solution. The space portion of the solution was determined using normal modes of free vibration of the complex link. An elastic mechanism constraint equation, relating the elastic link angles to the foreshortening of the elastic link, provided the necessary auxiliary conditions. Determination of the stability boundaries and steady-state solution of the Hill's equations with and without damping was presented. In a companion paper [41] they applied their technique to an example mechanism and the results were compared with those of the experiment conducted by them. They confirmed that a good qualitative as well as quantitative agreement existed between analytical and experimental results.

1.2 Objectives of the Present Work

From the above survey of the past research work, it is observed that the efforts aimed at eliminating or reducing the shaking force and/or shaking moment transmitted to the machine foundations, were based on the consideration of the effect of inertia forces, produced due to accelerations resulting from gross rigid body motion of the mechanism, towards the unbalance in the mechanism. Whereas in a real situation, specially when the mechanism runs at high speed and has elastic links, there are inertia forces arising out of the accelerations due to the vibrations of the links. The

contribution of these vibratory inertia forces towards the shaking force and the shaking moment, to the best of author's knowledge, has not been taken into account in earlier works. One may think of making the cross-sections of the links heavier in order to reduce their vibrations. But a careful study can reveal that this may further worsen the situation due to the increased rigid body inertia forces. On the other hand, a reduction in the cross-sectional areas of the links results in a reduction in the rigid body inertia forces thereby reducing the shaking force and the shaking moment transmitted to the supports. This can be adopted if the stresses in the links are determined at each stage and kept within allowable limits. However, a reduction in the cross-sectional areas of the links increases the vibratory accelerations of the links. As such, though the inertia of the links is decreased, the vibratory inertia forces may be higher. Furthermore, the stresses in the links have not been taken into consideration while redistributing the link masses to achieve a reduction in the unbalance shaking forces or shaking moments. In fact, the stress distribution is changed when the link masses are redistributed by placing counterweights.

The major objectives of the present work may be stated as follows:

(i) The shaking force and the shaking moment resulting from vibratory inertia forces will be taken into consideration to design a mechanism with optimal balancing characteristics.

(ii) The method of changing the kinematic design to achieve a reduction in the shaking force and the shaking moment [15] shall be adopted to design an optimally balanced mechanism with constraints on stresses in the links and/or constraints on deflection of strategic points on the mechanism.

(iii) The method of redistributing link masses to reduce the shaking forces and the shaking moment will be used with constraints on stresses and/or on deflections to obtain optimum design of a mechanism.

(iv) The areas of cross-sections of the links will be varied and its effect on the balancing characteristics will be investigated.

(v) The determination of the maximum stresses in the links and the KED inertia forces is a time consuming process, therefore the investigation of problems involving optimization with KED inertia forces and with stress constraints becomes, in general, impracticable. To overcome this difficulty the gradient of these functions will be used to predict their values at a new design point and its validity will be investigated.

(vi) Lastly, to evaluate the gradients of the above mentioned functions and the gradient of the minimizing function at a design point, it will be assumed that for small variations in the components of the design vector the maximum values of these functions occur in the vicinity of the positions at which they have occurred at the base point. The validity of this assumption will be determined.

CHAPTER II

KINETOELASTODYNAMIC ANALYSIS

2.1 Introduction

When a mechanism runs at a certain speed the resulting rigid body inertia forces and the external forces acting on the mechanism cause elastic deflections in the links which become substantial when the running speed is high. Since the rigid body inertia forces as well as the effect of the external forces on individual link vary during the motion of the mechanism, they produce forced vibrations in the links of the mechanism causing the links to deflect further about their rigid body position at any instant. The present chapter is aimed to make this kinetoelastodynamic analysis of the mechanism and determine the stresses in the links due to elastic deformations. The elastic accelerations of the links obtained during this analysis are then used to determine vibratory inertia forces.

Section 2.2 presents the various assumptions made for this analysis and the mathematical model adopted for the mechanism. Section 2.3 deals with the element analysis. In section 2.4 a procedure for the assembly of element matrices into system matrices is presented. The equation

of motion and a method of determining transformation matrix are given in section 2.5 and 2.6 respectively. Section 2.7 describes a method to eliminate the rigid body degree of freedom. Section 2.8 gives the solution of the equation of motion and the determination of stresses in the links. In section 2.9 the determination of quasi-static stresses is presented. Lastly, section 2.10 deals with an alternative procedure of determining the deflections and stresses by suppressing the rigid body degree of freedom.

2.2 Assumptions and Mathematical Model

All the links of the mechanism are considered to be completely elastic. The important assumptions made during the analysis that follow are:

(i) The elastic deflections are independent of the rigid body motion,

(ii) the deflections are so small that linear theory can be used,

(iii) the load vector, the stiffness matrix and the mass matrix remain constant during the small intervals into which the complete cycle of motion of the mechanism is discretised,

(iv) the effects of the friction, tolerance, clearances and impact are neglected.

A planar four bar mechanism having straight links with uniform cross-sections is considered for presenting the procedure of analysis.

$O_1A_1B_1O_2$ represents the initial rigid body configuration of the mechanism at the instant $\tau = \tau_o$. The load vector, the mass matrix and the stiffness matrix are determined at this position which are assumed to remain constant during a chosen interval $\Delta\tau$. Under the action of rigid body inertia forces produced by gross rigid body accelerations and the external forces the mechanism gets deflected as an elastic structural system to a new position $O_1A_2B_2O_2$ shown in Fig. 2.1. Using the displacements and the accelerations the stresses in the links and vibratory inertia forces are determined, respectively. From the deflected position $O_1A_2B_2O_2$ the mechanism is allowed to move as a rigid link mechanism through the interval $\Delta\tau$ to reach the position $O_1A_3B_3O_2$, which is treated as the instantaneous structure for the next interval of time $\Delta\tau$. The displacements and velocities of the elements obtained at the end of one interval are used as the 'initial conditions' for the next interval. Starting from some initial configuration the above procedure is repeated until the cycle is complete or the steady state condition is reached.

2.3 Element Analysis

The links of the mechanism are considered as beam elements with six coordinates, three at each end. Out of these three, two represent linear displacements, one along

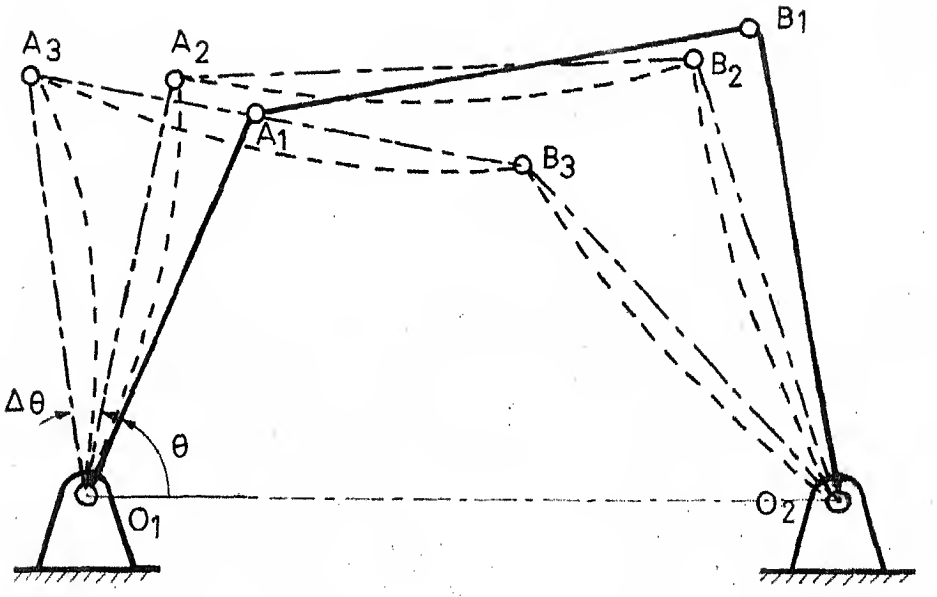

Fig 2.1 Diagram Showing Elastic and Rigid Body Displacements During Interval Δt

the element axis and the other perpendicular to it. The third represents the rotation at the end. The displacements at these coordinates are taken as $\bar{u}_1(\tau)$ to $\bar{u}_6(\tau)$. To represent the continuous deflection of the element (Fig. 2.2) in terms of these nodal displacements the following polynomial relations are assumed

$$u_x^a = C_1 + C_2 x \tag{2.1}$$

$$u_y^b = C_3 + C_4 x + C_5 x^2 + C_6 x^3 \tag{2.2}$$

where u_x^a is the continuous axial displacement due to axial forces only and u_y^b is the continuous transverse displacement due to bending only. C_1 to C_6 are functions of time τ only. These polynomials agree to the accuracy of the engineering theory of static bending of beams and also permit rigid body motions in addition to elastic displacements [43].

The additional transverse deflection due to shear is determined as follows:

$$\frac{\partial u_y^s}{\partial x} = -\frac{S_F}{GA_s} \tag{2.3}$$

and

$$EI \frac{\partial^3 u_y^b}{\partial x^3} = S_F \tag{2.4}$$

where, u_y^s = the transverse deflection due to shear effects only

S_F = the shear force acting at a position x of the link

A_s = the effective shear area of the position x

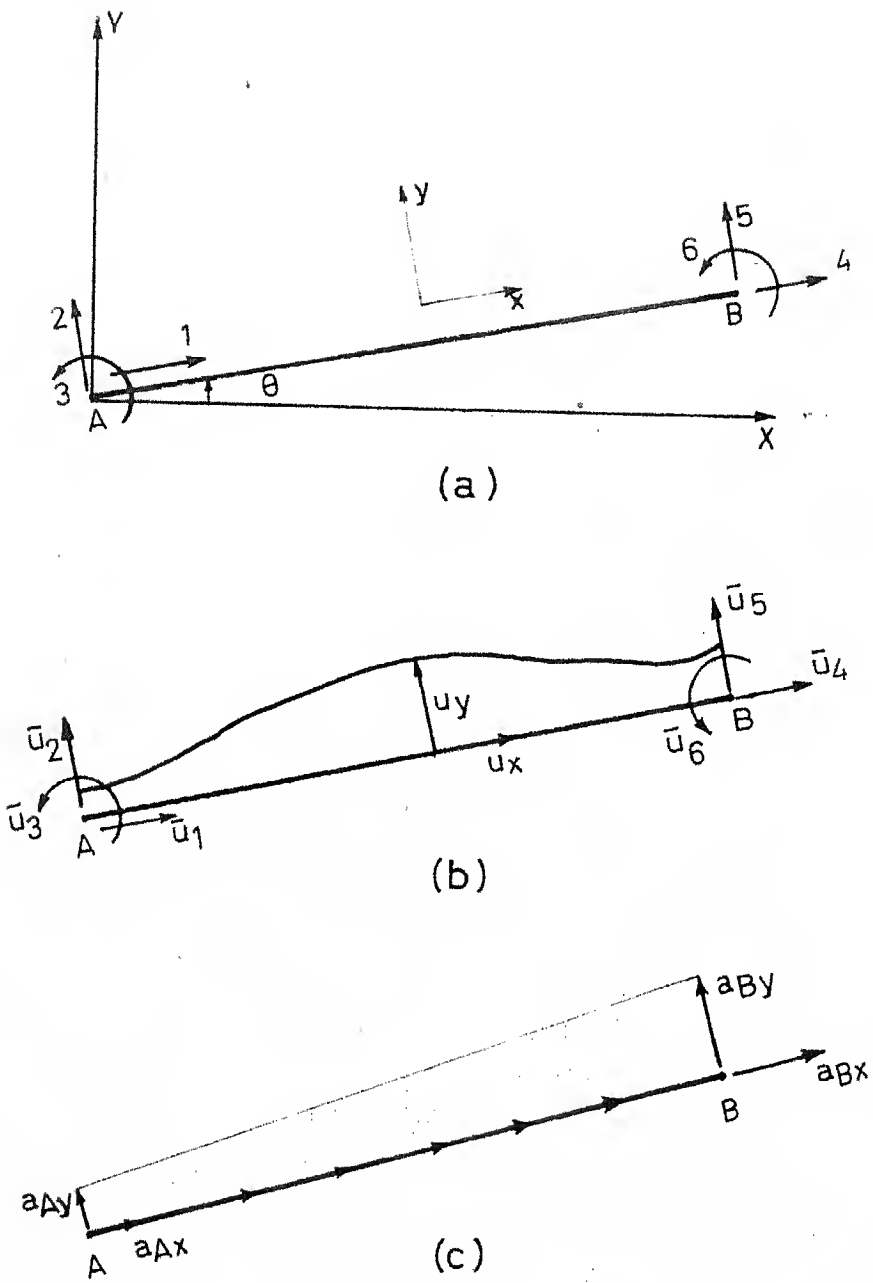

Fig 2.2 Element Coordinates

G = the shear modulus of elasticity

E = the Young's modulus of elasticity

I = second moment of area of the cross-section.

Using eqs. (2.3) and (2.4) S_F is eliminated to get

$$\frac{\partial u_y^s}{\partial x} = \frac{EI}{GA_s} \frac{\partial^3 u_y^b}{\partial x^3} \tag{2.5}$$

Integrating this equation the substituting equation (2.2) into it yields the following

$$u_y^s = C_5 \frac{2EI}{GA_s} + C_6 \frac{6EI}{GA_s} x + C \tag{2.6}$$

The total displacement is given by

$$\begin{aligned} u_y &= u_y^b + u_y^s \\ &= C_3' + C_4 x + C_5(x^2 + \frac{2EI}{GA_s}) + C_6(x^3 + \frac{6EI}{GA_s}x) \end{aligned} \tag{2.7}$$

where the constant of integration C in eq. (2.6) is absorbed with constant C_3 into C_3' in eq. (2.7).

To determine C_3' to C_6 the following boundary conditions are employed

$$\begin{aligned} &\text{At } x = o \qquad u_y = \bar{u}_2, \quad \frac{\partial u_y^b}{\partial x} = \bar{u}_3 \\ &\text{At } x = l \qquad u_y = \bar{u}_5, \quad \frac{\partial u_y^b}{\partial x} = \bar{u}_6 \end{aligned} \tag{2.8}$$

The resulting transverse deflection can thus be expressed as

$$u_y = \frac{1}{1+\varphi} \begin{bmatrix} 1 - 3\xi^2 + 2\xi^3 + (1-\xi\varphi) \\ \xi - 2\xi^2 + \xi^3 + \frac{1}{2}(\xi - \xi^2)\varphi \\ 3\xi^2 - 2\xi^3 + \varphi\xi \\ -\xi^2 + \xi^3 - \frac{\varphi}{2}(\xi - \xi^2) \end{bmatrix}^t \begin{Bmatrix} \bar{u}_2 \\ \bar{u}_3 l \\ \bar{u}_5 \\ \bar{u}_6 l \end{Bmatrix} \qquad (2.9)$$

where, $\varphi = \frac{12EI}{GA_s l^2}$; $\xi = \frac{x}{l}$; l = length of the element.

Using the engineering bending theory the longitudinal displacement u_x^b due to bending is determined as follows

$$u_x^b = -\frac{\partial u_y^b}{\partial x} y = \frac{1}{1+\varphi} \begin{bmatrix} (6\xi - 6\xi^2)\zeta \\ \{-1+4\xi-3\xi^2 - (1-\xi)\varphi\}\zeta \\ -(6\xi - 6\xi^2)\zeta \\ (2\xi - 3\xi^2 - \xi\varphi)\zeta \end{bmatrix}^t \begin{Bmatrix} \bar{u}_2 \\ \bar{u}_3 l \\ \bar{u}_5 \\ \bar{u}_6 l \end{Bmatrix} \qquad (2.10)$$

where $\zeta = y/l$; y = distance of the point from neutral axis. C_1 and C_2 in equation (2.1) are obtained by applying the boundary conditions on axial displacements, i.e. $u_x^a = \bar{u}_1$ at $x = 0$ and $u_x^a = \bar{u}_4$ at $x = l$. The total axial displacement u_x is given by

$$u_x(x,y,\tau) = u_x^a(x,\tau) + u_x^b(x,y,\tau) \qquad (2.11)$$

Therefore, the continuous displacement $u = \{u_x, u_y\}$ is obtained from the nodal displacement $\bar{u} = \{u_1, \ldots, u_6\}$ as follows

$$u = a\bar{u} \tag{2.12a}$$

and as such

$$\dot{u} = a\dot{\bar{u}} \tag{2.12b}$$

and $$\ddot{u} = a\ddot{\bar{u}} \tag{2.12c}$$

where the parameter a is called the shape function and is given by

$$a = \frac{1}{1+\varphi}\begin{bmatrix} (1+\varphi)(1-\xi) & 6(\xi-\xi^2)\zeta & \{-1+4\xi-3\xi^2-(1-\xi)\varphi\}l\zeta \\ 0 & 1-3\xi^2+2\xi^3+(1-\xi)\varphi & \{-2\xi^2+\xi^3+\frac{1}{2}(\xi-\xi^2)\varphi\}l \end{bmatrix}$$

$$\begin{bmatrix} (1+\varphi)\xi & 6(-\xi+\xi^2)\zeta & (2\xi-3\xi^2-\xi\varphi)l\zeta \\ 0 & 3\xi^2-2\xi^3+\xi\varphi & \{-\xi^2+\xi^3-\frac{1}{2}(\xi-\xi^2)\varphi\}l \end{bmatrix} \tag{2.13}$$

According to linear theory the normal strain and the sharing strain at any point of the link are obtained in terms of deflections as follows

$$e_{xx}(x,y,\tau) = \frac{\partial u_x}{\partial x} \tag{2.14}$$

$$e_{xy}(x,y,\tau) = \frac{\partial u_y}{\partial x} + \frac{\partial u_x}{\partial y} \tag{2.15}$$

Using eq. (2.12) along with eqs. (2.14) and (2.15) the continuous element strains at any point of the element in terms of the nodal displacement $\bar{u}$ are given by

$$e = \begin{Bmatrix} e_{xx} \\ e_{xy} \end{Bmatrix} = b\bar{u} \tag{2.16}$$

where the element strain matrix b is

$$b = \begin{Bmatrix} b_1 \\ b_2 \end{Bmatrix} = \frac{-1}{(1+\varphi)l} \begin{bmatrix} -(1+\varphi) & 6(1-2\xi)\zeta & (4-6\xi+\varphi)l\zeta \\ 0 & -\varphi & -(\varphi l/2) \\ (1+\varphi) & 6(-1+2\xi)\zeta & (2-6\xi-\varphi)l\zeta \\ 0 & \varphi & -(\varphi l/2) \end{bmatrix} \tag{2.17}$$

From the element strains, the element stresses at any point of the element are obtained as follows

$$\sigma = \begin{Bmatrix} \sigma_{xx} \\ \sigma_{xy} \end{Bmatrix} = \chi\, b\bar{u} \tag{2.18}$$

where $$\chi = \begin{bmatrix} E & 0 \\ 0 & \frac{GA_s}{A} \end{bmatrix} \tag{2.19}$$

and A = nominal area of cross-section.

The inertia forces due to rigid body accelerations are regarded as the continuous body forces $B(\xi, \tau)$ acting over the element. The components of these body forces at any point of the element are given by

$$B(\xi, \tau) = -\rho \begin{bmatrix} a_{Ax} + (a_{Bx} - a_{Ax})\xi \\ a_{Ay} + (a_{B_y} - a_{A_y})\xi \end{bmatrix} \tag{2.20}$$

where ρ = density of the material, a_{Ax} and a_{Bx} are the absolute rigid body normal accelerations and a_{Ay}, a_{By} are

the tangential accelerations at the end points A and B of the element respectively. These accelerations are obtained by the kinematic analysis of the mechanisms which is presented in Appendix A.

The element stiffness matrix $\bar{k}$, the element mass matrix $\bar{m}$ and the element load vector $\bar{p}$ in the element oriented coordinates are obtained using the principle of virtual work [42] as follows

$$\bar{k} = \int_v b^t \chi b \, dv \tag{2.21}$$

$$\bar{m} = \int_v \rho \, a^t \, a \, dv \tag{2.22}$$

$$\bar{p} = \int_v a^t \, B \, dv \tag{2.23}$$

where t indicates the transpose of a matrix. Integrations are taken over the whole volume v of the element and dv is elemental volume of the element.

The explicit expressions for these matrices are given in Appendix B.

Since the orientations of various links in a mechanism are different it is necessary to define a common coordinate system called as global coordinate system (or simply system coordinates). The element matrices are transformed into system coordinates from their respective element oriented coordinates before they are assembled into system matrices. To achieve this transformation, a rotation matrix R is defined as below

$$R = \begin{bmatrix} R_1 & 0 \\ 0 & R_1 \end{bmatrix} \qquad (2.24)$$

where R_1 is the rotation matrix for one end of the element. If θ is the angle made by the x-axis of the element with the X-axis of the system coordinates the rotation matrix R, is given by

$$R_1 = \begin{bmatrix} \cos\theta & \sin\theta & 0 \\ -\sin\theta & \cos\theta & 0 \\ 0 & 0 & 1 \end{bmatrix} \qquad (2.25)$$

The nodal displacements $\hat{u}$ of the element in the system coordinates are obtained using the following coordinate transformation

$$\bar{u} = R\ \hat{u} \qquad (2.26)$$

Using the contragradient law of transformation, the element load vector $\hat{p}$, the stiffness matrix $\hat{k}$ and the mass matrix $\hat{m}$ in the system coordinates are given by

$$\hat{p} = R^t\ \bar{p} \qquad (2.27)$$

$$\hat{k} = R^t\ \bar{k}\ R \qquad (2.28)$$

$$\hat{m} = R^t\ \bar{m}\ R \qquad (2.29)$$

The initial element displacement and velocity in system coordinates are obtained in a similar way from the initial element displacement and velocity in the element oriented coordinates as follows

$$\hat{u}_o = R^t \bar{u}_o \qquad (2.30)$$

$$\dot{\hat{u}}_o = R^t \dot{\bar{u}}_o \qquad (2.31)$$

The above analysis is applied to all the elements present in the mechanism.

2.4 Assembly of Element Matrices

Many methods are available to assemble the element matrices into system matrices for the complete mechanism. Some of them are connectivity matrix [28,24], permutation vector method [43,27] and 'code-system' method [44,35]. The 'code-system' method has the advantage over the others that no regular order is to be followed during numbering the element coordinates and the system coordinates at any joint. Thus any set of coordinates can be grouped together as the last set among the generalized system coordinates which is advantageous in placing the coordinates corresponding to the rigid body degree of freedom and the fixed ends supports as the last set among the generalized coordinates.

In this method the elements of the mechanism are numbered according to any choice. The system coordinates are also assigned numbers as required. An integer matrix NS is now defined such that in each row the columns contains the number corresponding to system coordinates for that element whose identification number matches with the row

number in the order in which the element coordinates are defined. The integer matrix NS for the mechanism shown in Fig. 2.3 is given in Table 2.1.

A sample programme to perform the required assembly of the element matrices into the system matrices is shown in Table 2.2.

2.5 Equation of Motion

Having determined the system mass matrix M, the stiffness matrix K and the load vector P after the above assembly, the special features of the mechanism are incorporated. For example, a flywheel is present at output end of the rocker its moment of inertia is added to the diagonal element of the mass matrix M corresponding to the system coordinate associated with the rotation of that rocker end. Similarly the forces or torques exerted at the input end shaft are included in the corresponding elements of the load vector P.

After all the special features of the mechanism are accounted for the final equation of motion for the complete mechanism is given by

$$M\ddot{U} + C\dot{U} + KU = P \qquad (2.32)$$

for $\tau_o < \tau < \tau_o + \Delta\tau$, with the initial conditions:

$$U(\tau_o) = U_o \quad \text{and} \quad \dot{U}(\tau_o) = \dot{U}_o \qquad (2.33)$$

Table 2.1 Integer Matrix NS

$$\begin{bmatrix} 14 & 15 & 13 & 1 & 2 & 3 \\ 1 & 2 & 4 & 5 & 6 & 7 \\ 5 & 6 & 8 & 16 & 17 & 12 \\ 1 & 2 & 4 & 9 & 10 & 11 \end{bmatrix}$$

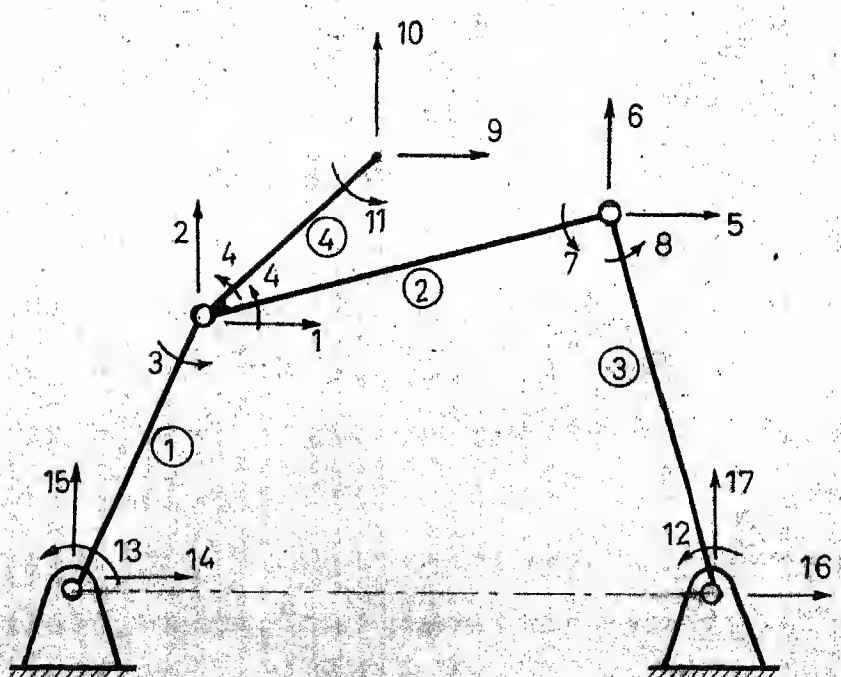

Fig 2.3 System Coordinates

TABLE 2.2. SAMPLE PROGRAM FOR ASSEMBLY OF ELEMENT MATRICES

```
      DO 1 ILINK = 1,MNE
      DO 1 I=1,NEC
      IROW = NS(ILINK,I)
      SP(IROW) = SP(IROW) + EP(I,ILINK)
      SD(IROW) = ED(I,ILINK)
      SV(IROW) = EV(I,ILINK)
      DO 1 J=1,NEC
      ICOL = NS(ILINK,J)
      SM(IROW,ICOL) = SM(IROW,ICOL)+EM(I,J,ILINK)
      SK(IROW,ICOL) = SK(IROW,ICOL) + EK(I,J,ILINK)
    1 CONTINUE
```

where MNE = number of links in the mechanism; NEC = number of element coordinates; EP,ED,EV,EM and EK are the element load vectors, element initial displacement vectors, element initial velocity vectors, element mass matrices and element stiffness matrices in system coordinates of the elements of the mechanism; SP, SD,SV,SM and SK are the system load vector, system initial displacement vector, system initial velocity vector, system mass matrix and system stiffness matrix respectively.

where C, $U(\tau)$, U_o and $\dot{U}_o$ are the damping matrix, displacement vector, initial displacement vector and initial velocity vector, respectively.

2.6 Determination of Transformation Matrix

The equation of motion (2.32) will be solved using normal mode method. For this purpose, it is first required to determine the solution of the following eigenvalue problem

$$M\ddot{X} + KX = 0 \qquad (2.34)$$

In the case of a mechanism, the stiffness matrix K is singular [28] and the degree of singularity of the matrix K is same as the number of rigid body degrees of freedom of the mechanism. To overcome this difficulty in solving eq. (2.34) the equation is modified using the following procedure [35].

The total set of the coordinates X of eq. (2.34) is divided into a subset X_B called 'slave coordinates' so that no rigid body displacement is possible through the remaining subset X_A called 'master coordinates'. The total coordinates in X_B are same as the number of rigid body degrees of freedom in the mechanism. There are many possible combinations to form the set of coordinates X_B, but it is more advantageous to take the coordinates corresponding to input motion as the slave coordinates. The eq. (2.34) is partitioned according to these subsets as shown below,

$$\begin{bmatrix} M_{AA} & M_{AB} \\ M_{BA} & M_{BB} \end{bmatrix} \begin{Bmatrix} \ddot{X}_A \\ \ddot{X}_B \end{Bmatrix} + \begin{bmatrix} K_{AA} & K_{AB} \\ K_{BA} & K_{BB} \end{bmatrix} \begin{Bmatrix} X_A \\ X_B \end{Bmatrix} = 0 \qquad (2.35)$$

When a small rigid body displacement dX_B is given at the slave coordinates then the corresponding rigid body displacements dX_A at the master coordinates are given by the relation

$$dX_A = T\, dX_B \qquad (2.36)$$

where T is called the displacement transformation matrix [42] and is a function of the geometry of the mechanism only. The displacement transformation matrix T, for any mechanism, can be determined as given below.

Since no elastic forces are developed when purely rigid body displacements take place in a mechanism mathematically one can say

$$\begin{bmatrix} K_{AA} & K_{AB} \\ K_{BA} & K_{BB} \end{bmatrix} \begin{Bmatrix} dX_A \\ dX_B \end{Bmatrix} = 0 \qquad (2.37)$$

from which one gets

$$\begin{aligned} K_{AA}\, dX_A + K_{AB}\, dX_B &= 0 \\ K_{BA}\, dX_A + K_{BB}\, dX_B &= 0 \end{aligned} \qquad (2.38)$$

Substituting eq. (2.36) in eq. (2.38) the following relations are obtained.

$$T = -K_{AA}^{-1} K_{AB} \tag{2.39}$$

$$K_{BA} T + K_{BB} = 0 \tag{2.40}$$

Eq. (2.39) is used to determine T. The matrix K_{AA} is non-singular and thus its inverse exists.

2.7 Elimination of Rigid Body Degrees of Freedom

Let a small virtual rigid body displacements δX_B be given at the slave coordinates. The corresponding virtual rigid body displacements at the master coordinates are given by (using eq. (2.36)),

$$\delta X_A = T \, \delta X_B \tag{2.41}$$

Applying the principle of virtual work to the equilibrium eq. (2.35) and remembering the fact that the elastic forces do not produce any work due to rigid body displacements and work is done by the inertia forces only, the following equation is obtained.

$$\delta X_A^t (M_{AA} \ddot{X}_A + M_{AB} \ddot{X}_B) + \delta X_B^t (M_{BA} \ddot{X}_A + M_{BB} \ddot{X}_B) = 0 \tag{2.42}$$

Substituting eq. (2.41) in eq. (2.42) and remembering the fact that δX_B is arbitrary, and $\ddot{X} = -\omega^2 X$, the following relation between X_A and X_B is obtained

$$X_B = T^* X_A \tag{2.43}$$

where $$T^* = -(T^t M_{AB} + M_{BB})^{-1} (T^t M_{AA} + M_{BA}) \tag{2.44}$$

Resolving X_A for small values into two parts [42] as given in eq. (2.45) and substituting it in eq. (2.43) the eq. (2.46) is obtained

$$X_A = X_{Ae} + TX_B \tag{2.45}$$

where X_{Ae} represents the displacement at the master coordinates relative to the rigid body configuration when $X_B=0$.

$$X_B = (I - T^*T)^{-1} T^* X_{Ae} \tag{2.46}$$

The size of the matrix $(I-T^*T)$ is equal to the total number of the rigid body degrees of freedom.

Eliminating X_A and X_B with the help of eqs. (2.45) and (2.46) and making use of eq. (2.39), eq. (2.35) can be written in terms of X_{Ae} as follows,

$$(-\omega^2 M' + K_{AA})\, X_{Ae} = 0 \tag{2.47}$$

where ω = natural frequency of vibration of the system,

M' = effective mass matrix in the free-vibration of the mechanism and is given by

$$M' = M_{AA} + (M_{AA}T + M_{BB})(I-T^*T)^{-1}T^* \tag{2.48}$$

The size of the matrices K_{AA} and M' are $(n-w)x(n-w)$ where n is number of system coordinates and w is the number of degrees of freedom of the mechanism. In case of single degree of freedom system $(I-T^*T)$ is scalar and therefore M' is symmetric. Since K_{AA} is non-singular the equation (2.47

can now be solved [45]* and the natural frequencies and natural modes can be obtained. Let φ' be the modal matrix obtained by solving eq. (2.47), the modal matrix φ corresponding to eq. (2.35) is obtained using eqs. (2.45) and (2.46) as given below

$$\varphi = \begin{Bmatrix} \varphi_A \\ \varphi_B \end{Bmatrix} \tag{2.49}$$

where $$\varphi_B = (I - T^* T)^{-1} T^* \varphi' \tag{2.50}$$

and $$\varphi_A = \varphi' + T \varphi_B \tag{2.51}$$

2.8 Solution of Equations and Determination of Stresses

The vector U in eq. (2.32) allows the rigid body motions along with the elastic motions (by virtue of the polynomials in eqs. (2.1) and (2.2)), but the modal matrix φ contains only the elastic modes and no rigid body modes. Thus, to determine the solution of the equation of motion (2.32) by normal mode method the system coordinates U are transformed to normal coordinates with the help of the following relation

$$U = \varphi \eta \tag{2.52a}$$

where $\eta(\tau)$ represent the displacement vector in the normal coordinate system.

Since φ is assumed to remain constant during the chosen interval $\Delta\tau$, the following relations may readily be obtained

*Abstract of the method from this reference is presented in Appendix C.

for velocity and acceleration in normal coordinate system by successive differentiation of eq. (2.52a)

$$\dot{U} = \varphi\dot{\eta} \tag{2.52b}$$

and

$$\ddot{U} = \varphi\ddot{\eta} \tag{2.52c}$$

Plugging eqs. (2.52) into eq. (2.32) and premultiplying by φ^t, the following equation results

$$\bar{M}\ddot{\eta} + \bar{C}\dot{\eta} + \bar{K}\eta = \bar{P} \tag{2.53}$$

where,

$$\bar{M} = \varphi^t M\varphi; \quad \bar{C} = \varphi^t C\varphi$$
$$\bar{K} = \varphi^t K\varphi; \quad \bar{P} = \varphi^t P \tag{2.54}$$

Using eqs. (2.53), the initial conditions are given by

$$\eta_o = (\varphi^t\varphi)^{-1}\varphi^t U_o \tag{2.55}$$

$$\dot{\eta}_o = (\varphi^t\varphi)^{-1}\varphi^t \dot{U}_o \tag{2.56}$$

Since the modes in φ are orthogonal with respect to the matrices M and K, $\bar{M}$ and $\bar{K}$ are diagonal matrices. If daping matrix C is taken proportional to either M or K or a linear combination of them, the matrix $\bar{C}$ also becomes a diagonal matrix, and eq. (2.53) is decoupled. The standard practice is to take $\bar{C}$ as proportional to the critical damping of the system at the normal modes [42]. Thus the following uncoupled equations are obtained

$$m_i\ddot{\eta}_i + 2\xi_i\omega_i m_i\dot{\eta}_i + k_i\eta_i = p_i \tag{2.57}$$
$$i = 1,2,\ldots,m.$$

where, m = number of normal coordinates

η_i = displacement at the i-th normal coordinate

$\dot{\eta}_i$ = velocity at the i-th normal coordinate

$\ddot{\eta}_i$ = acceleration at the i-th normal coordinate

m_i = i-th diagonal element of $\bar{M}$

k_i = i-th diagonal element of $\bar{K}$

p_i = i-th element of $\bar{P}$

ω_i = i-th natural frequency

$2m_i \omega_i$ = critical damping at the i-th normal mode

ξ_i = damping ratio (actual damping to critical damping) at the i-th normal mode.

In general the nature of system daping is such that the effect of higher modes is suppressed, therefore, the common practice is to take higher values of ξ_i for the successively higher modes. The damping matrix $\bar{C}$ as taken here in the eq. (2.53) can be expressed as follows

$$\bar{C} = 2 \begin{bmatrix} \omega_1 \xi_1 & & \\ & \ddots & \\ & & \omega_m \xi_m \end{bmatrix} [\bar{M}] \qquad (2.58)$$

Since it is assumed that load vector P (and as such $\bar{P}$) remains constant during the interval $\Delta\tau$, the solution of eq. (2.53) is obtained as shown below

$$\eta_i(\tau) = e^{-\sigma_i \tau} (I_i \cos \mu_i \tau' + J_i \sin \mu_i \tau') + \frac{p_i}{k_i} \qquad (2.59)$$

$$\dot{\eta}_i(\tau) = e^{-\sigma_i \tau'} [(-\sigma_i I_i + \mu_i J_i) \cos \mu_i \tau' - (\sigma_i J_i + \mu_i I_i) \sin \mu_i \tau'] \tag{2.60}$$

$$\text{and} \quad \ddot{\eta}_i(\tau) = \frac{p_i}{m_i} - \omega_i^2 \eta_i - 2 \omega_i \xi_i \dot{\eta}_i \tag{2.61}$$

$$i = 1, 2, \ldots, m$$

for $\tau_o < \tau < \tau + \Delta\tau$.

where $\tau' = \tau - \tau_o = \Delta\tau$

$$\sigma_i = \xi_i \omega_i$$

$$\mu_i = \sqrt{1 - \xi_i^2}\, \omega_i$$

$$I_i = \eta_i^o - p_i/k_i$$

$$J_i = (\dot{\eta}_i^o + \xi_i \omega_i I_i)/\mu_i$$

η_i^o = i-th element of the initial vector η_o in eq. (2.55)

and $\dot{\eta}_i^o$ = i-th element of the initial vector $\dot{\eta}_o$ in eq. (2.56)

The displacement η, velocity $\dot{\eta}$ and acceleration $\ddot{\eta}$ as obtained from eqs. (2.59) to (2.61) are transformed into system coordinates using eq. (2.52). The element displacement, velocity and acceleration vectors in system coordinates are obtained from the system vectors using integer matrix NS. These vectors are then finally transformed into element oriented coordinates with the help of eq. (2.26). The displacements thus obtained are used to determine the stresses in the links of the mechanism with the help of eq. (2.18). The acceleration vector obtained is used to determine the vibratory inertia forces.

2.9 Determination of Quasi-Static Stresses

If the load vector P_A corresponding to the master coordinates calculated at any instant is allowed to act on the mechanism as static forces the elastic deflection produced in the mechanism in the system coordinates (assuming the mechanism fixed at the input end, i.e. the crank as cantilever) is given by

$$U_{static} = K_{AA}^{-1} P_A \qquad (2.62)$$

This displacement vector is transformed into element displacement vector in system coordinates using integer matrix NS. The element displacement vector thus obtained is transformed into element oriented displacement vector using eq. (2.26). Plugging these element displacements in eq. (2.18) the quasi-static stresses in the links of the mechanism are obtained.

2.10 System Analysis by Suppressing Rigid Body Degree of Freedom

It has been pointed out in section 2.6 that the matrix k in eq. (2.34) is singular. Thus to solve eq. (2.34), a way of modifying the equation by eliminating the rigid body degree of freedom has been presented in the previous sections. Another alternative is to treat the input crank end as fixed, like a cantilever beam, thereby suppressing the rigid body degree of freedom. This is achieved by deleting the

rows and columns of the matrices M and K corresponding to the coordinate representing rigid body degree of freedom and also by deleting the element corresponding to this from the vector U in equation of motion (2.32). Thus, the resulting stiffness matrix denoted by K_{AA} is non-singular and the equation of motion can now be written as

$$M_{AA}\ \ddot{U}_A + C_{AA}\dot{U}_A + K_{AA}\ U_A = P_A \qquad (2.63)$$

where M_{AA} is the resulting mass matrix, C_{AA} the damping matrix for this problem, P_A the corresponding load vector and U_A the resulting displacement vector.

Eq. (2.63) can now be solved using normal mode method. For this purpose solution of the following eigenvalue problem is sought

$$M_{AA}\ \ddot{X}_A + K_{AA}\ X_A = 0 \qquad (2.64)$$

Since K_{AA} is non-singular the above equation is solved as before and the natural frequencies and natural modes are obtained. The rest of the procedure is same as outlined in section 2.8, and the stresses in the links of the mechanisms are obtained.

CHAPTER III

KINEMATIC SYNTHESIS AND DYNAMIC FORCE ANALYSIS

3.1 Introduction

A method of kinematic synthesis for a planar four bar mechanism is presented in section 3.2. To determine the maximum unbalance shaking force and shaking moment during a complete cycle of motion of the mechanism and also to determine the amount of the input torque required to maintain equilibrium at each interval into which the complete cycle of motion of the mechanism is discretised, it is required to make complete dynamic force analysis of the mechanism at the configuration corresponding to each interval. Section 3.3 deals with a procedure for this dynamic force analysis. In section 3.4 a method is developed to make the dynamic force analysis when counterweights are attached to the links in order to redistribute their masses with the aim of reducing the shaking force and/or the shaking moment. In section 3.5, a procedure is developed to determine the contribution due to the KED inertia towards the shaking force and shaking moment. Section 3.6 deals with the determination of system mass matrix when counterweights are attached at the ends of the links.

3.2 Kinematic Synthesis

The kinematic synthesis of mechanism has received a great deal of attention till to date. A number of methods for the kinematic synthesis are now available [46-48]. The present study does not aim at discussing the merits and demerits of these methods. Since the complex number method of the kinematic synthesis is most widely used for planar mechanisms, it is adopted in the present study.

Though the method is a general one and can be used to synthesise a planar mechanism for any use, i.e. path generation, function generation or rigid body guidance, it is discussed here with reference to rigid body guidance.

Suppose it is proposed to guide a rigid body through finitely separated positions. Let the firm lines in Fig. 3.1 show the intial configuration when the rigid body is in its first position at P_1 coincident with the coupler point P. O_1 and O_2 are the fixed supports and O is any base point. Z_0 to Z_5 represent the vectorial positions of the first support from the base point and the various links of the mechanism as indicated in Fig. 3.1. The vector Z_6 represents the position of the coupler point P from the second joint of the coupler, shown by dotted line in Fig. 3.1. Let the vectors R_1, R_2 and R_3 represent the three finitely separated positions of the rigid body attached to the coupler point P.

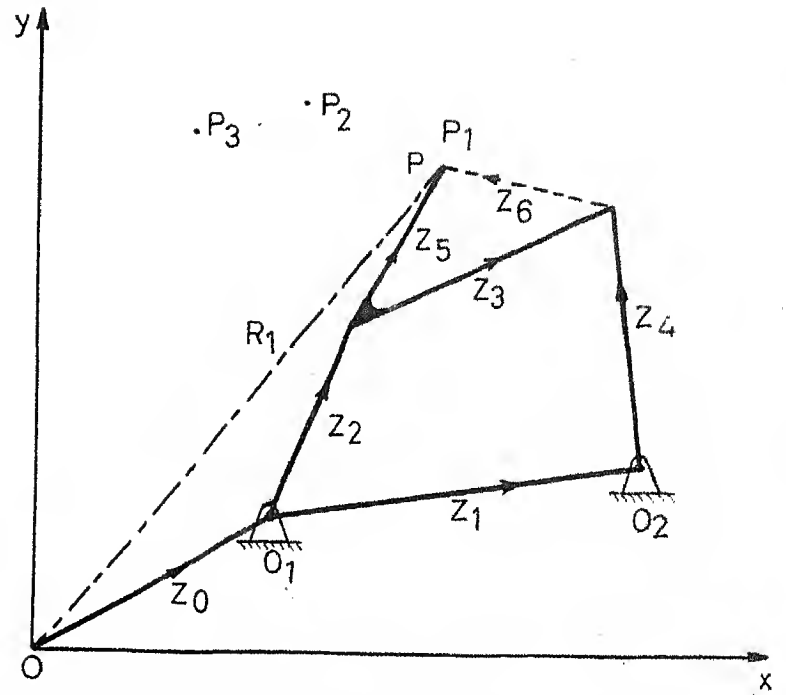

Fig 3.1 Vectorial Representation of Four-Bar Mechanism for Rigid Body Guidance

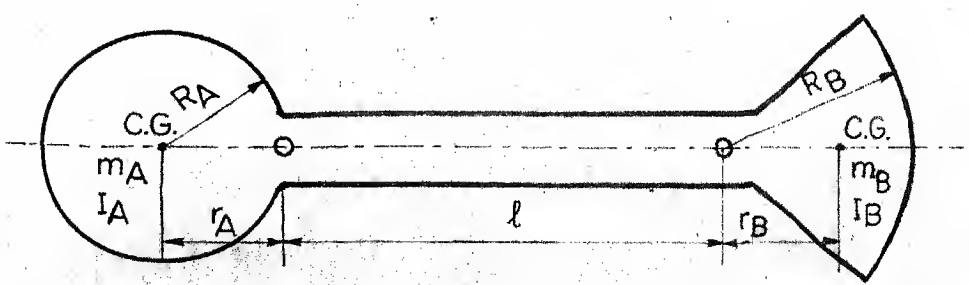

Fig 3.2 Link with Counterweights

The loop closure equations for the point P at the initial position is written in the following two ways.

$$\begin{aligned} Z_o + Z_2 + Z_5 &= R_1 \\ Z_o + Z_1 + Z_4 + Z_6 &= R_1 \end{aligned} \tag{3.1}$$

When the mechanism moves and the rigid body occupies the jth position, let the links be rotated through θ_j (crank ψ_j (coupler) and φ_j (follower) from their initial positions respectively, then the above loop closure equations for the jth position are

$$\begin{aligned} Z_o + Z_2 e^{i\theta_j} + Z_5 e^{i\psi_j} &= R_j \\ Z_o + Z_1 + Z_4 e^{i\varphi_j} + Z_6 e^{i\psi_j} &= R_j \end{aligned} \tag{3.2}$$

Subtracting equations (3.1) from equation (3.2) the followin relations are obtained.

$$\begin{aligned} Z_2 (e^{i\theta_j} - 1) + Z_5 (e^{i\psi_j} - 1) &= r_j \\ Z_4 (e^{i\varphi_j} - 1) + Z_6 (e^{i\psi_j} - 1) &= r_j \end{aligned} \tag{3.3}$$

where r_j is the relative displacement vector of the jth position of the rigid body from its initial position. For three rigid body positions j is equal to 2 thus one has

$$
\begin{aligned}
Z_2 (e^{i\theta_1} - 1) + Z_5 (e^{i\psi_1} - 1) &= r_1 \\
Z_2 (e^{i\theta_2} - 1) + Z_5 (e^{i\psi_2} - 1) &= r_2 \\
Z_4 (e^{i\varphi_1} - 1) + Z_6 (e^{i\psi_1} - 1) &= r_1 \\
Z_4 (e^{i\varphi_2} - 1) + Z_6 (e^{i\psi_2} - 1) &= r_2
\end{aligned}
\qquad (3.4)
$$

These are four equations in four complex variables. The angular rotations of the links may be arbitrarily chosen or some of them may be specified in the problem, generally θ's are specified, and Z_2, Z_4, Z_5 and Z_6 are determined using equations (3.4). Z_1 and Z_3 are then determined using the links closure equation and the closure equation of the coupler triangle as given below

$$
\begin{aligned}
Z_2 + Z_3 &= Z_1 + Z_4 \\
Z_3 + Z_6 &= Z_5
\end{aligned}
\qquad (3.5)
$$

Therefore the equations (3.4) and (3.5) yield all the link lengths of the mechanism to serve the required aim. However, the number of possible solution are infinite since arbitrary values can be assigned to ψ's and φ's.

3.3 Dynamic Force Analysis

At each stage of iteration during the optimization process it is required to determine the maximum shaking force, the maximum shaking moment etc. during a complete

cycle of motion of the mechanism. The following procedure is adopted for this purpose.

In Chapter II a transformation matrix has been obtained (section 2.6) which relates the small rigid body displacements at the 'slave' set of coordinates to the corresponding small displacement at the 'master' set of coordinates. The same logic is extended when the coordinates representing the two translational rigid body degrees of freedom at each fixed bearing are also included [35]. These four co-ordinates, two at each fixed bearing, that allow additional rigid body degrees of freedom, are grouped together with the rotational degree of freedom at the input crank end, placing them as the last system coordinates. This set of coordinates forms the group of 'slave' coordinates and is represented by the subscript C. The remaining set of coordinates, which are termed as 'master' coordinates, is denoted by the subscript A.

At any given configuration the mechanism is in equilibrium under the action of the external forces acting on it, the inertia forces, the torque applied at the input crank end and the reactions at the fixed bearings. Applying the principle of virtual work and remembering the fact that the elastic forces do not produce any work during rigid body displacements the following equation is readily obtained

$$T_C + F_C + T_R^t F_A = 0 \qquad (3.6)$$

where T_C is the vector of the unknown reactions at the slave coordinates, F_C is the known force vector that include the inertia forces and external forces at the slave coordinates and F_A is the known inertia forces and the external forces at the master coordinates. The transformation matrix T_R which relates the small rigid body displacements at the slave coordinates to the corresponding small rigid body displacements at the master coordinates is obtained following a procedure similar to that described in section 2.6, giving T_R as follows

$$T_R = -K_{AA}^{-1} K_{AC} \tag{3.7}$$

where K_{AA} and K_{AC} are the submatrices of the partitioned stiffness matrix K as indicated below

$$[K] = \begin{bmatrix} K_{AA} & K_{AC} \\ K_{CA} & K_{CC} \end{bmatrix} \tag{3.8}$$

Having determined the vector T_C using eq.. (3.6) the shaking force and the shaking moment about a point midway between the two fixed supports are given by

$$FS = \sqrt{(T_{c2}-T_{c4})^2 + (T_{c3} - T_{c5})^2} \tag{3.9}$$

$$MS = \frac{l_o}{2} (T_{c5} - T_{c3}) - T_{c1} \tag{3.10}$$

where FS is the shaking force, MS the net shaking moment exerted on the foundations, l_o the distance between the two

attached to the link respectively. Let the suffix A and B stand for the parameters of the counterweights at the left and right ends of the link respectively. Let ω and α are the angular velocity and angular acceleration and a_{Ax}, a_{Ay} and a_{Bx}, a_{By} are the linear accelerations in the x and y directions at the left and right ends of the link respectively. The additional nodal inertia forces due to the counterweights are then given by

$$\begin{aligned} p_1 &= -m_A (a_{Ax} + r_A \omega^2) \\ p_2 &= -m_A (a_{Ay} - r_A \alpha) \\ p_3 &= -I_A \alpha - p_2 r_A \\ p_4 &= -m_B (a_{Bx} - r_B \omega^2) \\ p_5 &= -m_B (a_{By} + r_B \alpha) \\ p_6 &= -I_B \alpha + p_5 r_B \end{aligned} \qquad (3.11)$$

where p_1 to p_6 are the component of the additional nodal inertia forces due to the counterweights acting at the six coordinates of the element (link). These nodal forces are added to the previously calculated element nodal forces due to the inertia of the link alone. This resultant set of the nodal forces gives the element load vector in element oriented coordinates due to the combined rigid body inertia of the link and its counterweights.

fixed supports, T_{c1} is the first element of the vector, T_c, which corresponds to the input torque at the crank end and T_{c2} to T_{c5} are the remaining elements of the vector T_c which correspond to bearing reactions.

3.4 Dynamic Force Analysis with Counterweights

When the masses of the links are redistributed by placing counterweights in order to reduce the shaking force or shaking moment, the inertia forces acting at the nodes, determined using the finite element approach, due to the links of uniform cross-section, are modified. The additional nodal forces due to the inertia of the attached counterweights are determined as follows.

The counterweights that are attached to a link are generally either circular with circumference passing through the center of the joint of the link, or the sector of a circle with its centre coincident with the center of the joint or simply an extension of the link beyond the joint having similar cross-section as the link. Figure 3.2 shows a link with counterweight attached at both ends. A link may not have counterweights at its both ends but to generalize the presentation counterweights are assumed to be present at both the ends. Let m, r and I represent the mass, the distance of the centroid from the joint of the link and the mass moment of inertia of the counterweight

section 3.4 for determining the contribution towards the rigid body inertia forces due to the counterweights. The only change made in the equations (3.11) is that the accelerations due to elastic motion are substituted in place of the rigid body accelerations. Thus one gets

$$\begin{aligned} p_{e1} &= -m_A (a_{e1} - r_A v_{e3}) \\ p_{e2} &= -m_A (a_{e2} - r_A a_{e3}) \\ p_{e3} &= -I_A a_{e3} - p_{e2} r_A \\ p_{e4} &= -m_B (a_{e4} - r_B v_{e6}^2) \\ p_{e5} &= -m_B (a_{e5} + r_B a_{e6}) \\ p_{e6} &= -I_B a_{e6} + p_{e5} r_B \end{aligned} \qquad (3.13)$$

where p_{e1} to p_{e6}, v_{e1} to v_{e6} and a_{e1} to a_{e6} are elements of the KED inertia load vector $\bar{p}_e$ due to counterweights, velocity vector $\bar{v}_e$ and acceleration vector $\bar{a}_e$ of the element (link) in the element oriented coordinates, respectively. The other variables are same as explained in section 3.4. The velocity vector and acceleration vector mentioned above are the ones that are obtained at the end of the previous interval by the kinetoelastodynamic analysis of the mechanism.

3.5.3 Determination of Total KED Inertia Forces

Having determined the KED inertia load vector as above it is added to the element resultant load vector

determined in section 3.4. This final element inertia load vector in element oriented coordinate is transformed into element load vector in system coordinates using the eq. (2.26). These transformed elements load vectors are assembled to yield system inertia load vector. The inertia load vector thus obtained is added to the system inertia load vector P_e determined in section 3.5.1 to give the final system inertia load vector due to the combined rigid body and KED inertia for the complete mechanism, i.e. including all the links and their counterweights. It is this inertia load vector which is used to determine the shaking force, the shaking moment and the input end torque at any configuration of the mechanism as outlined in section 3.3.

3.6 Determination of System Mass Matrix with Counterweights

When the counterweights are attached at the ends of the links the system mass matrix M in eq. (2.33), obtained considering the regular links with uniform cross-section, needs modification. To achieve this it is assumed that as if the whole of the counterweight mass is situated at the joint of the link near to that counterweight to account its contribution corresponding to the translational coordinates of the joint. To account the contribution of the counterweight corresponding to the rotational coordinate at the joint the moment of inertia of the counterweight about the center of the joint is determined. These masses or

moment of inertia are added to the corresponding diagonal elements of the element mass matrix in element coordinates. The element mass matrices, thus obtained, are first transformed into element mass matrices in system coordinates, and they are then assembled to give system mass matrix M.

CHAPTER IV

OPTIMIZATION PROBLEM AND SOLUTION PROCEDURE

4.1 Introduction

In mechanism design one of the two methods may be followed, namely: (a) Direct design methods, (b) Mathematical programming techniques. In the former procedure a set of equations is formed based on design criteria (kinematic or dynamic or both) relating the design variables. These equation are then solved by various means to find the design variables. This procedure is not suitable if the required design has to satisfy certain inequality constraints. One alternative is to design a mechanism using this procedure and see whether the constraints are satisfied. If they are violated the design is revised by trial and error. Furthermore for complex problems, where there are a number of possible design objectives, including both kinematic and dynamic performance criteria and where there are a number of design constraints this procedure is not applicable. In such situations it is advantageous to adopt mathematical programming techniques. Using this technique it is also possible to make a trade-off study between

various competitive objectives. The application of mathematical programming techniques to problems in mechanism design has been presented in a review paper by Fox and Gupta [49]. They have discussed the available tools of optimization as applied to mechanism design. In the present study, where two stages of mechanism design, namely, balancing of mechanism and strength considerations are both combined into a single design objective, this is the most convenient procedure to be followed. Therefore the problems in the present study are solved as nonlinear programming problems.

4.2 Nonlinear Programming Problem

A nonlinear programming problem can mathematically be posed as:

Minimize,

$$f(\bar{X})$$

subject to,

$$g_i(\bar{X}) < 0 \qquad i = 1, 2, \ldots, m$$

and,

$$L_j(\bar{X}) = 0 \qquad j = 1, 2, \ldots, p$$

where f is the objective function of n variables $\bar{X}$ to be minimized, g_i are m inequality constraints and L_j are p equality constraints which must be satisfied at the optimum point.

4.3 Problems Undertaken During Present Study

As pointed out in Chapter I the present study is categorized into two types of problems and hence the following two nonlinear programming problems are formulated.

4.3.1 First Problem

In this problem it is required to synthesize a suitable mechanism which serves a specified aim (such as rigid body guidance, path generation or function generation) with optimal dynamic characteristics with reference to unbalance in the mechanism. Thus the objective is to minimize the shaking force and/or the shaking moment transmitted to the machine foundation.

The design parameters for this problem are the unknown relative angular positions of the coupler and the follower when the crank moves through given positions (angles) to guide the rigid body through required positions. The cross-sectional areas of the links are taken as variables. A single proportionality factor is taken for this purpose for all the links in order to limit the number of variables.

The major constraints imposed on the optimization process are as follows:

(i) From kinematic point of view the mobility conditions must be satisfied and also the transmission angle at any position of the mechanism should not be less

than a specified minimum. Assuming the mechanism to be crank rocker type the mobility conditions (known as Grashof criteria) and other constraints are expressed in terms of link lengths and transmission angle λ as follows

$$\begin{aligned}
(l_1+l_2) - (l_3+l_4) &< 0 \\
l_3-l_4 - l_1-l_2 &< 0 \\
l_2-l_1 &< 0 \\
l_2-L_{min} &< 0 \\
\left|90-\lambda_{max}\right| - \theta_{min} &< 0
\end{aligned} \qquad (4.1)$$

where l_i $(i = 1,2,3,4)$ are the lengths of ground link, crank, coupler and follower respectively, L_{min} is the minimum permissible length of the crank and θ_{min} is the least permissible value of the maximum deviation of the transmission angle from 90°. The first three of the above constraints are Grashof criteria, the fourth one takes into account the minimum practical limit for the crank length and the last one is from the transmissibility consideration of the forces.

(ii) The stresses in the links are kept within a specified maximum limit to safeguard against possible failure due to want of strength. Mathematically it can be expressed as

$$\sigma_i - \sigma_{max} < 0 \qquad (4.2)$$

$$i = 1,2,3$$

where σ_i are the maximum stresses during a complete cycle of motion of the mechanism produced in the crank, coupler and follower, respectively. σ_{max} is the maximum allowable stress for the material of the links.

(iii) The deflections of the strategic points in the mechanism are not allowed to exceed beyond a specified limit so that the required goal is met within a tolerable accuracy. However, in the solution of present problem no constraints are imposed on deflections.

An example has been solved taking into account the effect of KED inertia during the determination of the shaking force and the shaking moment transmitted to the machine foundation. In another example the contribution due to KED inertia is not included and it is solved taking into consideration only the contribution due to rigid body inertia to investigate the effect of KED inertia on the design.

4.3.2 Second Problem

For a given mechanism (i.e. with fixed link lengths) the link masses are redistributed by placing counterweights to achieve optimum dynamic characteristics with reference to unbalance in the mechanism. Therefore, the objective in this case also is to minimize the shaking force and/or shaking moment transmitted to the foundation.

The design variables are the size and position of counterweights to be attached to the links. The cross-sectional areas of the links are allowed to vary. To reduce the number of variables, the cross-sectional areas of all the links are varied in the same proportion by taking a common proportionality factor.

The major constraints considered are:

(i) The stresses in the links are constrained to take a value less than a specified maximum permissible value so that the links have sufficient strength. Mathematically it can be represented as

$$\sigma_i - \sigma_{max} < 0 \qquad (4.3)$$

$$i = 1, 2, 3$$

where σ_i and σ_{max} are same as defined in 4.3.1.

(ii) If it is desired to limit the deflections of vital points in the mechanism then constraints can be imposed on them. However, in the present problem these constraints are not included.

(iii) In case the shaking force alone is minimized a constraint on shaking moment and input torque are imposed.

In this case also in one example the contribution of KED inertia towards the shaking force and shaking moment has been considered. However to estimate the effect of KED inertia the same problem is solved excluding KED inertia.

Berkof and Lowen [6] showed that in a four bar mechanism with a coupler having symmetry about the line of joints the shaking force could be minimized by placing appropriate counterweights at the end of the crank and follower jointed to the fixed supports in such a way that their centroid lie on the line of joints of the respective link produced. Since in the present problem a symmetric coupler is taken, the centroids of the counterweights attached to the crank and follower are kept at 180° with line of joints of the respective links. These counterweights are taken as circular with their circumference passing through the center of the pin of the joint of the respective link. Two sector type weights are attached at the coupler ends. The radii as well as the angles of the sectors are taken as variables. These counterweights are taken as result of an observation in which it is noted that they have a favourable effect on coupler stresses. As such, the design variables for this problem are the radii of the four counterweights and the angles of the two sector type counterweights.

4.4 Procedure Adopted for Evaluating the Maximum Shaking Force etc. and Maximum Stresses

The shaking force etc. as well as the stresses in the links of a mechanism are not only functions of the various parameters of the mechanism but they also depend upon the configuration of the mechanism and as such they

continuously vary during the complete cycle of motion of the mechanism. It is not possible to express them explicitly as a function of input angle. The general practice is to calculate them at discrete positions during the complete cycle of motion. The accuracy in the values of the shaking force etc. and stresses depends upon the size of the interval. A smaller interval size gives a better accuracy but requires a larger number of calculations during a cycle thereby incurring more computer time in determining the maximum shaking force etc. and the maximum stresses in the links. Thus a compromise is made between the accuracy desired and the available time. Furthermore when the parameters of the mechanism are changed, not only the magnitudes of the maximum shaking force etc. and maximum stresses in the links are changed but the positions (i.e. angles) of the crank at which these maxima occur also change.

4.4.1 Determination of Maximum Stresses

The determination of the maximum stresses in the links of a completely elastic mechanism is a time consuming process. Moreover most of the methods available todate yield unsteady state stresses initially. To obtain the steady state stresses the process has to be repeated for a number of cycles which differ in different cases. The determination of stresses even for one cycle is very time consuming therefore the calculation of steady state stresses

by continuing the analysis for many cycles cannot be justified in an optimization problem where the minimizing function or its gradient has to be evaluated a large number of times. Therefore the determination of stresses is restricted to first cycle of motion only. Invariably in most of the cases the steady state stresses are smaller than the first cycle stresses and the design will be safe.

To cut down the computational time further the gradients of the stresses in the links are determined at the initial point and then while taking various steps in the design space during one dimensional minimization to find out the optimum step length these gradients are used to determine the subsequent values of the maximum stresses in the links. These type of approximations have been successfully used in a number of other problems. It is found to work well in this case also.

4.4.2 Determination of Maximum Shaking Force etc.

For problems in which contribution of KED inertia towards shaking force and shaking moment etc. is included, the shaking force, the shaking moment, and the input torque are determined at each position of the mechanism into which the cycle of motion is discretised while determining stresses, using the method outlined in Chapter III. The maximum values of these functions during the complete cycle of

motion are noted. As explained in section 4.4.1 the kineto-elastodynamic analysis of the mechanism is a time consuming process the gradients of the maximum shaking force, the maximum shaking moment and the maximum input torque are used to predict these functions at subsequent design points during one dimensional minimization. These approximations are also found to work successfully.

In case the contribution of KED inertia is not taken into consideration the shaking force, the shaking moment and the input torque are obtained using direct equations as outlined in Appendix D at intervals into which the complete motion of the mechanism is divided. A larger interval may be taken for this purpose. Having determined the maximum value of the shaking force and the position, i.e. the crank angle at which it occurs, a finer interval is taken and the shaking force is calculated about this crank position and a more accurate value of the maximum shaking force is obtained. If desired this procedure can be adopted to obtain accurate values for the maximum shaking moment and/or maximum input torque.

4.5 Solution Procedure

The procedures available to solve a constrained minimization problem fall into two categories: (i) converting the problem into an unconstrained problem by suitable means, (ii) direct methods [50,51].

Without going into a discussion of their merits and demerits, which is not the purpose here, the interior penalty function method of unconstrained minimization is used that fall under the first category. The interior penalty function method has an advantage over the exterior penalty function method that one can stop at any level of optimization process with the design still in the feasible region.

The interior penalty function for problems having inequality constraints only is defined as

$$\varphi\ (\bar{X}, r) \;=\; f(\bar{X}) - r \sum_{i=1}^{m} \frac{1}{g_i(\bar{X})} \qquad (4.4)$$

where r is penalty function parameter.

The function φ is minimized as unconstrained minimization problem over $\bar{X}$ for a fixed positive value of r. In the next step r is decreased and φ is minimized. The process is continued sequentially till there is no improvement during the minimization process. It is reasonable to take such values of r initially which makes the function φ about 1.5 to 2 times the objective function f. Any suitable reduction factor is taken to reduce the value of r for the next step. Most commonly a reduction factor of 10 is taken.

As pointed out earlier, gradients of the maximum stresses in the links shall be used to predict them at the

neighbouring design point so as to reduce the computational time. Therefore, it is appropriate to use a gradient method for unconstrained minimization. The Davidson-Fletcher-Powell (DFP) method (also known as variable-metric method) has been adopted to solve the problems under study. This is very effective even for highly eccentric and distorted functions. Golden section method of one dimensional minimization is used to determine the optimum step length in a certain move direction. This method is preferred over the cubic interpolation since it requires lesser number of overall functions evaluations thereby incurring lesser computer time in determining optimum step length.

4.6 Determination of Gradients

The gradients of the maximum shaking forces etc. and the maximum stresses are used to determine these functions at subsequent design points. Moreover, the DFP method of optimization requires the determination of the gradient of the penalty function at each iteration of optimization. Since these functions are not available in the form of explicit equations, it is not possible to have closed form expressions for these gradients. Therefore, the finite difference method of gradient calculation is resorted to. The backward difference formula is used for this purpose. If the number of design variables is large sufficient

computational time is needed when the stresses in the links are calculated, each time a design variable is perturbed, upto the complete cycle of motion of the mechanism. To overcome this problem the kinetoelastodynamic analysis is made for the complete cycle of motion of the mechanism at the base point only and subsequently, when each design variable is changed by a small amount in turn, the kinetoelastodynamic analysis is made up to a few degrees beyond that crank angle at which the maximum stress in the links or the maximum shaking force or the maximum shaking moment or the maximum input torque (whichever corresponds to largest crank angle) has occurred at the base point. This procedure of determining the graduents has worked well and has saved sufficient computational time.

CHAPTER V

RESULTS AND DISCUSSION

5.1 Introduction

The optimization problems formulated in Chapter IV are solved by taking numerical examples. Several computer programs have been written for this purpose, which are run on DEC 1090 computer to solve these examples. However, before taking up the actual optimization problems a study has been made to observe the effect of various mechanism parameters on the results of the kinetoelastodynamic analysis of the mechanism. This analysis is also expected to be useful in arriving at reasonable values of initial parameters of the mechanism for the optimization problems. Therefore, the analysis results are presented first in section 5.2 and then the results for the optimizations are given in section 5.3.

5.2 Analysis Results

The following four bar mechanisms are solved for the purpose of studying the effect of various parameters of the mechanism. Any system of units can be chosen for the numerical examples. However, FPS system of units has been adopted in the present study so that a direct comparison can be made with the previous works, wherever possible.

Mechanism A

Length of the crank = 12.0"; length of the coupler = 36.0"; length of the follower = 30.0"; length of the ground link = 36.0". The other parameters, unless specified otherwise are as follows: material aluminium of sp.wt. = 0.101 lbs/in^3 and Young's Modulus = 0.1 x 10^8 lbs/in^2; cross-section of all the links = 1" x 1"; material damping ratio = 0.05; angular interval in which the complete cycle of motion is discretized = 4^o; speed of the input crank (assumed constant) = 300 rpm.

Mechanism B

Length of the crank = 14.42"; length of the coupler = 29.28"; length of the follower = 21.26"; length of the ground link = 26.26". Other parameters are the same as for mechanism A.

5.2.1 Kinetoelastodynamic Analysis

Table 5.1 shows the effect of the size of interval in which the complete cycle of motion of the mechanism is discretized for computational work. The balancing torque present at the input end is determined considering the rigid body (RB) inertia forces only. The analysis is continued for the first three cycles. A change in the angular interval ($\Delta\theta$) from 5^o to 4^o causes an increase in the link stresses specially that of the crank during the

able 5.1 Effect of Angular Interval ($\Delta\theta$)-I

(ζ = 0.05 ; Links X-section=1"X 1" ; RPM=300)

ANGULAR INTERVAL ($\Delta\theta$)	CYCLE OF MOTION	MAXIMUM STRESSES IN LINKS (lb/sq in)			MAXIMUM SHAKING FORCE (lb)		MAXIMUM INPUT END TORQUE(lb in)	
		CRANK	COUPLER	FOLLOWER	RB ONLY	KED ONLY	RB ONLY	KED ONLY
5°	FIRST	- 4396	- 2506	1500	282	247	1825	241
	SECOND	- 5001	- 1756	1117	-	260	-	285
	THIRD	- 5001	- 1756	1117	-	260	-	285
4°	FIRST	- 7738	- 2621	1865	282	324	1825	329
	SECOND	- 5441	- 1759	1173	-	354	-	295
	THIRD	- 5441	- 1759	1173	-	354	-	295
2°	FIRST	- 7801	- 2669	1994	282	653	1825	240
	SECOND	- 5316	- 1587	1255	-	487	-	213
	THIRD	- 5317	- 1588	1254	-	487	-	213

Table 5.2 Effect of Angular Interval ($\Delta\theta$)-II

(ζ = 0.05 ; Links X-section=1"X1"; RPM=300)

ANGULAR INTERVAL ($\Delta\theta$)	CYCLE OF MOTION	MAXIMUM STRESSES IN LINKS(lb/sq in)			MAXIMUM SHAKING FORCE (lb)		MAXIMUM INPUT END TORQUE(lb in)	
		CRANK	COUPLER	FOLLOWER	RB ONLY	KED INCLUDED	RB ONLY	KED INCLUDED
5°	FIRST	- 4504	- 2517	1635	282	371	1825	2024
	SECOND	- 4905	- 1866	1339	-	381	-	1875
	THIRD	- 4906	- 1866	1339	-	381	-	1875
4°	FIRST	- 7738	- 2577	1803	282	525	1825	1828
	SECOND	- 5391	- 2332	1454	-	470	-	1807
	THIRD	- 5391	- 2332	1454	-	470	-	1807
2°	FIRST	- 8112	- 2659	2004	282	653	1825	1914
	SECOND	- 5346	- 1976	1251	-	591	-	1817
	THIRD	- 5346	- 1976	1251	-	591	-	1817

first cycle of motion. This could be due to the reason that some useful information might have been suppressed by choosing a larger interval ($\Delta\theta = 5^{o}$). However, the difference in the link stresses is not much when the interval is further reduced from 4^{o} to 2^{o}. Figs. 5.1 and 5.2, which give an account of the coupler stress versus crank angle, for the intervals of 4^{o} and 2^{o}, respectively, further enhance this conclusion. An examination of the contribution of KED inertia towards the shaking force shows a continuous increase with the reduction in the interval. It can also be noted that the contribution of KED inertia towards the shaking force is not only comparable to the contribution of rigid body inertia towards the shaking force but the former is even higher than the latter for finer intervals. Furthermore, the steady state is reached, as can be observed, during the second cycle of motion, and the stresses are more or less settled to the same maximum magnitude in all the three cases.

Table 5.2 shows the effect of the inerval size when the contribution of KED inertia towards the input end torque is also included in the analysis. Looking at Tables 5.1 and 5.2 it can be concluded that the addition of torque at the input end due to KED inertia has no significant effect on the results. This is because that the contribution of KED inertia towards the input end torque is very small in comparison to that of rigid body inertia.

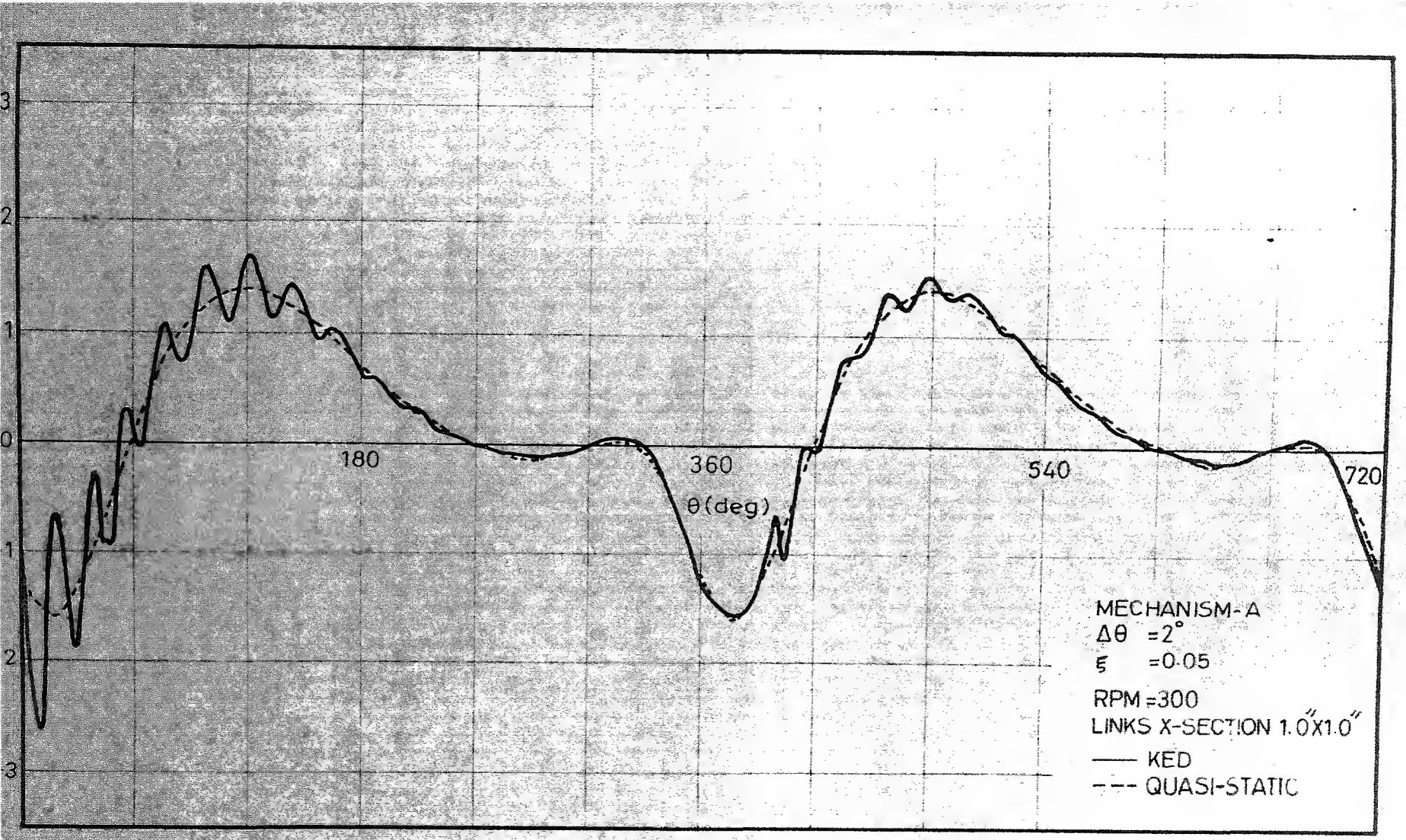

Fig 5.2 Coupler Mid-Point Stress vs Crank Rotation

Table 5.3 gives a comparison between the KED analysis results when different values for the material damping ratio are assumed during the solution process. It is interesting to note that although there is an increase in the link stresses during the first cycle of rotation with a decrease in damping ratio, but the maximum crank stress is settled, more or less, to the same steady state value in all the three cases considered. However, the coupler and follower stresses are settled to slightly higher values with lower damping ratio. The effect of damping ratio on the stress distribution in the links can be fully understood by observing Figs. 5.1 and 5.3 which depict the coupler stress against the crank angle for damping ratios of 0.05 and 0.01, respectively. It can be observed that the stress fluctuates about some mean value. The fluctuations are more pronounced when the damping ratio is smaller. Observing the stress during the second cycle of rotation, it can be concluded that the fluctuations are reduced in the steady state as compared to the fluctuations during the first cycle of motion which depicts the transient state. This behaviour is common to all dynamic response problems. The contribution of KED inertia towards the maximum shaking force is more for lower damping ratio. Furthermore, the maximum shaking force in the steady state is more than that in the transient state, i.e. first cycle of motion.

Table 5.3 Effect of Damping-I

($\Delta\theta = 4^{\circ}$; Links X-section=1" X 1" ; RPM=300)

DAMPING RATIO (ξ)	CYCLE OF MOTION	MAXIMUM STRESSES IN LINKS (lb/sq in)			MAXIMUM SHAKING FORCE (lb)		MAXIMUM INPUT END TORQUE(lb in)	
		CRANK	COUPLER	FOLLOWER	RB ONLY	KED ONLY	RB ONLY	KED ONLY
0.05	FIRST	- 7738	- 2621	1865	282	324	1825	329
	SECOND	- 5441	- 1759	1173	-	354	-	295
	THIRD	- 5441	- 1759	1173	-	354	-	295
0.02	FIRST	- 8646	- 2757	1932	282	554	1825	471
	SECOND	- 5495	- 2031	1255	-	690	-	648
	THIRD	- 5495	- 2053	1207	-	686	-	644
0.01	FIRST	- 9071	- 2981	1958	282	984	1825	758
	SECOND	- 5453	- 2164	1713	-	1154	-	1103
	THIRD	- 5466	- 2281	1702	-	1126	-	1020

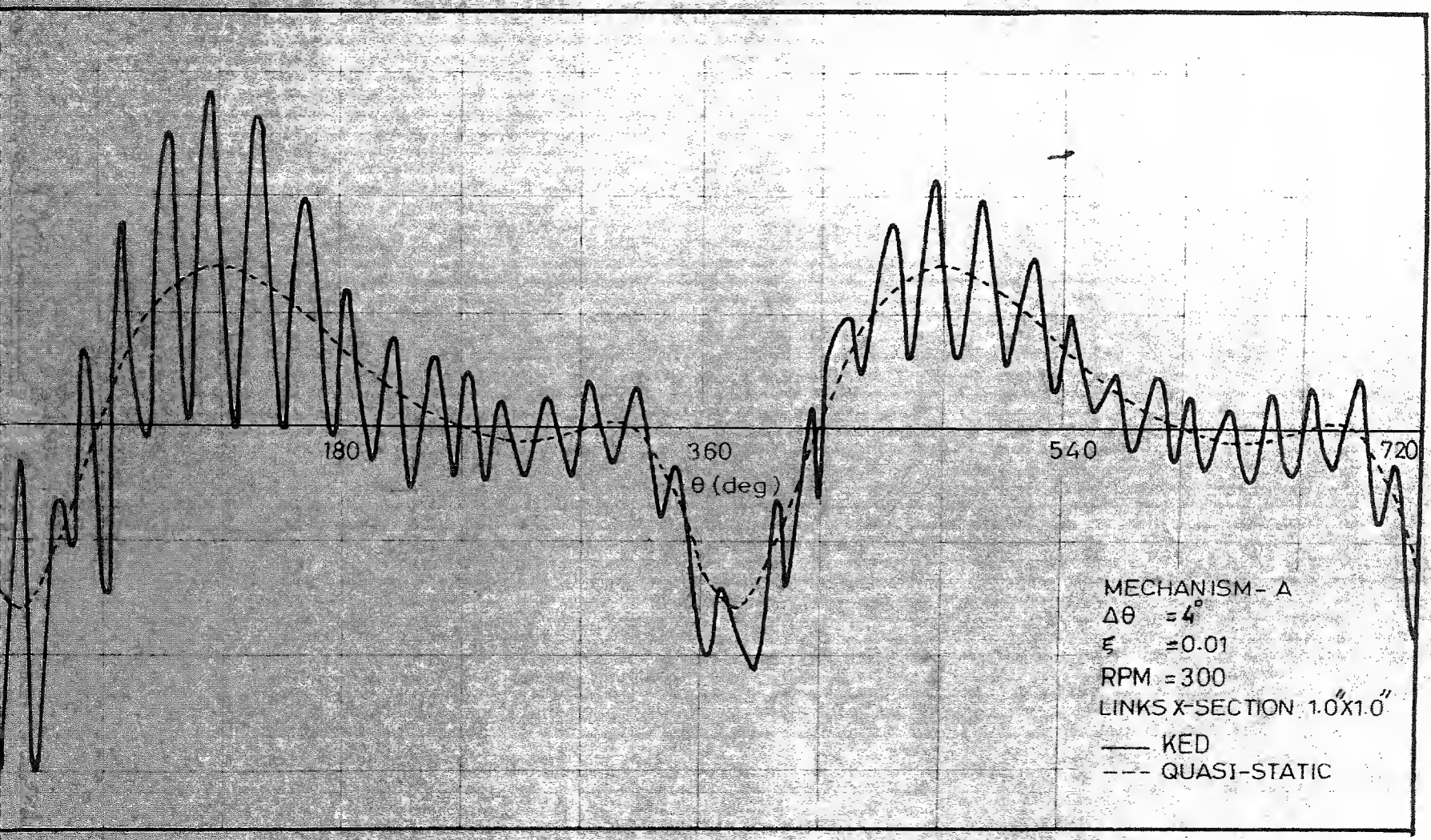

Fig 5.3 Coupler Mid-Point Stress vs. Crank Rotation

Table 5.4 shows the results with different assumed material damping ratios when the contribution of KED inertia towards input end torque is also included. The results have the same trend as for the case when the torque due to rigid body inertia only is considered to be acting at the input end.

Table 5.5 presents the effect of the crank speed of the mechanism on the results of kinetoelastodynamic analysis. As the running speed increases the stresses in all the links are increased more or less in a ratio which is the square of the speed ratio. This is in accordance with normal expectations. Since the acceleration is proportional to the square of the input speed the load vector, which consists of forces due to inertia only, is increased as the square of the speed ratio. Thus, the increase in the link stresses is also of the same order. The shaking force and the input end torque due to rigid body inertia are also correspondingly increased as the square of the speed ratio. The shaking force and the input end torque due to KED inertia are increased in a proportion which is even higher than the square of the speed ratio. Here one can observe that it is extremely important to take KED inertia into account at high speeds. Since the input torque due to KED inertia become very high with the increase in speed, the link stresses, when the torque at input end due to KED

Table 5.4 Effect of Damping-II

($\Delta\theta = 4^{\circ}$; Links X-section=1″X1″ ; RPM=300)

DAMPING RATIO (ξ)	CYCLE OF MOTION	MAXIMUM STRESSES IN LINKS (lb/sq in)			MAXIMUM SHAKING FORCE (lb)		MAXIMUM INPUT END TORQUE(lb in)	
		CRANK	COUPLER	FOLLOWER	RB ONLY	KED COMBINED	RB ONLY	KED COMBINED
0·10	FIRST	- 6787	- 2447	1710	282	405	1825	1768
	SECOND	- 5332	- 1628	1186	-	381	-	1810
	THIRD	- 5332	- 1628	1186	-	381	-	1810
0·05	FIRST	- 7738	- 2577	1803	282	525	1825	1828
	SECOND	- 5391	- 2332	1454	-	470	-	1806
	THIRD	- 5391	- 2332	1454	-	470	-	1806
0·03	FIRST	- 8295	- 3281	1825	282	541	1825	1867
	SECOND	- 5447	- 3514	1614	-	741	-	1805
	THIRD	- 5445	- 3497	1592	-	716	-	1809

Table 5.5 Effect of Crank Speed

($\Delta\theta = 4^{\circ}$; $\xi = 0.05$; Links X-section=1"X1")

INPUT END TORQUE	CRANK SPEED (rpm)	MAXIMUM STRESSES IN LINKS (lb/sq in)			MAXIMUM SHAKING FORCE (lb)		MAXIMUM INPUT END TORQUE(lb in)	
		CRANK	COUPLER	FOLLOWER	RB ONLY	KED ONLY/ COMBINED	RB ONLY	KED ONLY/ COMBINED
DUE	300	- 7738	- 2621	1865	282	324	1825	329
TO	600	- 31080	- 9707	8456	1129	3310	7302	4032
RB ONLY	1200	- 137000	- 66220	48750	4517	15953	29206	13916
DUE TO	300	- 7738	- 2577	1803	282	525	1825	1828
RB AND KED	600	- 33720	- 16580	13280	1129	5137	7302	4406
COMBINED	1200	-499000	-110300	46200	4517	130380	29206	110800

inertia is also included, are much higher than those when the torque present at the input end is due only to the rigid body (RB) inertia.

The effect of varying the cross-section of the links on the maximum link stresses, the maximum shaking force, and the maximum input torque is presented in Table 5.6. The load vector due to rigid body inertia is directly proportional to the cross-sectional area of the links, whereas the link stresses vary inversely as the thickness of the links. Thus, when only the thickness of the links is changed there is no change in the maximum link stresses (refer to link stresses in Table 5.6 for cross-sections of 1" x 1" and 1" x 4", which are exactly the same). However for the same cross-sectional area of the links when the width to thickness ratio is increased the link stresses are markedly reduced. This can be observed by looking at the link stresses given in Table 5.6 for the set of cross-sections having the same area, namely, 1.5" x 1.5" and 2.25" x 1" or 2" x 2" and 4" x 1". When the contribution due to KED inertia towards the input end torque is also included the trend is the same as discussed above as far as the maximum link stresses are concerned. The contribution due to the KED inertia towards the maximum shaking force, when considered separately, is reduced when the width to thickness ratio is increased (refer to the maximum shaking force due to KED inertia alone

Table 5.6 Effect of Links cross-section

($\Delta\theta = 4^{\circ}$; $\xi = 0.05$; RPM = 300)

INPUT END TORQUE	CROSS SECTION OF LINKS (inxin)	MAXIMUM STRESSES IN LINKS (lb/sq in)			MAXIMUM SHAKING FORCE (lb)		MAXIMUM INPUT END TORQUE (lb in)	
		CRANK	COUPLER	FOLLOWER	RB ONLY	KED ONLY/ COMBINED	RB ONLY	KED ONLY/ COMBINED
DUE TO RB ONLY	1.0 X 1.0	- 7738	- 2621	1865	282	324	1825	329
	1.5 X 1.5	- 4013	- 1588	1123	635	482	4106	318
	2.0X2.0	- 2324	- 1020	933	1128	850	7300	258
	2.25X1.0	- 2545	- 956	703	635	247	4106	360
	4.0X1.0	- 1195	- 392	492	1128	286	7300	261
	1.0X4.0	- 7738	- 2621	1865	1128	1296	7300	1315
DUE TO RB AND KED COMBINED	1.0X4.0	- 7738	- 2577	1803	282	525	1825	1825
	1.5X1.5	- 3983	- 1589	1157	635	877	4106	4074
	2.0X2.0	- 2309	- 1020	933	1128	1290	7300	7288
	4.0X1.0	- 1195	- 393	496	1128	1256	7300	7066
	1.0X4.0	- 7738	- 2577	1803	1128	2099	7300	7313

for the set of cross-sections 1.5" x 1.5" and 2.25" x 1" or 2" x 2" and 4" x 1"). However when the effect of KED inertia and RB inertia is considered together there is no appreciable difference in the maximum shaking force with the change in width to the thickness ratio (refer the values of the maximum shaking force in Table 5.6 for the set of cross-sections 2" x 2" and 4" x 1").

Table 5.7 shows the results of KED analysis for two different materials, of which the mechanism links are made. These two materials are steel and aluminium. Since the steel is heavier than aluminium, the maximum shaking force and maximum input torque in the case of links made of steel are higher than those in the case of links made of aluminium. The maximum stresses in the links made of steel are also higher than those in the links made of aluminium. This is because that the inertia load in the former case is higher than that in the latter one.

Table 5.8 presents a comparison of the results when the mechanisms with different link lengths are taken. There is a large variation in the link stresses when a different mechanism is taken. This table also shows the effect of adding a flywheel (having moment of inertia = 0.7 lbs-in-sec^2) at the output end. It is observed that the maximum follower stress is greatly increased by the addition of flywheel. In the case of first mechanism there

Table 5.7 Effect of Links material

($\Delta\theta = 4^\circ$; $\xi = 0.05$, Links X-section = 1" X 1" ; RPM = 300)

MATERIAL	INPUT END TORQUE	MAXIMUM STRESSES IN LINKS (lb/sq in)			MAXIMUM SHAKING FORCE (lb)		MAXIMUM INPUT END TORQUE (lb in)	
		CRANK	COUPLER	FOLLOWER	RB ONLY	KED ONLY/ COMBINED	RB ONLY	KED ONLY/ COMBINED
STEEL	RB ONLY	- 18200	- 7405	4643	755	1712	4880	1621
	KED COMBINED	- 18200	- 7436	4616	755	1255	4880	4824
ALUMINIUM	RB ONLY	- 7738	- 2621	1865	282	525	1825	329
	KED COMBINED	- 7738	- 2577	1803	282	314	1825	1828

Table 5.8 Effect of Links Length, Flywheel and Input End Boundary Condition

($\Delta\theta = 4^{\circ}$; $\xi = 0.05$, Links X-section = 1"X1"; RPM=300)

LINK LENGTHS (in)				CRANK END BOUNDARY CONDITION	FLYWHEEL AT OUTPUT END	MAXIMUM STRESSES IN LINKS (lb/sq in)		
GROUND	CRANK	COUPLER	FOLLOWER			CRANK	COUPLER	FOLLOWER
36.00	12.00	36.00	30.00	ELEMINATING RIGID BODY DEGREE OF FREEDOM	WITHOUT	- 7738	- 2621	1865
					WITH	- 8713	- 2642	5026
				FIXED AS CANTILEVER BEAM	WITHOUT	- 8870	- 2905	3614
					WITH	- 8864	- 2570	7259
26.26	14.42	29.28	21.26	ELEMINATING RIGID BODY DEGREE OF FREEDOM	WITHOUT	- 18060	- 8138	4974
					WITH	- 26110	- 19450	35970
				FIXED AS CANTILEVER BEAM	WITHOUT	- 28890	- 15290	11100
					WITH	- 35370	33080	- 36500

is no effect on the maximum stresses in the crank and the coupler due to the addition of flywheel. Whereas for the second mechanism the maximum stress in each of the links increases with the addition of flywheel. In Table 5.8 the analysis is also presented when the input end of the crank is instantaneously taken fixed as a cantilever beam. It is observed that for the first mechanism the difference between the maximum link stresses for the two cases, namely, when the rigid body degree of freedom is eliminated by the method outlined in section 2.7 of Chapter II, and when the crank is instantaneously assumed as cantilever, is small. However, for the second mechanism the maximum stresses in the links when the crank is taken as a cantilever beam are much higher than those when the rigid body degree of freedom is eliminated.

Figs. 5.4 to 5.6 give an account of the distribution of stresses in the crank, coupler and follower, respectively, versus crank angle for the mechanism A. The damping ratio is assumed 0.01 and the stresses are analysed at intervals ($\Delta\theta$) of 2° up to five cycles of motion of mechanism. However, the stresses are plotted only for the first two cycles except for the coupler stress in Fig. 5.5, which is shown for the fifth cycle also. The dotted curves in these figures represent the quasi-static stresses in the respective links. It can be observed that the link stresses

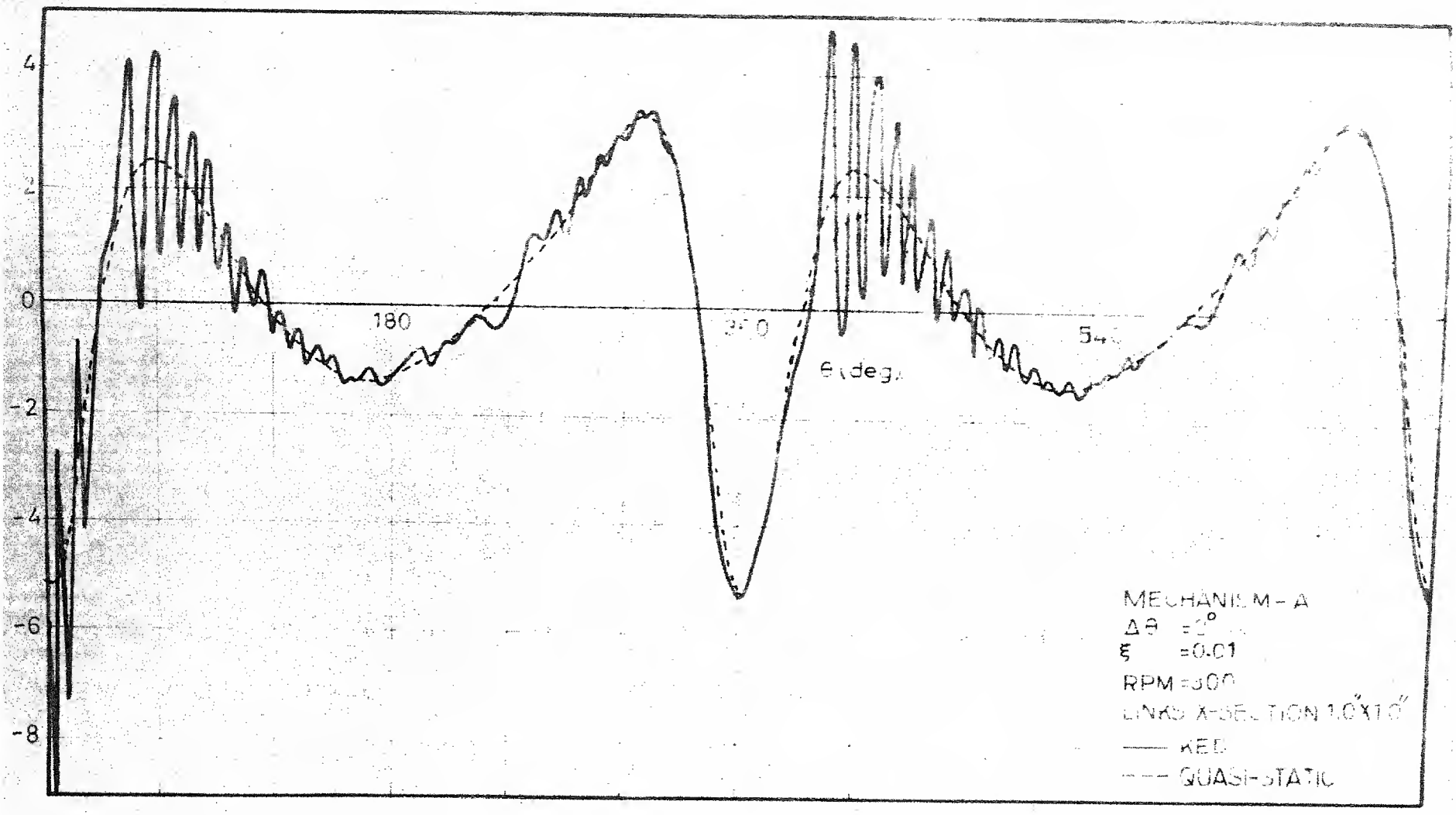

Fig 5.4 Crank Mid-Point Stress vs. Crank Rotation

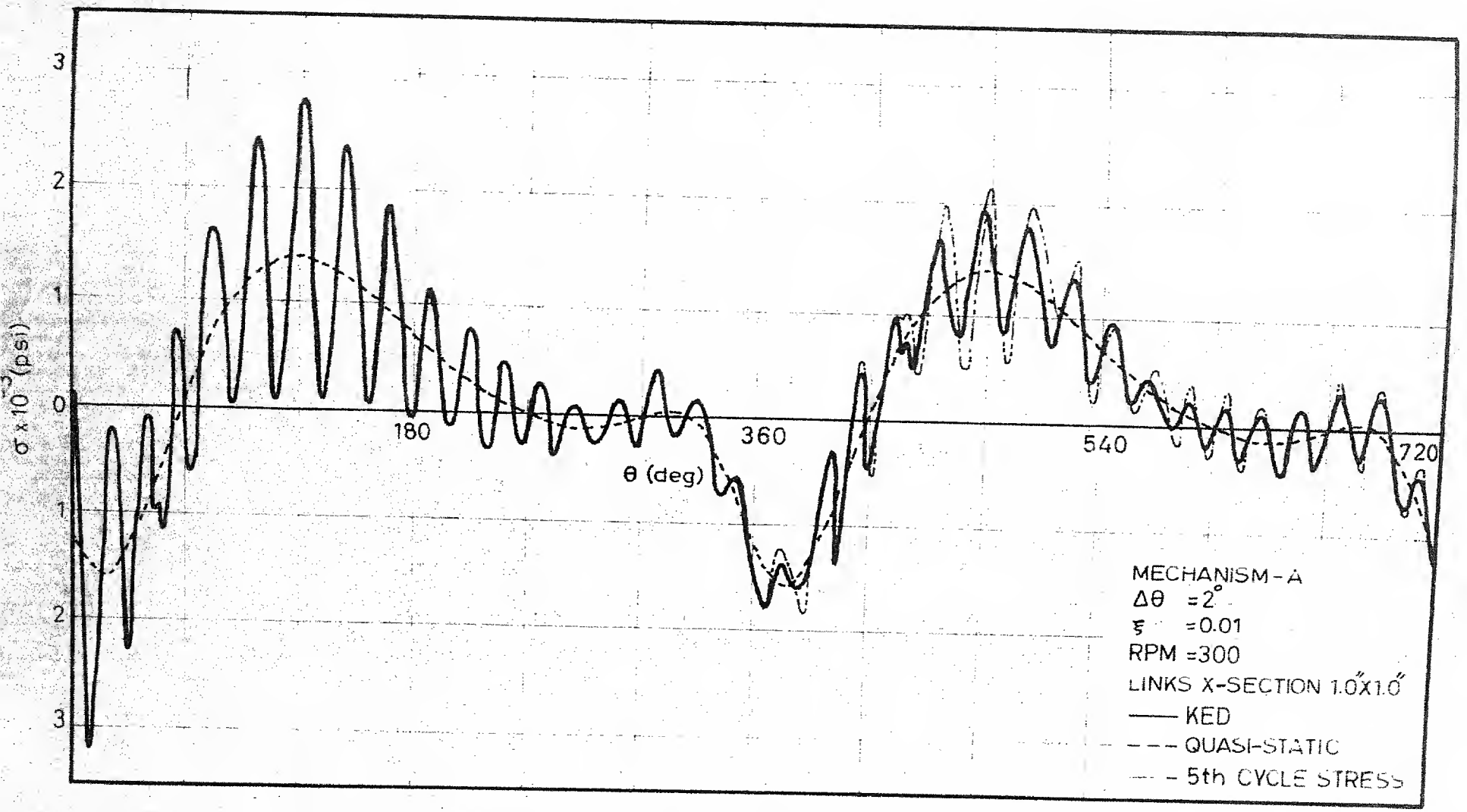

Fig 5.5 Coupler Mid-Point Stress vs. Crank Rotation

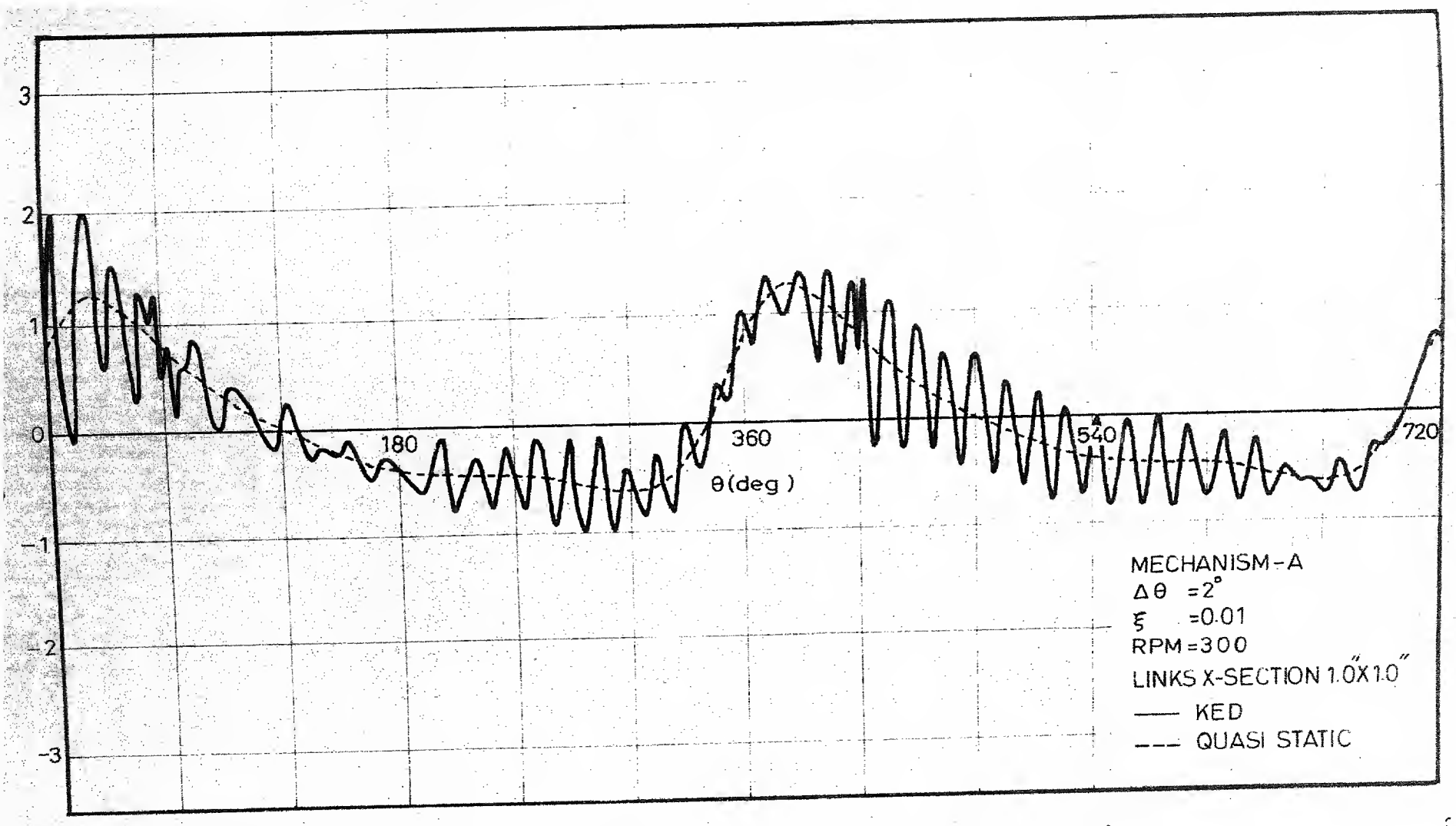

Fig 5.6 Follower Mid-Point Stress vs. Crank Rotation

determined by complete KED analysis fluctuate about the quasi-static stress curve. This behaviour is as expected in general dynamic response problems and therefore confirms the validity of the analysis. The maximum stresses in the links obtained by complete KED analysis are greater than those obtained by quasi-static analysis. The maximum stresses in the former case are more by about 70%, 114% and 92% than those in the latter one for the crank, coupler and follower, respectively, during the first cycle of motion, i.e. transient state. However, in the steady state the difference is only 2%, 43% and 8% between the maximum stresses in the crank, coupler and follower, respectively, for the two cases. Thus, except for the coupler stress the steady state stresses in the other links, when determined using complete KED analysis, are very close to the quasi-static stresses for the mechanism considered.

Figs. 5.7 to 5.9 represent the distribution of stresses in the crank, coupler and follower, respectively, of the same mechanism as above, when the analysis is made by assuming the crank instantaneously fixed as a cantilever beam, i.e. by considering the mechanism as structure. The quasi-static stresses are also shown in these figures by dotted curves. A comparative examination of these figures reveals that the behaviour is better represented when the mechanism is analysed by eliminating the rigid body degree

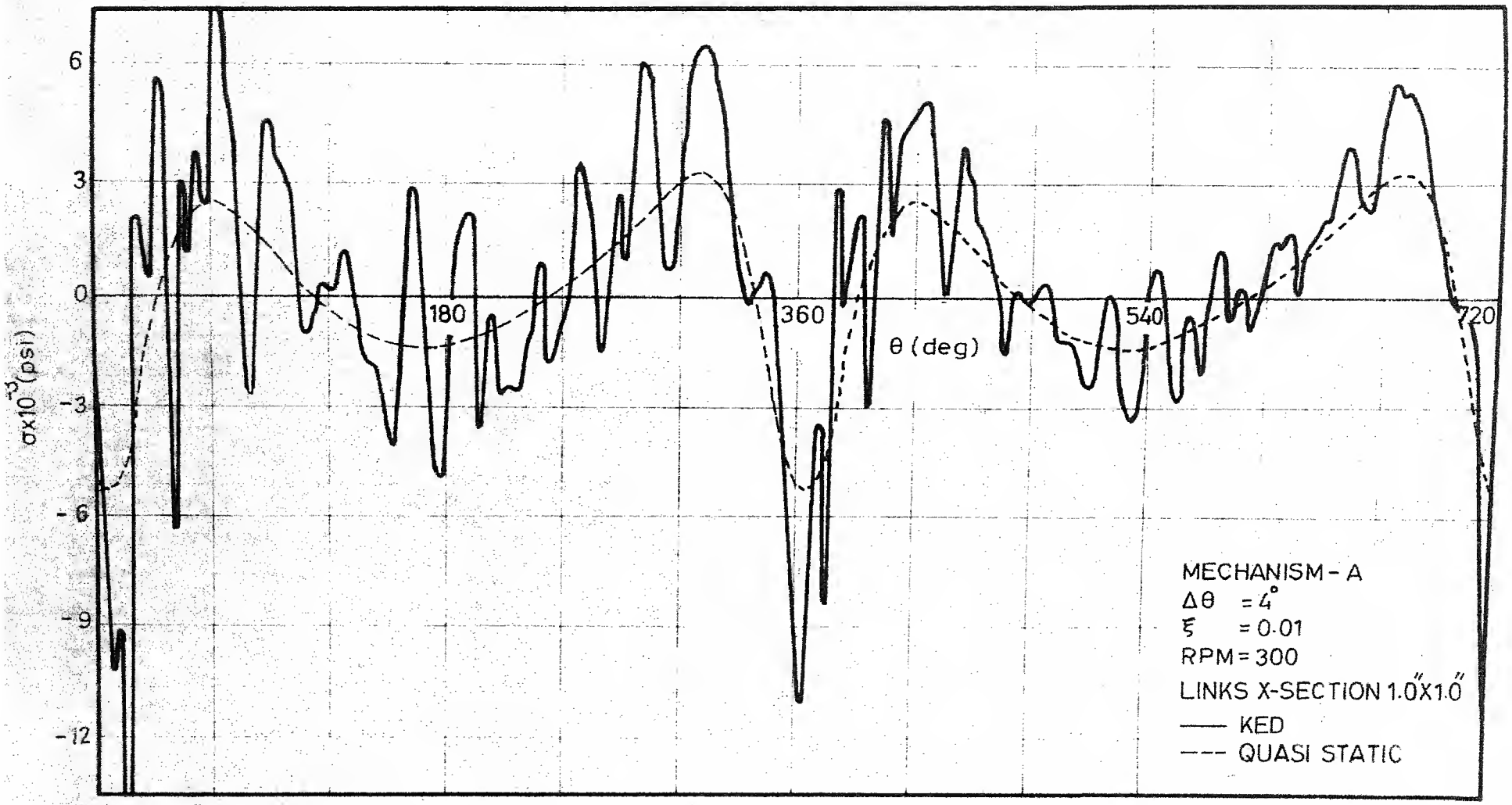

Fig 5.7 Crank Mid-Point Stress vs. Crank Rotation (with Crank Input End Fixed)

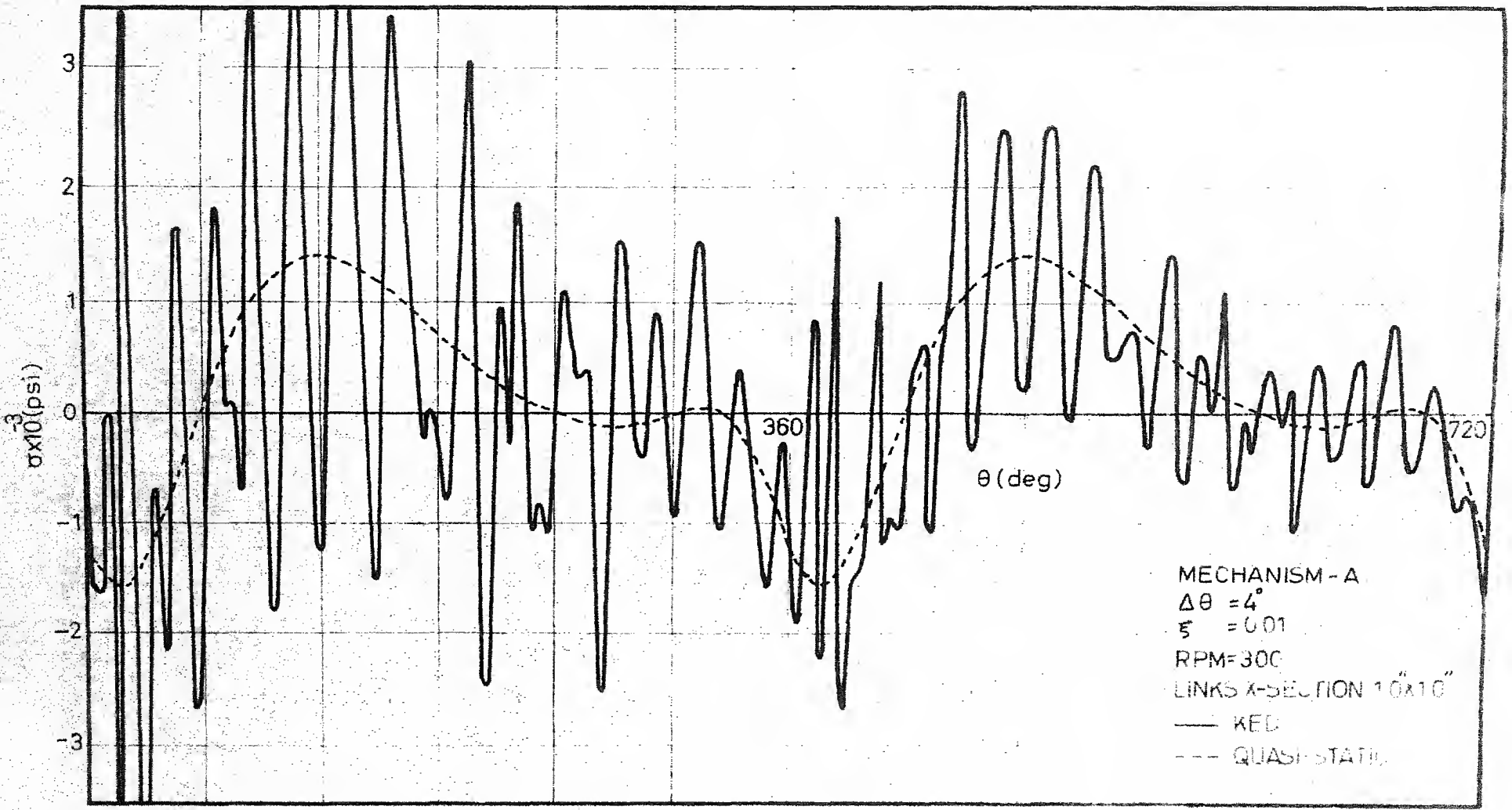

Fig 5.8 Coupler Mid-Point Stress vs. Crank Rotation (with Crank Input End Fixed)

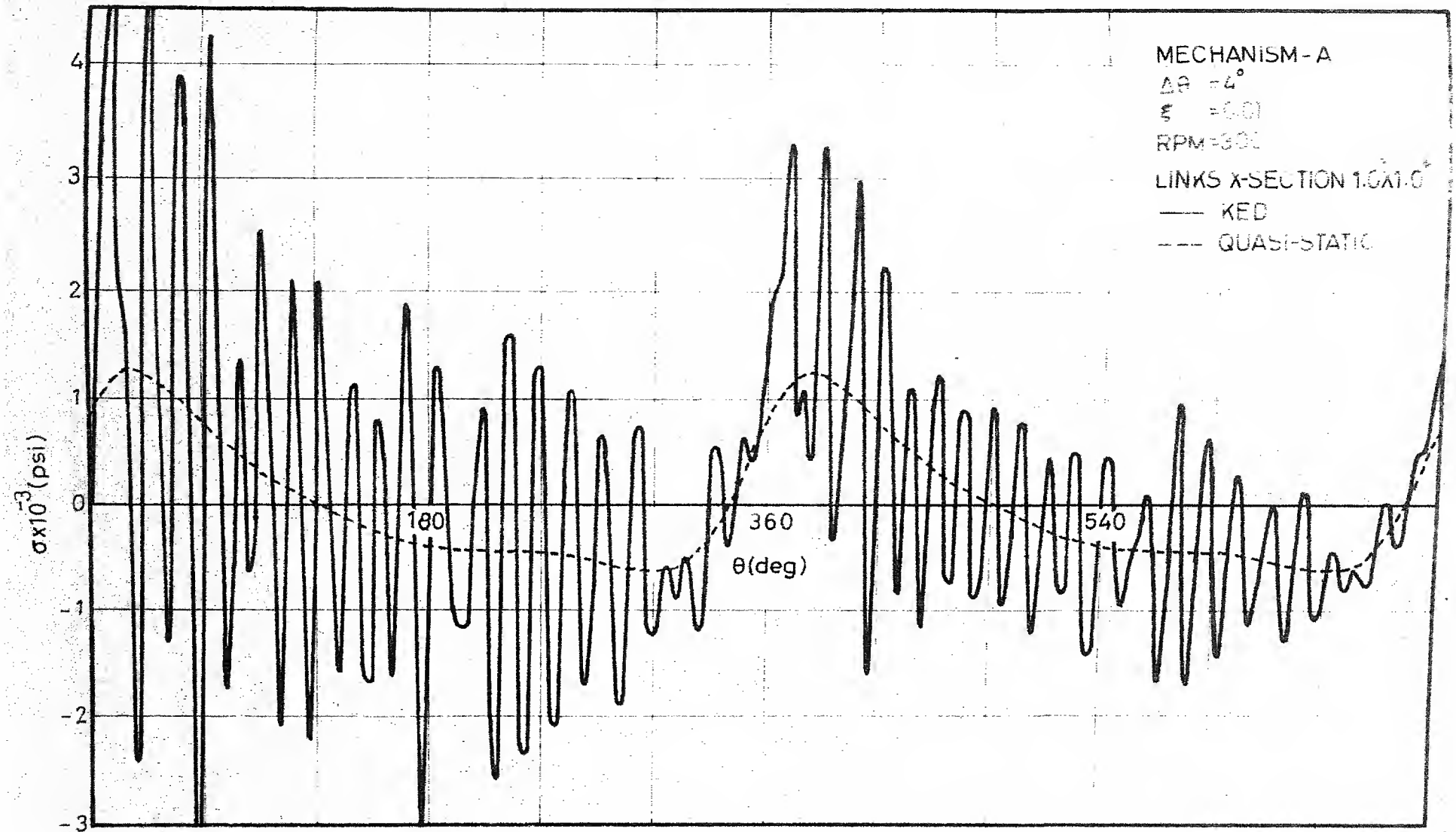

Fig 5.9 Follower Mid-Point Stress vs. Crank Rotation (with Crank Input End Fixed)

of freedom. Though the example cited here is different, the result of analysis, when mechanism is considered by eliminating its rigid body degree of freedom, show a trend which is similar to the one obtained during the experimental determination of stresses or strains in the links in some of the previous works [34,52].

5.2.2 Balancing Analysis and Shaking Force Minimization

For mechanism A the shaking force due to rigid body inertia only is minimized using counterweights. Two circular weights, with circumference passing through the center of the joint, are attached, one to the crank and the other to the follower ends, which are supported at the ground pivots. The radii of these counterweights as well as angular position of their centers are taken as variables. The thickness of these counterweights is equal to the thickness of the respective link to which they are attached. Extensions at both the ends of the coupler are assumed to the present; the width of each extension is taken equal to the coupler width but the thickness is taken equal to twice the coupler thickness. The extension lengths are taken as variables. The whole arrangement is depicted in Fig. 5.10.

The complete problem is solved as non-linear programming problem. In one case the objective function is the shaking force. In another case constraints on the maximum

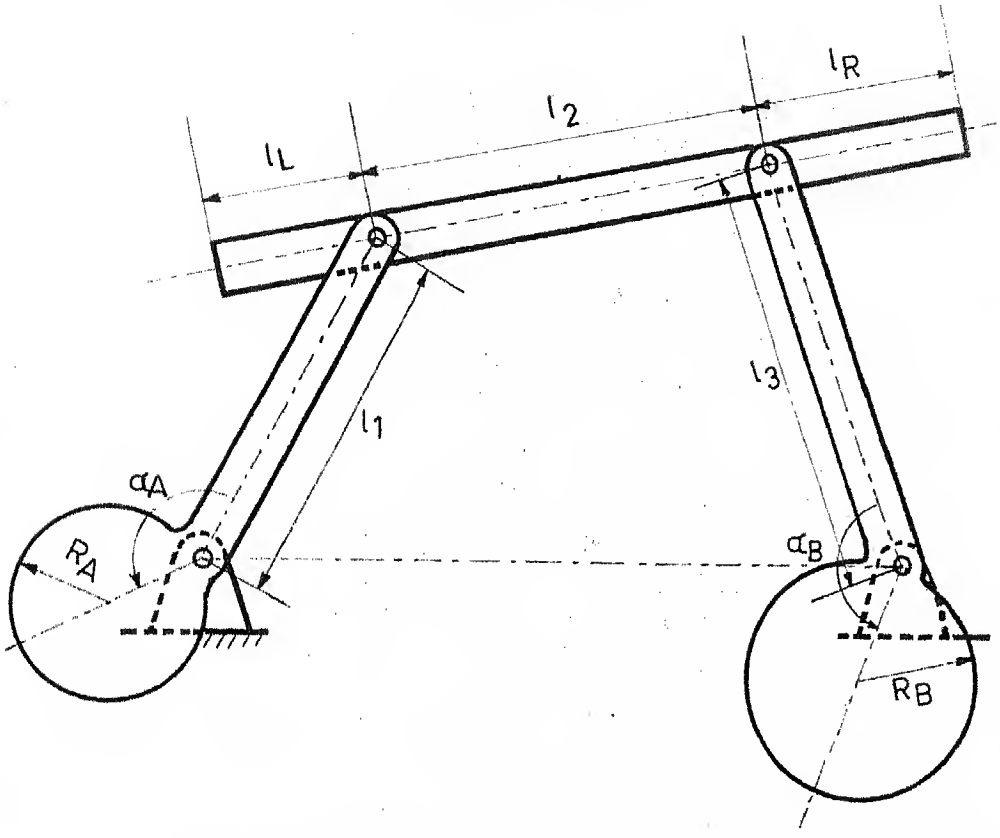

Fig 5.10 Arrangement of Counterweights-I

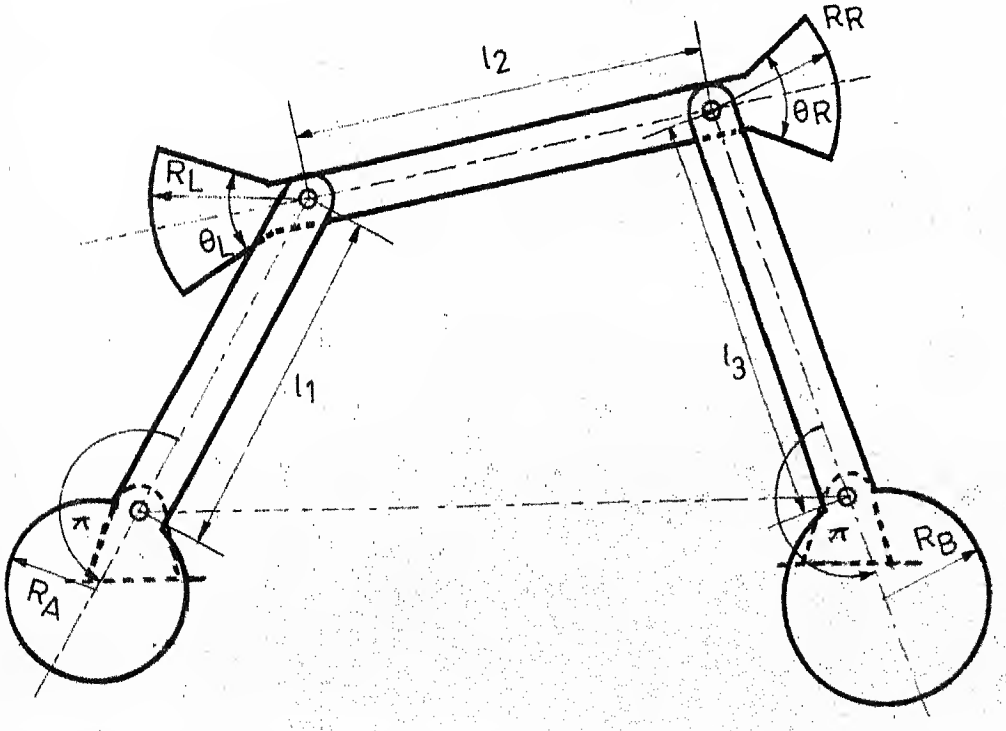

Fig 5.11 Arrangement of Counterweights-II

shaking moment, the maximum bearing reaction and the maximum input end torque are applied and the shaking force is minimized. In a third case the objective function is a combination of the shaking force and the shaking moment. To make the contribution due to the shaking force and the shaking moment towards the objective function approximately equal in the beginning, the shaking force is multiplied by a weightage factor of 40. The various results are shown in Table 5.9. In this table the results are also given when the coupler extensions are not provided and only two circular counterweights, one at the crank and the other at the follower ends, are used. In both the cases when full force balance is achieved the maximum shaking moment, the maximum bearing reaction and the maximum input torque have all increased compared to an unbalanced mechanism. However, by putting constraint on the shaking force, the bearing reaction and the input end torque, they can be restricted to be within a desired value but at the expense of achieving only partial force balance.

In another example the extensions of the coupler are taken as circular sectors in place of rectangular bars. The radii and the angles of the sectors are taken as variables. Two circular weights are taken at the crank and follower ends as before. The center of each circular weight is assumed to be at 180° with respect to the line of joints of the

Table 5.9 Results of Shaking Force Optimization Using Counterweights- I

OBJECTIVE FUNCTION	CONSTRAINTS	ENDS COUNTER WEIGHTS RADII ** CRANK	FOLLOWER	ANG.POSITION* CRANK	FOLLOWER	LENGTH OF** BAR TYPE WTS. COUPLER L.END	R.END	MAXIMUM SHAKING FORCE (lb)	MAXIMUM SHAKING MOMENT (lb in)	MAXIMUM BEARING REACTION (lb)	MAXIMUM INPUT TORQUE (lb in)
WITHOUT COUNTERWEIGHTS	-	-	-	-	-	-	-	282	5163	311	175+
INITIAL	-	2.00	2.00	3.14	3.14	2.00	2.00	308	6009	354	200+
SHAKING FORCE	-	4.82	7.30	3.15	3.15	-2.49	-4.46	1	9155	525	326+
SHAKING FORCE	SM<6100 BR<380, T<2100	5.13	5.76	3.05	3.23	1.86	-0.00	64	5712	356	2100
SHAKING FORCE	SM<5500 BR<350, T<1800	5.54	3.42	2.96	3.19	2.50	-0.04	135	4742	314	1798
SHAKING FORCE AND MOMENT	-	4.77	7.14	3.16	3.66	-1.77	-0.12	4	7264	430	2622
SHAKING FORCE (USING 2-WTS.)	-	4.53	7.70	3.13	2.32	-	-	2	8189	461	291+
SHAKING FORCE (USING 2-WTS.)	SM<5500 BR<350, T<1800	5.35	3.19	2.89	3.22	-	-	139	4798	298	179+
SHAKING FORCE (USING 2-WTS.)	SM<6100 BR<380, T<2100	4.91	5.70	3.05	3.16	-	-	64	5648	343	2092
SHAKING F. AND M. (USING 2-WTS.)	-	4.50	7.03	3.15	3.54	-	-	3	7125	410	254+
FULLY FORCE BALANCED	-	4.52	6.81	3.14	3.14	-	-	1	6835	396	244+

* in radians ** in inches

respective link and the circumference passing through the center of the joint (the complete system is shown in Fig. 5.11). The radii of these circular weights are taken as variables. The optimization results for various cases are given in Table 5.10. The results are similar to ones obtained with bar type weights at the coupler ends.

Table 5.11 shows the effect of adding arbitrary masses at the ends of the links of the mechanism A on the stresses in the links and on the contribution of KED inertia towards the shaking force etc. The stress analysis is made with an assumed value of damping ratio of 0.05 and angular interval is taken as 5^{o}. The first row contains the maximum link stresses and the maximum shaking force etc. when there are no counterweights attached to the ends of the links. The rows that follow the first row show the maximum stresses and the maximum shaking force etc. when a counterweight is attached in turn to the end of each link. The counterweight attached to the coupler ends is circular sector having radius as indicated in the table and the angle of the sector is one radian. The counterweight placed at the crank or the follower end is circular with its center at 180^{o} with respect to the line of joints and circumference passing through the center of the joint. The addition of counterweight at the crank end produces a reduction in the shaking force, particularly that one which is

Table 5.10 Results of Shaking Force Optimization Using Counterweights-II

OBJECTIVE FUNCTION		CONSTRAINTS	RADII OF ENDS COUNTERWEIGHTS (in)				SECTOR ANGLE (rad)		MAXIMUM SHAKING FORCE (lb)	MAXIMUM SHAKING MOMENT (lb in)	MAXIMUM BEARING REACTION (lb)	MAXIMUM INPUT TORQUE (lb in)
			CRANK	COUPLER LEFT	COUPLER RIGHT	FOLLOWER	LEFT END	RIGHT END				
WITHOUT COUNTERWEIGHTS		-	-	-	-	-	-	-	282	5163	311	1764
SHAKING FORCE AND MOMENT	INITIAL	-	2.00	2.00	2.00	2.00	3.14	3.14	308	6018	355	2003
	OPTM.	-	5.87	-2.79	0.18	6.87	3.86	3.96	1	7016	492	2522
SHAKING FORCE	INITIAL	SM<6100 BR<380 T<2100	2.00	2.00	2.00	2.00	3.14	3.14	308	6018	355	2003
	OPTM.		5.21	-1.14	0.09	5.70	3.64	2.33	70	5490	358	2100

Table 5.11 Effect of Counterweights

RADII OF ENDS COUNTERWEIGHTS(in)				MAXIMUM SHAKING FORCE (lb)		MAXIMUM SHAKING MOMENT (lb in)		MAXIMUM INPUT END TORQUE(lb in)		MAXIMUM STRESSES IN LINKS(lb/sq in)		
CRANK	COUPLER LEFT	COUPLER RIGHT	FOLLOWER	RB ONLY	KED ONLY	RB ONLY	KED ONLY	RB ONLY	KED ONLY	CRANK	COUPLER	FOLLOWER
0.0	0.0	0.0	0.0	282	247	5163	6476	1822	241	-4396	-2506	1500
5.0	0.0	0.0	0.0	185	228	4350	6706	1822	792	-9014	-2703	2353
0.0	5.0	0.0	0.0	352	368	5827	5472	1934	1059	-4640	-1875	1625
0.0	0.0	5.0	0.0	448	443	10503	4092	3559	297	12800	1248	1486
0.0	0.0	0.0	5.0	197	585	5767	9404	1922	923	-4919	-2500	4926

due to rigid body (RB) inertia, but the maximum stress in the crank is increased. The addition of counterweight at the follower end causes a reduction in the maximum shaking force due to rigid body inertia but the maximum shaking force, the maximum shaking moment and the maximum input torque due to RED inertia are increased. The maximum stress in the follower is also increased. The addition of counterweights of the amount indicated at the coupler ends has adverse effect on balancing of the mechanism but it produces a reduction in the maximum stress in the coupler.

5.3 Optimization Results

5.3.1 First Problem

The example chosen for this problem is a crank rocker mechanism to guide a rigid body through three given positions. The following data is assumed:

When the crank is turned through 30° and 90° from some initial reference position, the rigid body is displaced in the x-direction and y-direction by an amount -7.0" and 2.0" and -20.0" and -4.0", respectively, from some initial position. The initial cross-section of the crank is taken as 3" x 1" and that of the coupler and follower as 2" x 1". The cross-sectional area of the each link is varied by taking a variable in the design vector which is used to divide the initial width of the link to determine width at

a new design point. The width to the thickness ratio is maintained as 2 unless the thickness is reduced to the extent of 0.2", when it is kept constant at 0.2" and in this case only the width is allowed to vary. The upper bound on the maximum link stresses is taken as 1500 lb/sq in. Since the coupler point, where the body to be guided is attached, comes out to be very close to the line of joints of the coupler (distance l_6 in Fig. 5.12) initially as well in the final design for this example, the effect of coupler extension is neglected during the KED analysis to reduce the computational time.

Table 5.12 shows the initial design and the optimum design with and without including the effect of KED inertia. The objective function in both the cases is the shaking force. The maximum shaking force, the maximum shaking moment and the maximum input end torque are reduced by approximately 1/15th, 1/8th and 1/11th times the original values, respectively, for the case in which the contribution due to KED inertia is included along with the contribution due to rigid body inertia towards the shaking force etc. This reduction is partly achieved due to a change in the link lengths and partly due to a reduction in the link cross-sectional areas. The stress constraints are far from being active. Here apparently, one may think that since the link stresses are small compared to the allowable limit,

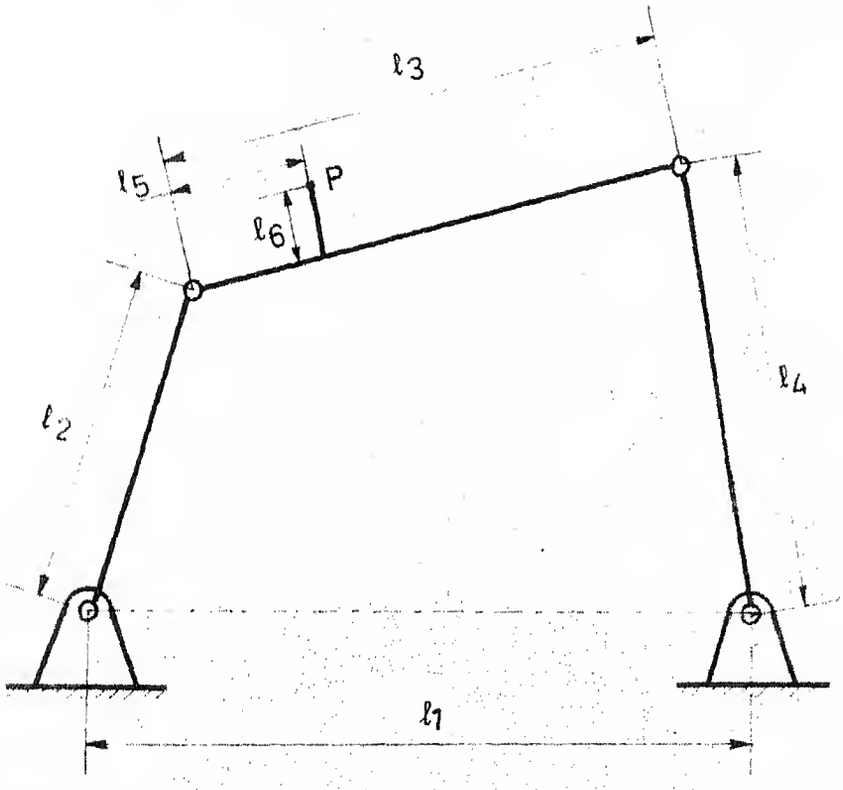

Fig 5.12 Four-Bar Mechanism of Problem-I
(Rigid Body Guidance)

Table 5.12 Optimization Results-Problem I(a) and (b)

CASE		LINK LENGTHS (in.)				COUPLER EXTENSION		CROSS-SECTIONS OF LINKS (inxin)			MAXIMUM STRESSES IN LINKS (lb/sq in)			MAXIMUM SHAKING FORCE (lb)	MAXIMUM SHAKING MOMENT (lb in)	MAXIMUM INPUT TORQUE (lb in)
		GROUND	CRANK	COUPLER	FOLLOWER	X (in)	Y (in)	CRANK	COUPLER	FOLLOWER	CRANK	COUPLER	FOLLOWER			
WITH KED	INIT.	26.26	14.42	29.28	21.26	6.35	-2.62	3.00 1.00	2.00 1.00	2.00 1.00	-5978	-1371	945	2699	26666	16853
	OPT.	32.80	14.41	31.80	21.36	8.65	1.20	1.44 0.48	0.96 0.48	0.96 0.48	-3560	-4176	2108	175	3294	1528
WITHOUT KED	INIT.	26.26	14.42	29.28	21.26	6.35	-2.62	3.00 1.00	2.00 1.00	2.00 1.00	-5978	-1371	922	1264	21988	16893
	OPT.	33.59	14.42	33.12	23.70	7.57	-0.51	0.60 0.20	0.40 0.20	0.40 0.20	-11120	-9695	8585	31	513	261

one may reduce the area of cross-section further and achieve a further reduction in the shaking force. No doubt reducing the link cross-sectional areas further may reduce the contribution due to the rigid body inertia towards the shaking force etc. but the contribution due to KED inertia towards the shaking force may increase due to high elastic accelerations because of slender links. This fact is depicted in Table 5.13 where results are given when the link cross-sectional areas are changed arbitrarily at the optimum design point. There appears to be two local minima close to each other. The significance of these local minima can be explained as follows. Around the first local minimum the reduction in the shaking force due to rigid body (RB) inertia is less compared to the increase in it due to the KED inertia when link cross-sectional areas are reduced at first. However, the reduction in the shaking force due to RB inertia again over compensates the increase in the shaking force due to KED inertia when link cross-sectional areas are further reduced about the first local minimum giving another minimum close to the first one. Around the second local minimum the increase in the shaking force due to KED inertia, when link cross-sectional areas are reduced, is more pronounced and the net shaking force increases for ever. It can also be observed from Table 5.13 that the maximum link stresses increase with decrease in the link

Table 5.13 Effect of Arbitrary Variation in Links Areas at Final Optimum Design - Problem I(a)

CASE	AREA REDUCTION FACTOR	MAXIMUM SHAKING FORCE (lb)	MAXIMUM SHAKING MOMENT (lb in)	MAXIMUM INPUT END TORQUE (lb in)	MAXIMUM STRESSES IN LINKS (lb/sq in)		
					CRANK	COUPLER	FOLLOWER
OPTIMUM	10.42	177	3257	1531	-3592	-4226	2138
ARBITRARY VARIATION IN AREA REDUCTION FACTOR WITH SMALLER VARIATION NEAR OPTIMUM	9.50	367	4554	1732	-3673	-3397	1461
	10.00	346	3449	1660	-3430	-3961	1896
	10.30	185	3343	1582	-3463	-4175	2079
	10.40	177	3277	1539	-3568	-4221	2129
	10.50	182	3136	1493	-3705	-4253	2174
	10.60	179	2922	1445	-3855	-4275	2215
	10.70	170	2658	1399	-3998	-4287	2251
	10.80	162	2598	1356	-4123	-4291	2283
	10.90	167	2590	1317	-4236	-4290	2309
	11.00	171	2572	1283	-4344	-4285	2330
	11.50	236	3759	1173	-4740	-4237	2352
	12.00	283	4780	1077	-5061	-4292	2353

cross-sectional areas. The progress of optimization process is shown in Table 5.14. It can be observed that the process is first converged to an optimum design without any significant change in the link cross-sectional areas. One of the Grashof constraints becomes active. Thus at first the reduction in the shaking force is only due to a change in the link lengths. At this design point arbitrary variation in the area reduction factor is made and the effect is observed. The results, which are shown in Table 5.15, indicate that a further reduction in shaking force is possible by a reduction in the link cross-section areas. Therefore, the problem is further optimized starting from the first optimum design point. However to save computational time the link cross-sectional areas at the initial point are arbitrarily reduced to halves of their values at the first optimum design point. The progress of this optimization process is also shown in Table 5.14. The fact that optimum design thus obtained is a final one has already been explained with the help of results shown in Table 5.13.

When the effect of KED inertia is not taken into account the maximum shaking force, the maximum shaking moment and the maximum input torque continue to decrease till one or more stress constraints become active. The progress of optimization process is shown in Table 5.16. Here also it can be observed that at first the reduction

Table 5.14 Details of Optimization Progress - Problem-1(a)

OPTIMIZATION STEP	PENALTY PARAMETER	AREA REDUCTION FACTOR	OBJECTION FUNCTION	ϕ FUNCTION	MIN.* TRANSMISSION ANGLE	CONSTRAINTS BASED ON GRASHOF CRITERIA |G1|	|G2|	|G3|	MAXIMUM STRESSES IN LINKS (lb/sq in) CRANK	COUPLER	FOLLOWER
INITIAL	50.0	5.00	2699	3850	21.1	0.493	0.191	0.592	-5978	-1371	945
FIRST	50.0	4.98	677	1602	37.6	0.148	0.546	0.772	-1922	-732	526
SECOND	5.0	4.99	598	708	34.0	0.101	0.538	0.785	-1769	-749	390
THIRD	0.5	5.01	562	577	26.7	0.061	0.524	0.797	-1626	-731	-457
FOURTH	0.05	5.01	539	540	24.8	0.050	0.528	0.823	-1499	-713	-548
INITIAL	10.0	10.0	222	564	24.3	0.051	0.530	0.832	-3391	-1772	1177
FIRST	10.0	10.42	177	341	33.7	0.302	0.397	0.922	-3592	-4228	2138
SECOND	1.0	10.42	175	191	33.8	0.298	0.398	0.920	-3560	-4176	2108

* in degrees

Table 5.15 Effect of Arbitrary Variation in Links Areas at the First Optimum Design - Problem 1(a)

AREA REDUCTION FACTOR	MAXIMUM SHAKING FORCE (lb)		MAXIMUM SHAKING MOMENT (lb in)		MAXIMUM INPUT END TORQUE (lb in)		MAXIMUM STRESSES IN LINKS (lb/sq in)		
	RB ONLY	KED ONLY	RB ONLY	KED ONLY	RB ONLY	KED ONLY	CRANK	COUPLER	FOLLOWER
4.0	991	257	13037	3346	7639	298	-1179	-581	-461
4.5	783	222	10301	2822	6036	147	-1553	-666	-488
5.0	635	184	8345	5491	4889	467	-1443	-727	-551
5.5	524	172	6896	1010	4041	288	-1642	-766	-568
6.0	440	228	5794	4115	3395	525	-1929	-759	670
7.0	324	206	4257	3546	2494	342	-1976	-1121	704
8.0	248	81	3259	755	1910	143	-2824	-1325	1006
9.0	196	106	2575	1950	1509	243	-3047	-1437	1167
10.0	159	107	2086	1054	1222	108	-3331	-1723	1161
11.0	131	107	1724	1368	1010	147	-3067	-1767	1258
12.0	110	74	1449	930	849	95	-3954	-2022	1466

Table 5.16 Details of Optimization Progress - Problem I(b)

OPTIMIZATION STEP	PENALTY PARAMETER	AREA REDUCTION FACTOR	OBJECTIVE FUNCTION	ϕ FUNCTION	* MIN. TRANSMISSION ANGLE	CONSTRAINTS BASED ON GRASHOF CRITERIA			MAXIMUM STRESSES IN LINKS (lb /sq in)		
						|G1|	|G2|	|G3|	CRANK	COUPLER	FOLLOWER
INITIAL	50.0	5.00	1269	2421	20.1	0.493	0.192	0.592	5978	-1371	922
FIRST	50.0	5.16	660	1476	36.2	0.221	0.530	0.817	-1931	-829	730
INITIAL	50.0	1.00	702	1519	36.2	0.219	0.530	0.817	-1792	-822	590
FIRST	50.0	1.94	217	1020	31.7	0.329	0.430	0.800	-4244	-3197	2167
RESTART	50.0	2.51	128	825	38.7	0.579	0.522	1.430	-4692	-6695	2192
SECOND	5.0	3.91	50	125	38.7	0.517	0.539	1.240	-4814	-8066	4421
THIRD	0.5	5.01	31	40	34.7	0.441	0.488	0.959	-11120	-9695	5688

* in degrees

in shaking force is due to a change in the link lengths and there is no appreciable change in the link cross-sectional areas. The area reduction factor is then scaled down and the problem is further optimised. At the final optimum design point the link stresses are close to the allowable limit. Observing the trend from the table it can be expected that any further reduction in areas of the links will cause the link stresses to cross the allowable limit. The link areas at the optimum design point are much smaller in this case than those in which the effect due to KED inertia is also included.

5.3.2 Second Problem.

The shaking force is minimized for mechanism A when it is running at 300 rpm. The initial cross-section of the crank is taken as 1.5" x 0.5" and that of the coupler and the follower as 1.0" x 0.5". Two circular counterweights are taken one at the crank and the other at the follower end with their centres at 180^{o} with respect to the line of pivots of the respective links. The circumference of the counter-weights passes through the center of the respective fixed pivots. Two sector type counterweights are taken one each at the two ends of the coupler. The complete arrangement is indicated in Fig. 5.11. The design variables are the radii of the four weights and the angles of the sectors. The variation in the link areas is achieved by taking a variable

in the design vector and dividing the width of the each link by this variable at each design point. The ratio of the width to the thickness is maintained at 2 till the thickness is reduced to 0.2" at which stage it is taken as a constant (0.2") and only the width is allowed to vary. The thickness of the each counterweight is taken equal to the thickness of the link to which it is attached. Non-negativity constraints on the sector angles are imposed. Also the sector angles are not allowed to increase beyond 2π by putting constraints. The upper bound on the maximum stresses in the links is taken as 1500 psi. The initial radii of the counterweights are taken as 2" and the sector angles as one radian.

The results of optimization are shown in Table 5.17 with and without KED inertia effects. The objective function in both the cases is the maximum shaking force. The reduction achieved at the optimum design in the maximum shaking force, the maximum shaking moment and the maximum input torque is approximately 80%, 56% and 66% of their original values, respectively, when the contribution due to KED inertia is taken into account. The change in the radii of the counterweights is very little (except the radius of the counterweight attached to the crank end) at the optimum design compared to their values at the initial design point. However, the reduction in shaking force at the optimum design point cannot be claimed only due to the reduction in cross-

Table 5.17 Optimization Results – Problem II(a) and (b)

CASE		RADII OF ENDS COUNTERWEIGHTS (lb)				SECTOR ANGLE (rad)		CROSS SECTIONS OF LINKS (in x in)			MAXIMUM STRESSES IN LINKS (lb/sq in)			MAX. SHAKING FORCE (lb)	MAX. SHAKING MOMENT (lb in)	MAX. INPUT TORQUE (lb in)
		CRANK	COUPLER LEFT	COUPLER RIGHT	FOLLOWER	LEFT END	RIGHT END	CRANK	COUPLER	FOLLOWER	CRANK	COUPLER	FOLLOWER			
WITH KED	INIT.	2.00	2.00	2.00	2.00	1.00	1.00	1.50 0.50	1.00 0.50	1.00 0.50	1869	-2473	1843	254	4497	1025
	OPT.	1.69	2.17	2.08	1.90	1.30	1.19	0.84 0.28	0.56 0.28	0.56 0.28	-6767	-4035	4426	56	1963	363
WITHOUT KED	INIT.	2.00	2.00	2.00	2.00	1.00	1.00	1.50 0.50	1.00 0.50	1.00 0.50	-1830	-2469	1848	149	2826	981
	OPT.	0.01	0.01	-0.05	2.87	3.27	3.16	0.45 0.20	0.30 0.20	0.30 0.20	-12590	12160	12870	17	296	99
*		3.19	0.00	0.00	4.56	0.00	0.00	0.45 0.20	0.30 0.20	0.30 0.20	-14260	-12610	28800	0.3	366	139

* with counterweights that give full force balance

sectional areas of the links. This fact is made clear by determining the maximum shaking force, the maximum shaking moment and the maximum stresses in the links when the link cross-sectional areas are reduced arbitrarily without any counterweight attached to the links. The results are shown in Table 5.18. It can be observed that the shaking force does not decrease below a value of about 140 lb. However, with counterweights the optimum value of the shaking force attained is 56 lb. Any further reduction in the link cross-sectional areas at the optimum design point does not produce a reduction in the maximum shaking force. In fact the shaking force ever increases when the link cross-sectional areas are reduced from the optimum value with the optimum set of counterweights. These results are shown in Table 5.19. The progress of optimization progress for this case is shown in Table 5.20.

In the second case, in which the contribution due to KED inertia towards the shaking force is not included, the reduction in the maximum shaking force is achieved partly due to the adjustment in the counterweight parameters and partly due to a reduction in the link areas. The progress of optimization process is shown in Table 5.20. It can be observed that the link stresses are approaching to their constraint boundaries near the optimum design point. Thus a further reduction in the link areas may cause a reduction in the shaking force but the link stresses may cross the upper

Table 5.18 Effect of Arbitrary Variation in Links Areas of Original Mechanism - Problem II (a)

CASE	AREA REDUCTION FACTOR	MAXIMUM SHAKING FORCE (lb)	MAXIMUM SHAKING MOMENT (lb in)	MAXIMUM INPUT END TORQUE (lb in)	MAXIMUM STRESSES IN LINKS (lb/sq in) CRANK	COUPLER	FOLLOWER
ARBITRARY VARIATION IN LINKS CROSS SECTIONAL AREAS OF ORIGINAL MECHANISM (WITHOUT COUNTER-WEIGHTS)	1.00	165	3710	567	- 2485	- 2477	1586
	1.25	210	3327	555	- 3436	- 3375	2358
	1.50	201	2295	450	- 2673	4232	3064
	1.60	233	-	-	- 4140	4880	3261
	1.70	141	4687	-	- 7455	- 5032	4507
	1.75	319	5201	352	6623	8568	4654
	1.80	287	4781	324	- 5593	7810	5058
	1.90	200	4525	293	- 6769	5394	4193
	2.00	140	4704	237	- 7367	- 5008	4391
	2.05	141	4687	-	- 7455	- 5032	4507
	2.10	170	4456	225	7805	5609	4780
	2.20	315	3986	220	13120	10010	6287

Table 5.19 Details of Optimization Progress - Problem II(a)

OPTIMIZATION STEP	PENALTY PARAMETER	AREA REDUCTION FACTOR	OBJECTIVE FUNCTION	Φ FUNCTION	RADII OF ENDS COUNTERWEIGHTS (in)				SECTOR ANGLE(rad)		MAXIMUM STRESSES IN LINKS (lb/sq in)		
					CRANK	COUPLER LEFT	COUPLER RIGHT	FOLLOWER	LEFT END	RIGHT END	CRANK	COUPLER	FOLLOWER
INITIAL	10.0	1.00	254	470	2.00	2.00	2.00	2.00	1.00	1.00	1869	-2473	1843
FIRST	10.0	1.62	76	268	1.89	2.36	1.98	1.89	1.43	1.06	-5334	-3900	3709
REST-ART	10.0	1.71	60	249	1.68	2.21	2.09	1.89	1.30	1.19	-5990	-3931	3828
SECOND	1.0	1.72	59	78	1.66	2.22	2.10	1.88	1.32	1.20	-6821	-3992	4003
REST-ART	1.0	1.70	61	80	1.65	2.23	2.11	1.87	1.33	1.22	-6520	-3963	3897
THIRD	0.1	1.785	57	59	1.68	2.19	2.09	1.87	1.30	1.19	-6443	-3954	4145
RESTA-RT	0.1	1.786	56	58	1.69	2.17	2.08	1.90	1.30	1.19	-6767	-4035	4426
RESTA-RT	0.1	1.787	60	62	1.69	2.16	2.07	1.91	1.30	1.19	-6778	-4021	4439

Table 5.20 Details of Optimization Progress - Problem II(b)

CASE	AREA REDUCTION FACTOR	MAXIMUM SHAKING FORCE (lb)	MAXIMUM SHAKING MOMENT (lb-in)	MAXIMUM INPUT END TORQUE (lb-in)	MAXIMUM STRESSES IN LINKS (lb/sqin) CRANK	COUPLER	FOLLOWER
OPTIMUM	1.79	58	1963	63	6766	-4028	4284
ARBITRARY VARIATION IN AREA REDUCTION FACTOR NEAR OPTIMUM	1.60	103	3715	460	-5421	-3790	3592
	1.65	88	2479	462	-6239	-3895	3744
	1.70	70	1919	438	-6559	-3977	3944
	1.75	65	1512	400	-6863	-3987	4223
	1.80	73	2266	356	-6874	-4066	4440
	1.85	124	4153	341	-6644	4850	4935
	1.90	133	4904	363	-5902	6026	5396
	1.95	159	5048	348	-4429	6854	5501
	2.00	180	5322	324	3649	7609	5335
	2.10	206	5375	307	4720	8483	5145
	2.20	227	4913	321	-2114	9570	9011
	2.40	460	8595	267	21200	22090	-19700

limit. The counterweight at the crank end reduces to nearly zero, which is contrary to the earlier observations shown in Tables 5.9 and 5.10, where the shaking force due to rigid body inertia only is minimized without stress constraints. This is because that the counterweight at the crank end causes an increase in its stress, on which a constraint has been imposed, thus it does not allow a counterweight to be present at that end. As such, it is not possible to achieve full force balance by redistribution of link masses when stress constraints are present.

In the last row of Table 5.17, the results are presented when the counterweights, determined according to the method presented by Berkof and Lowen [6], are attached to the crank and the coupler ends to achieve full force balance The maximum shaking force becomes practically zero but the maximum shaking moment and maximum input torque are 20% and 40% more than their values at the optimum design point obtained using the present procedure. Moreover the maximum stress in the follower is very high and has surpassed the allowable limit.

CHAPTER VI

CONCLUSIONS AND PROPOSALS FOR FUTURE WORK

2.1 Conclusions

In the present work only one example in each of the two types of the procedures to achieve balance in a planar mechanism has been solved. Since it takes a long computational time to solve each problem (about 60 min. of CPU time on the average on DEC 1090), it is not feasible to solve many examples. However, the results of the numerical example in the each category can be interpreted to give general conclusions for not only a four bar planar mechanism but for any planar mechanism in general. The following conclusions are drawn from the results of the two numerical examples solved.

(1) It is extremely important to take into account the contribution due to KED inertia towards the shaking force and the shaking moment to achieve a balance in mechanisms with elastic links in a real sense.

(2) The inclusion of the effect of the KED inertia limits the amount of balance that can be achieved.

(3) It is not possible to achieve full force or/and full moment balance by redistribution of the link masses

because the contribution due to KED inertia towards the shaking force and the shaking moment cannot be completely balanced by any combination of counterweights. However, a reduction in the shaking force and/or shaking moment due to KED inertia is possible by using a suitable set of the counterweights.

(4) When the effect of KED inertia is not included and the mechanism is fully force balanced using suitable counterweights the dynamic stresses produced in the links are very high because of the increased inertia of the links. Thus a kinetoelastodynamic analysis must be made to determine the link stresses when a mechanism with elastic links is to be fully force balanced using counterweights even if the contribution due to KED inertia towards the shaking force is neglected.

(5) It was established by Conte and his group [15] that the shaking force, shaking moment and input end torque due to rigid body inertia forces could be reduced by altering the kinematic design. The present study reveals that this procedure is also effective in reducing the contribution due to KED inertia towards the shaking force, shaking moment and input end torque.

(6) The reduction in the link areas is very effective in minimizing the unbalance in the mechanisms. However, the link stresses must be determined at each stage to check that they do not cross the allowable limit.

(7) When the contribution due to KED inertia towards the shaking force and the shaking moment is not included, the link cross-sectional areas continue to decrease with the unbalance in the mechanism becoming smaller and smaller till one or more of the link stresses approach the allowable limit.

(8) The assumption made in determining the gradients of the various function as outlined in Chapter V has worked well. It has reduced the computational time considerably for the second problem in which the maximum values of the various functions occur mostly during the first quarter part of the motion cycle of the mechanism. However, for the first problem, at the latter stages of optimization process, the maximum values of some of the functions occur during the last quarter of the motion cycle of the mechanism therefore the analysis has to be carried out till the end of the complete cycle of motion for most of the time. Thus there is very little saving in computational time in this case.

(9) The use of the gradients of the link stresses and maximum shaking force to predict them at a new design point during one dimensional minimization has successfully worked. This has also resulted in a considerable saving in the computational time.

2.2.2 Second Category

Under the second category the following suggestions are proposed.

(a) In the present work only one design variable is used to make a change in the area of all the links to save the computational time by limiting the number of design variables as far as possible. However, the maximum stress developed in a link and the contribution due to KED inertia of a link towards the shaking force and shaking moment are different for different links. Therefore to be more realistic, the variation in the area of each link must be independently made. Moreover, the ratio of the width to the thickness of a link is taken a constant (2 in the present study). For a mechanism of given link lengths and input crank speed the rigid body inertia forces depend only on the link cross-sectional areas and are independent of the shape of the link cross-sections. On the other hand, the KED inertia forces depend on the shape of the link cross-sections since the elastic deformations and as such the elastic accelerations depend on them. Thus, the width to the thickness ratio of each link may also be allowed to vary or some other shape of the link cross-sections may be chosen to arrive at a better design.

2.2.2 Second Category

Under the second category the following suggestions are proposed.

(a) In the present work only one design variable is used to make a change in the area of all the links to save the computational time by limiting the number of design variables as far as possible. However, the maximum stress developed in a link and the contribution due to KED inertia of a link towards the shaking force and shaking moment are different for different links. Therefore to be more realistic, the variation in the area of each link must be independently made. Moreover, the ratio of the width to the thickness of a link is taken a constant (2 in the present study). For a mechanism of given link lengths and input crank speed the rigid body inertia forces depend only on the link cross-sectional areas and are independent of the shape of the link cross-sections. On the other hand, the KED inertia forces depend on the shape of the link cross-sections since the elastic deformations and as such the elastic accelerations depend on them. Thus, the width to the thickness ratio of each link may also be allowed to vary or some other shape of the link cross-sections may be chosen to arrive at a better design.

(b) The KED analysis is made by considering the contribution due only to rigid body inertia forces towards the load vector. The additional inertia forces produced due to vibration of the links are not included in the load vector for displacement analysis. A more realistic approach be made by taking into account the contribution due to vibrational inertia forces towards the load vector used in making KED analysis.

2.2.3 Third Category

The effect of KED inertia forces on the unbalance in other planar mechanisms may be investigated and the effectiveness of the present procedure in arriving at an optimum design be determined.

REFERENCES

1. Sherwood, A.A., 'The Optimum Distribution of Mass in the Coupler of a Plane Four Bar Linkage', J. Mechanism, Vol. 1, 1966, pp 229-234.

2. Sherwood A.A. and Hockey B.A., 'The Optimisation of Mass Distribution in Mechanism Using Dynamically Similar Systems', J. Mechanism, Vol. 4, 1969, pp 243-260.

3. Skreiner M., 'Dynamic Analysis Used to Complete the Design of a Mechanism', J. Mechanism, Vol. 5, 1970, pp 105-119.

4. Hockey B.A., 'An Improved Technique for Reducing the Fluctuation of Kinetic Energy in Plane Mechanisms', J. Mechanism, Vol. 6, 1971, pp 405-418.

5. Hockey B.A., 'The Minimization of the Fluctuation of Input Shaft Torque in Plane Mechanisms', Mechanism and Machine Theory, Vol. 7, 1972, pp 335-346.

6. Berkof R.S. and Lowen G.G., 'A New Method of Complete Force Balancing of Simple Linkages', Trans. ASME, J. Engng. Ind., Vol. 91, 1969, pp 21-26.

7. Lowen G.G. and Berkof R.S., 'Survey of Investigations into the Balancing of Linkages', J. Mechanism, Vol. 3, 1968, pp 221-231.

8. Han C.Y., 'Balancing of High Speed Machinery', Trans. ASME, J. Engng. Ind., Vol. 89, 1967, pp 111-128.

9. Berkof R.S. and Lowen G.G., 'Theory of Shaking Moment Optimization of Force Balanced Four Bar Linkage', Trans. ASME, J. Engng. Ind., Vol. 93, 1971, pp 53-60.

10. Lowen G.G. and Berkof R.S., 'Determination of Force Balanced Four Bar Linkages with Optimum Shaking Moment Characteristics', Trans. ASME, J. Engng. Ind., Vol. 93, 1971, pp 39-46.

11. Kaufman R. E. and Sandor G.N., 'Complete Force Balancing of Spatial Linkages', Trans. ASME, J. Engng. Ind., Vol. 93, 1971, pp 620-626.

12. Tepper F. R. and Lowen G.G., 'General Theorems Concerning Full Force Balancing of Planar Linkages by Internal Mass Redistribution', Trans. ASME, J. Engng. Ind., Vol. 94, 1972, pp 789-796.

13. Berkof R.S. 'Complete Force and Moment Balancing of Inline Four-Bar Linkage', Mechanism and Machine Theory, Vol. 8, 1973, pp 397-410.

14. Tepper F.R. and Lowen G.G., 'Shaking Force Optimization of Four Bar Linkage with Adjustable Constraints on Ground Bearing Forces', Trans. ASME, J. Engng. Ind., Vol. 97, 1975, pp 643-651.

15. Conte F.L., George G.R., Mayne R.W. and Sadler J.P., 'Optimum Mechanism Design combining Kinematic and Dynamic Force Considerations', Trans. ASME, J. Engng. Ind., Vol. 97, 1975, pp 662-670.

16. Wiederrich J.L. and Roth B., 'Momentum Balancing of Four-Bar Linkages', Trans. ASME, J. Engng. Ind., Vol. 98, 1976, pp 1289-1295.

17. Elliott J.L. and Tesar D. 'The Theory of Torque, Shaking Force, and Shaking Moment Balancing of Four Link Mechanisms', Trans. ASME, Vol. 99, 1977, pp 715-722.

18. Walker M.J. and Oldham K., 'A General Theory of Force Balancing Using Counterweights', Mechanism and Machine Theory, Vol. 13, 1978, pp 175-185.

19. Carson W.L. and Stephens J.M., 'Feasible Parameter Design Spaces for Force and Root-Mean-Square Moment Balancing an In-line 4R 4-Bar Synthesized for Kinematic Criteria', Mechanism and Machine Theory, Vol. 13, 1978, pp 649-658.

20. Balasubramanian S. and Bagci C., 'Design Equations for the Complete Shaking Force Balance of 6R 6-Bar and 6-Bar Slider Crank Mechanisms', Mechanism and Machine Theory, Vol. 13, 1978, pp 659-674.

21. Walker M.J. and Oldham K., 'Extensions to the Theory of Balancing Frame Forces in Planar Linkages', Mechanism and Machine Theory, Vol. 14, 1979, pp 201-207.

22. Bagci C., 'Shaking Force Balancing of Planar Linkages with Force Transmission Irregularities Using Balancing Idler Loops', Mechanism and Machine Theory, Vol. 14, 1979, pp 267-284.

23. Erdman A.G. and Sandor G.N., 'Kineto-Elastodynamic - A Review of the State of the Art and Trends', Mechanism and Machine Theory, Vol. 7, 1972, pp 19-33.

24. Winfrey R.C. 'Elastic Link Mechanism Dynamics', Trans. ASME, J. Engng. Ind., Vol. 93, 1971, pp 268-272.

25. Erdman A.G., Sandor G.N. and Oakberg R.C., 'A General Method for Kineto-dynamic Analysis and Synthesis of Mechanisms', Trans. ASME, J. Engng. Ind., Vol. 94, 1972, pp 1193-1205.

26. Erdman, A.G., Imam I. and Sandor G.N., 'Applied Kineto-elastodynamics', Proceedings of the Second OSU Applied Mechanisms Conference, Stillwater.

27. Imam I., Sandor G. N. and Kramer S.N., 'Deflection and Stress Analysis in High Speed Planar Mechanisms with Elastic Links', Trans. ASME, J. Engng. Ind., Vol. 95, 1973, pp 541-548.

28. Hurty W.C. and Rubinstein M.F., 'Dynamic of Structure', Prentice-Hall, N.J., 1966.

29. Imam I. and Sandor G.N., 'A General Method of Kineto-Elastodynamic Design of High Speed Mechanisms', Mechanism and Machine Theory, Vol. 8, 1973, pp 497-516.

30. Imam I. and Sandor G.N., 'High Speed Mechanism Design - A General Analytical Approach', Trans. ASME, J. Engng. Ind., Vol. 97, 1975, pp 609-628.

31. Sadler J.P. and Sandor G.N., 'A Lumped Parameter Approach to Vibration and Stress Analysis of Elastic Systems', Trans. ASME, J. Engng. Ind., Vol. 95, 1973, pp 549-557.

32. Sadler J.P. and Sandor G.N., 'Non-linear Vibration Analysis of Elastic Four-Bar Linkages', Trans. ASME, J. Engng. Ind., Vol. 96, 1974, pp 411-419.

33. Alexander R.M. and Lawrence K.L., 'An Experimental Investigation of the Dynamic Response of an Elastic Mechanism', Trans. ASME, J. Engng. Ind., Vol. 96, 1974, pp 268-274.

34. Alexander R.M. and Lawrence K.L, 'Experimentally Determined Dynamic Strains in an Elastic Mechanism', Trans. ASME, J. Engng. Ind., Vol. 97, 1975, pp 791-794.

35. Nath P.K., 'Kinetoelastodynamic Analysis of High Speed Mechanisms', Ph.D. Dissertation, Indian Institute of Technology, Kanpur (India), 1976.

36. Sutherland G.H., 'Analytical and Experimental Investigation of a High Speed Elastic-Membered Linkage', Trans. ASME, J. Engng. Ind., Vol. 98, 1975, pp 788-794.

37. Meirovitch L.M., 'Analytical Methods in Vibration', 3rd Ed., Macmillan Company, New York, 1971.

38. Golebiewski E.P. and Sadler J.P., 'Analytical and Experimental Investigation of Elastic Slider-Crank Mechanisms', Trans. ASME, J. Engng. Ind., Vol. 98, 1976, pp 1266-1271.

39. Thompson B.S. and Barr A.D.S., 'A Variational Principle for the Elastodynamic Motion of Planar Linkages', Trans. ASME, J. Engng. Ind., Vol. 98, 1976, pp 1306-1312.

40. Jandarasits W.G. and Lowen G.G., 'The Elastic-Dynamic Behaviour of a Counterweighted Rocker Link with an Overhanging End Mass in a Four-Bar Linkage Part I: Theorem', Trans. ASME, J. Mechanical Design, Vol. 101, Jan. 1979, pp 77-78.

41. Jandarasits W.G. and Lowen G.G., 'The Elastic-Dynamic Behaviour of a Counterweighted Rocker Link with an Overhanging End Mass in a Four-Bar Linkage Part II: Application and Experiment', Trans. ASME, J. Mechanical Design, Vol. 101, Jan. 1979, pp 89-98.

42. Przemieniecki J.S., 'Theory of Matrix Structural Analysis', McGraw Hill Book Co., New York, 1968.

43. Zienkiewicz O.C., 'The Finite Element Method in Engineering Science,' 2nd Ed., McGraw Hill Book Co., New York, 1971.

44. Rubinstein M.F., 'Matrix Computer Analysis of Structures', Prentice Hall, Inc., 1966.

45. Grad J. and Brebner M.A., 'Eigenvalues and Eigenvectors of a Real General Matrix', Communication of the ACM, Vol. 11, 1968, pp 820-826.

46. Hartenberg R.S. and Denavit J., 'Kinematic Synthesis of Linkages', Mc-Graw-Hill Book Co., New York, 1964.

47. Hall A.S., 'Kinematic and Linkage Design', Balt Publishers, West Lafayette, Indiana, U.S.A., 1966.

48. Soni, A.H., 'Mechanism Synthesis and Analysis', McGraw Hill, New York, 1974.

49. Fox R.L. and Gupta, K.C. 'Optimization Technology as Applied to Mechanism Design', Trans. ASME, J. Engng. Ind., Vol. 95, 1973, pp 657-663.

50. Fox R.L., 'Optimization Methods for Engineering Design', 2nd Ed., Addison-Wesley Publishing Co., 1973.

51. Rao S.S., 'Optimization Theory and Applications', Wiley Eastern Limited, New Delhi, 1978.

52. Bagci C. and Kalaycioglu S., 'Elastodynamics of Planar Mechanism Using Planar Actual Finite Line Elements, Lumped Mass Systems, Matrix-Exponential Method, and the Method of 'Critical-Geometry Kineto-elasto-statics' (CGKES)', Trans. ASME, J. Mechanical Design, Vol. 101, 1979, pp 417-427.

53. Ralston A., 'A First Course in Numerical Analysis', McGraw-Hill, New York, 1965.

54. Sadler J.P. and Sandor G.N., 'Kineto-elastodynamic Harmonic Analysis of Four-Bar Path Generating Mechanisms', Presented at the 11th ASME Conference on Mechanisms, Columbus, Ohio, Nov. 1-4, 1970, ASME Paper No. 70-Mech-61.

55. Shigley, J.E., 'Dynamic Analysis of Machines', McGraw-Hill, New York, 1961.

56. Timoshenko S. and Young D.H., 'Advanced Dynamics', McGraw-Hill, New York, 1948.

57. Denavit J., Hartenberg, R.S., Razi R. and Uicker, J.J., Jr., 'Velocity, Acceleration and Static-Force Analysis of Spatial Linkages, Trans. ASME, J. Appl. Mech., Vol. 32, 1965, pp 903-910.

58. Uicker, J.J., Jr., 'Dynamic Force Analysis of Spatial Linkages', Trans. ASME, J. Appl. Mech., Vol. 34, 1967, pp. 418-424.

APPENDIX A

KINEMATIC ANALYSIS

A kinematic analysis is made to obtain positions, angular velocities and accelerations of the various links in a four bar mechanism when their values for input crank are given.

Referring to Fig. D.1(a), let l_1, l_2, l_3 and l_4 are the lengths of the crank, the coupler, the follower and the ground link, respectively, measured between their joint centers. θ_1, θ_2 and θ_3 are the angular positions of the crank, the coupler and the follower, respectively, measured in the counterclockwise direction with respect to X-axis as shown in Fig. D.1(a). The angular positions of the coupler and the follower are related to the crank position and link lengths as follows [53],

$$\cos\theta_2 = (A\,B + C_3\,C_6 C \sin\theta_1)/D$$

$$\sin\theta_2 = (A\,C_6 C - C_3 B \sin\theta_1)/D \qquad \text{(A-1)}$$

$$\cos\theta_3 = -E\cos\theta_2 + C\sin\theta_2$$

$$\sin\theta_3 = -E\sin\theta_2 - C\cos\theta_2$$

where

$$A = 1 - C_3\cos\theta_1$$

$$B = C_4 - C_5\cos\theta_1$$

$$C = \sqrt{[1 - (C_1 + C_2\cos\theta_1)^2]} \qquad \text{(A-2)}$$

...Contd.

$$D = C_3^2 - 2C_3 \cos\theta_1 + 1$$
$$E = C_1 + C_2 \cos\theta_1 \qquad \text{(A-2)}$$

and
$$C_1 = (l_2^2 + l_3^2 - l_1^2 - l_4^2)/2l_2l_3$$
$$C_2 = l_4l_1/l_2l_3$$
$$C_3 = l_1/l_4 \qquad \text{(A-3)}$$
$$C_4 = (l_1^2+l_2^2-l_3^2+l_4^2)/2l_2l_4$$
$$C_5 = l_1/l_2$$
$$C_6 = l_3/l_4$$

When the input crank runs at constant angular speed the angular velocities and accelerations of the coupler and the follower are given by

$$\omega_2 = \omega_1 l_1 \sin(\theta_1-\theta_3)/l_2\sin(\theta_2-\theta_3) \qquad \text{(A-4)}$$
$$\omega_3 = \omega_1 l_1 \sin(\theta_1-\theta_2)/l_3\sin(\theta_2-\theta_3)$$
$$\alpha_2 = -(l_1\omega_1^2 \cos(\theta_1-\theta_3) + l_2\omega_2^2 \cos(\theta_2-\theta_3) + l_3\omega_3^2)/ \omega l_2 \sin(\theta_2-\theta_3)$$
$$\alpha_3 = +(l_1\omega_1^2 \cos(\theta_1-\theta_2) + l_3\omega_3^2 \cos(\theta_2-\theta_3) + l_2\omega_2^2)/ l_3 \sin(\theta_2-\theta_3) \qquad \text{(A-5)}$$

where ω_1, ω_2 and ω_3 are the angular velocities of the crank, the coupler and the follower, respectively and α_2 and α_3 are the angular accelerations of the coupler and the follower, respectively.

APPENDIX B

ELEMENT MATRICES

The element stiffness matrix $\bar{k}$, mass matrix $\bar{m}$ and the load vector $\bar{p}$, which are referred in Chapter II (eqs. (2.21) to (2.23)), for an element of uniform cross-section in element oriented coordinates system are given by

$$\bar{k} = \frac{1}{l^3(1+\varphi)} \begin{bmatrix} EAl^2 & & & & & \\ 0 & 12EI & & & & \\ 0 & 6EIl & (4+\varphi)EIl^2 & & \text{Symmetric} & \\ -EAl^2 & 0 & 0 & EAl^2 & & \\ 0 & -12EI & -6EIl & 0 & 12EI & \\ 0 & 6EIl & (2-\varphi)EIl^2 & 0 & -6EIl & (4+\varphi)EIl^2 \end{bmatrix} \tag{B-1}$$

$$\bar{m} = \frac{\rho Al}{840(1+\varphi)^2} \begin{bmatrix} 280(1+\varphi)^2 & & & & & \\ 0 & (312+588\varphi+280\varphi^2) & & & & \\ 0 & (44+77\varphi+35\varphi^2)l & (8+140\varphi+7\varphi^2)l^2 & & \text{Symmetric} & \\ 140(1+\varphi)^2 & 0 & 0 & 280(1+\varphi)^2 & & \\ 0 & (108+252\varphi+140\varphi^2) & (26+63\varphi+35\varphi^2)l & 0 & (312+588\varphi+280\varphi^2) & \\ 0 & -(26+63\varphi+35\varphi^2)l & -(6+14\varphi+7\varphi^2)l^2 & 0 & -(44+77\varphi+35\varphi^2)l & (8+140\varphi+7\varphi^2)l^2 \end{bmatrix} \tag{B-2}$$

$$\bar{p} = -\frac{\rho A l}{120(1+\varphi)} \begin{bmatrix} 20(1+\varphi)(2a_{Ax}+a_{Bx}) \\ (42+40\varphi)a_{Ay} + (18+20\varphi)a_{By} \\ (6+5\varphi)l\, a_{Ay} + (4+5\varphi)l\, a_{By} \\ 20(1+\varphi)(a_{Ax}+2a_{Bx}) \\ (18+20\varphi)\, a_{Ay} + (42+40\varphi)a_{By} \\ -(4+5\varphi)l\, a_{Ay} + (6+5\varphi)l\, a_{By} \end{bmatrix} \qquad (B\text{-}3)$$

where l, A and I are the length, cross-sectional area and second moment of the cross-sectional area, respectively, of the element (link). ρ and E are the density and modulus of elasticity of the element material. a_{Ax}, a_{Ay}, a_{Bx} and a_{By} are components of the accelerations in the x and y directions of the two ends A and B of the element, respectively, as indicated in Fig. 2.2(c) of Chapter II.

APPENDIX C

ABSTRACT OF SOLUTION PROCEDURE FOR EIGENVALUE PROBLEM

To determine the eigenvalues and eigenvectors of the dynamical matrix of the eigenvalue problem (eq. (2.47)) given in Chapter II an algorithm due to Grad and Brebner [45] has been used. This algorithm gives all the eigenvalues and eigenvectors of a real general matrix. It involves QR double-step method to compute the eigenvalues and inverse iteration process is used to find out the corresponding eigenvectors. A brief summary of the procedure adopted in writing the algorithm is given below. For other details of the algorithm the original paper mentioned above can be referred.

To obtain a better accuracy in the results the following two modifications are first made. (i) The absolute sums of corresponding rows and columns are made approximately equal by scaling the matrix using a sequence of similarity transformations. (ii) The resulting matrix is normalized so that the value of Euclidean norm is equal to one.

The matrix is reduced to an upper-Hessenberg form using similarity transformations (Householder's method). Using QR double-step iterative process the Hessenberg matrix is reduced to a form so that all elements of the subdiagonal that converge

to zero are in modulus less than $2^{-t} \|H\|_E$, where t is the number of significant digits in the mantissa of binary floating-point number. The eigenvalues are then obtained from the reduced form.

Inverse iteration is applied to the upper-Hessenberg matrix until the absolute value of the greatest component of the right hand side vector is greater than the bound $2^t/(100N)$, where N is the order of matrix. Generally an additional step is performed to get the computed eigenvector after achieving the above bound. However, the residuals are determined at each step and if at any step they are greater in absolute value than that of the previous step, then the vector of the previous step is taken as the computer eigenvector.

APPENDIX D

EXPLICIT EQUATIONS FOR DYNAMIC FORCE ANALYSIS

D.1 Introduction

There are many methods available for the dynamic force analysis. Out of which most commonly used methods are directly based on Newton's second law or principle of virtual work [55,56]. Matrix methods [57,58] are also now available for this purpose. However, since in the present study a simple four-bar mechanism has been chosen for numerical examples, the dynamic force analysis is made by applying Newton's second law to the free body diagrams of the links, which readily gives a set of equations. The shaking force, the shaking moment, the input end torque and the bearing reactions are then determined using these equations. The complete procedure is presented in section D.2. Section D.3 deals with the procedure to determine equivalent dynamical system when counterweights are attached to the links.

D.2 Dynamic Force Analysis

In Fig. D.1(a) a planar four bar mechanism at an instant of time is shown. The links 1, 2, 3 and 4 are jointed together of which link 4 is fixed. When the mechanism

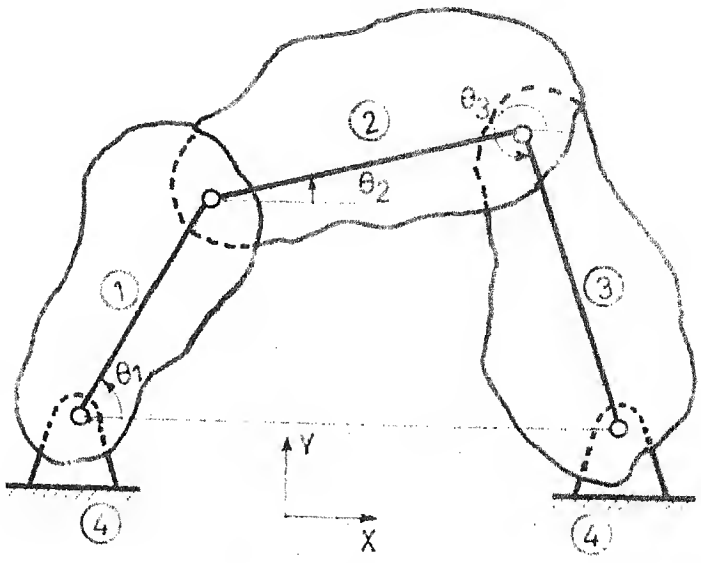

Fig.D.1(a) Mechanism Configuration at an Instant

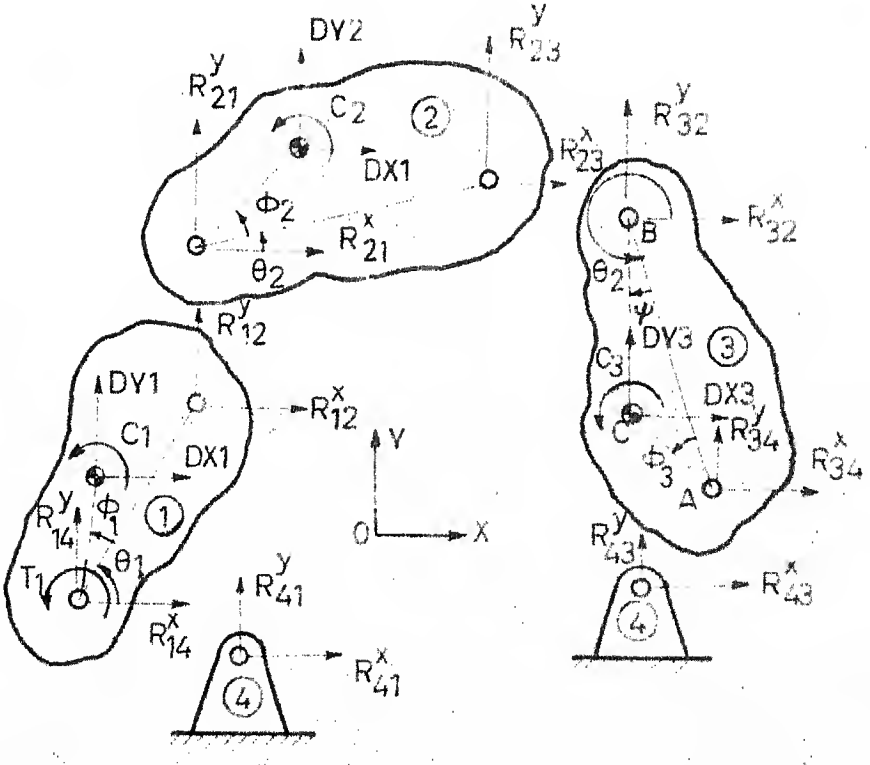

Fig D.1(b) Free Body Diagram of Links

is in motion the links are subjected to angular and linear accelerations which vary with respect to the mechanism configuration. This gives rise to varying rigid body inertia forces which in turn produce varying reactions at the ground bearings (supports).

To determine these reactions at any instant of time we consider the free body diagrams of the three movable links 1, 2 and 3 in the positions corresponding to the instant considered as shown in Fig. D.1(b).

Let l_i be the distance between two joints of ith link, θ_i be the angular position of the link, r_i the distance of the centroid of the link from the left end joint for the crank and the coupler whereas from the right end joint for the follower, φ_i be the angular position of the centroid with respect to the line of joints of the link. The angles are measured positive in the anticlockwise sense. R^x_{ij} and R^y_{ij} denote the X and Y components of the forces exerted by the jth link on the ith link at the joint. DXi, DYi and C_i are the components of inertia forces in the X and the Y directions and inertial torque of the ith link, respectively. T_1 is the input torque at the driving crank. Then from the free body diagrams of the links (Fig. D.1(b)) we have the following set of equilibrium equations.

$$R^x_{14} + R^x_{12} + DX1 = 0$$

$$R^y_{14} + R^y_{12} + DY1 = 0$$

$$R^x_{21} + R^x_{23} + DX2 = 0$$

$$R^y_{21} + R^y_{23} + DY2 = 0$$

$$R^x_{32} + R^x_{34} + DX3 = 0$$

$$R^y_{32} + R^y_{34} + DY3 = 0$$

$$T_1 + C_1 - R^x_{12}\, l_1 \sin\theta_1 + R^y_{12}\, l_1 \cos\theta_1 - \qquad \text{(D-1)}$$

$$- DX1 \cdot r_1 \sin(\theta_1 + \varphi_1) + DY1 \cdot r_1 \cos(\theta_1 + \varphi_1) = 0$$

$$C_2 - R^x_{23}\, l_2 \sin\theta_2 + R^y_{23}\, l_2 \cos\theta_2$$

$$- DX_2 \cdot r_2 \sin(\theta_2 + \varphi_2) + DY2 \cdot r_2 \cos(\theta_2 + \varphi_2) = 0$$

$$C_3 - R^x_{34}\, l_3 \sin\theta_3 + R^y_{34}\, l_2 \cos\theta_3$$

$$- DX3 \cdot BC \cdot \sin(\theta_3 - \psi_3) + DY3 \cdot BC \cdot \cos(\theta_3 - \psi_3) = 0$$

The new parameters BC and ψ_3 used in the last of the eqs. (D-1) are defined as follows from triangle ABC shown in the third link [Fig. D.1(b)].

$$BC^2 = l_3^2 + r_3^2 - 2 l_3 r_3 \cos\varphi_3 \qquad \text{(D-2)}$$

and $$\psi_3 = \sin^{-1}\left(\frac{r_3}{BC} \sin\varphi_3\right).$$

Keeping in mind the following identities the eqs. (D-1) relates the nine unknown quantities, i.e. the reactions

at the four joints in the two directions and the input torque.

$$
\begin{aligned}
R_{12}^{x} &= -R_{21}^{x} \\
R_{12}^{y} &= -R_{21}^{y} \\
R_{23}^{x} &= -R_{32}^{x} \\
R_{23}^{y} &= -R_{32}^{y} \\
R_{34}^{x} &= -R_{43}^{x} \\
R_{34}^{y} &= -R_{43}^{y} \\
R_{41}^{x} &= -R_{14}^{x} \\
R_{41}^{y} &= -R_{14}^{y}
\end{aligned}
\qquad \text{(D-3)}
$$

Thus using identities (D-3) in eqs. (D-1) one gets nine linear non-homogenous equations in nine unknowns which are solved to give these unknowns.

If m_i be the mass of the ith link, I_i the moment of inertia about center of gravity of the ith link, aX_i, aY_i and α_i are the components of the linear accelerations of the centroid in the X and Y directions and the angular acceleration, respectively, of the ith link, then one has

$$
\begin{aligned}
DXi &= -m_i\, aX_i \\
DYi &= -m_i\, aY_i \\
C_i &= -I_i \alpha_i
\end{aligned}
\qquad \text{(D-4)}
$$

The positions of the links, their angular velocities and accelerations for a given position and speed of the input crank is obtained from the kinematic analysis of the mechanism presented in Appendix A. The linear accelerations aX_i and aY_i of the links (i = 1,2,3) are then given by

$$\begin{aligned}
aX_1 &= -r_1[\omega_1^2 \cos(\theta_1+\varphi_1) + \alpha_1 \sin(\theta_1+\varphi_1)] \\
aY_1 &= -r_1[\omega_1^2 \sin(\theta_1+\varphi_1) - \alpha_1 \cos(\theta_1+\varphi_1)] \\
aX_2 &= -r_2[\omega_2^2 \cos(\theta_2+\varphi_2)+\alpha_2 \sin(\theta_2+\varphi_2)]-l_2\omega_1^2 \cos\theta_1 \\
aY_2 &= -r_2[\omega_2^2 \sin(\theta_2+\varphi_2)-\alpha_2 \cos(\theta_2+\varphi_2)]-l_1\omega_1^2 \sin\theta_1 \\
aX_3 &= +r_3[\omega_3^2 \cos(\theta_3+\varphi_3) + \alpha_3 \sin(\theta_3+\varphi_3)] \\
aY_3 &= +r_3[\omega_3^2 \sin(\theta_3+\varphi_3) - \alpha_3 \cos(\theta_3+\varphi_3)]
\end{aligned} \qquad \text{(D-5)}$$

where θ_i and α_i are the angular velocity and the angular acceleration of the ith moving link.

The components FS^x and FS^y of the shaking force in the X and Y directions, respectively, are given by

$$\begin{aligned}
FS^x &= R_{41}^x + R_{43}^x \\
FS^y &= R_{41}^y + R_{43}^y
\end{aligned} \qquad \text{(D-6)}$$

Using first six of the eqs. (D-1), identities (D-3) and eqs. (D-6) one gets

$$\begin{aligned}
FS^x &= DX1 + DX2 + DX3 \\
FS^y &= DY1 + DY2 + DY3 \\
FS &= \sqrt{[(FS^x)^2 + (FS^y)^2]}
\end{aligned} \qquad \text{(D-7)}$$

where FS denotes the net shaking force acting on the foundations.

If the X-axis is taken parallel to the ground link (i.e. fixed link 4) the shaking moment about a point midway between the two fixed supports due to ground bearing reactions is given by

$$MS' = \frac{1}{2}(R^y_{43} - R^y_{41})l_o \qquad (D\text{-}8)$$

where l_o is the distance between the fixed supports. The net shaking moment transmitted to the foundations is given by

$$MS = MS' - T_1 \qquad (D\text{-}9)$$

The bearing reactions at the four joints are given by

$$\begin{aligned} BR1 &= \sqrt{[(R^x_{41})^2 + (R^y_{41})^2]} \\ BR2 &= \sqrt{[(R^x_{11})^2 + (R^y_{12})^2]} \\ BR3 &= \sqrt{[(R^x_{23})^2 + (R^y_{23})^2]} \\ BR4 &= \sqrt{[(R^x_{34})^2 + (R^y_{34})^2]} \end{aligned} \qquad (D\text{-}10)$$

The maximum values of the shaking force FS, shaking moment SM, input end torque T_1 and the bearing reaction during the entire cycle of motion of the mechanism is determined by performing the above analysis for various configurations of the mechanism differing by a preselected angular interval ($\Delta\theta$) of the input crank from 0^o to 360^o.

D.3 Determination of Equivalent Dynamical System

Since a four bar mechanism is chosen for all the numerical problems solved in the present study, the determination of equivalent dynamical system is presented only with reference to the four bar mechanism.

Consider a mechanism with counterweights attached to its links as shown in Fig. 5.10 of Chapter V. The complete elaboration of the arrangement is also given in the same chapter. Let R_A and R_B are the radii of the circular counterweights attached one to the crank and the other to the follower, respectively α_A and α_B are the angular positions of the counterweights with respect to the line of joints of the respective links. The coupler extension lengths are l_L and l_R corresponding to the left and right ends of the coupler, respectively. Let m_i' and I_i' are the mass and the moment of inertia of the ith link about its centroid without counterweights, and m_i and I_i are the mass and the moment of inertia of the ith link about its centroid with counterweight(s), respectively.

The mass and the moment of inertia of the each circular counterweight about its center are given by

$$\begin{aligned} m_A &= \pi R_A^2 \, t_A \, \rho \\ m_B &= \pi R_B^2 \, t_B \, \rho \end{aligned} \qquad \text{(D-11)}$$

and

$$I_A = \frac{1}{2} m_A R_A^2$$
$$I_B = \frac{1}{2} m_B R_B^2 \qquad \text{(D-12)}$$

where t, m and I denote the thickness, mass and moment of inertia of the counterweight and the suffix A and B stand for the crank and the coupler counterweights, respectively. ρ is the density of the material of the counterweights.

The position of the centroid of the link and its attached counterweight combined, in a coordinate system in which x-axis is taken along the line of joints of the respective link and y-axis perpendicular to it and the origin is the center of the left end joint for the crank and the coupler, and that of the right end joint for the follower, is given by

$$x_1 = (\tfrac{1}{2}m_1' l_1 + m_A R_A \cos \alpha_A)/(m' + m_A)$$
$$y_1 = (m_A R_A \sin \alpha_A)/(m' + m_A) \qquad \text{(D-13)}$$

and

$$x_3 = (\tfrac{1}{2}m_3' l_3 + m_B R_B \cos \alpha_B)/(m' + m_B)$$
$$y_3 = (m_B R_B \sin \alpha_B)/(m' + m_B) \qquad \text{(D-14)}$$

where x_1, y_1 and x_3, y_3 are the coordinates of the centroids of the crank and the coupler, respectively.

The total moment of inertia and the mass of the each link with its counterweight are given by

$$I_1 = I_1' + m_1' \left[\left(x_1 - \frac{l_1}{2}\right)^2 + y_1^2\right] + I_A$$
$$+m_A \left[(x_1 - R_A \cos \alpha_A)^2 + (y_1 - R_A \sin \alpha_A)^2\right]$$
$$I_3 = I_3' + m_3' \left[\left(x_3 - \frac{l_3}{2}\right)^2 + y_3^2\right] + I_B \qquad \text{(D-15)}$$
$$+ m_B \left[(x_3 - R_B \cos \alpha_B)^2 + (y_3 - R_B \sin \alpha_B)^2\right]$$

and

$$m_1 = m_1' + m_A$$
$$m_3 = m_3' + m_B \qquad \text{(D-16)}$$

The radial distance and the angular position of the centroid for the crank and the coupler, respectively, are given by

$$r_1 = \sqrt{(x_1^2 + y_1^2)}$$
$$\varphi_1 = \sin^{-1} (y_1/r_1)$$
$$r_3 = \sqrt{(x_3^2 + y_3^2)} \qquad \text{(D-17)}$$
$$\varphi_3 = \sin^{-1} (y_3/r_3)$$

The mass of the coupler extension and its moment of inertia about its centroid are given by

$$m_L = l_L\, b_L\, t_L\, \rho$$
$$m_R = l_R\, b_R\, t_R\, \rho \qquad \text{(D-18)}$$
$$I_L = \frac{1}{12} m_L L_L^2$$
$$I_R = \frac{1}{12} m_R L_R^2 \qquad \text{(D-19)}$$

where ρ, b, t are the material density, width and thickness of the extension and the suffix R and L stand for the left and right ends of the coupler.

The position of the centroid of the coupler is given by

$$x_2 = [m_2' \frac{l}{2} + m_L(-l_L/2) + m_R (l_2+l_R/2)]/[m_2'+m_L+m_R] \tag{D-20}$$

$$y_2 = 0.$$

The total mass and moment of inertia are given by

$$m_2 = m_2' + m_L + m_R \tag{D-21}$$

$$I_2 = I_2' + I_L + m_L (x_2+l_L/2)^2 + I_R + m_R [x_2-(l_2+l_R/2)]^2 \tag{D-22}$$

The radial distance and angular position of the centroid of the coupler are given by

$$r_2 = x_2 \tag{D-23}$$

$$\varphi_2 = 0.$$

Eqs. (D-15) to (D-17) and (D-21) to (D-23) give the parameters of the equivalent dynamical system needed to make the dynamic force analysis of the mechanism with counterweights. It must be noted that the effect of the holes in links or the pins for the joints and any enlargement in the links at the joints have been neglected in the above equations, presented for determining equivalent dynamical system.

When sector type counterweights are used at the coupler ends the eqs. (D-18) to (D.20) and eq. (D-22) are modified as follows

$$m_L = \pi \theta_L R_L^2 t_L$$
$$m_R = \pi \theta_R R_R^2 t_R \qquad \text{(D-24)}$$

$$I_L = \tfrac{1}{2} m_L R_L^2$$
$$I_R = \tfrac{1}{2} m_R R_R^2 \qquad \text{(D-25)}$$

where θ_L and θ_R are the sector angles in radians of the left and right end counterweights, respectively. (Refer Fig. 5.11 in Chapter V.)

$$x_2 = [m_2' \frac{l_2}{2} + m_L(-\frac{4}{3} \frac{\sin(\theta_L/2)}{\theta_L} R_L) + m_R(l_2 + \frac{4}{3} \frac{\sin(\theta_R/2)}{\theta_R} R_R)] / [m_2' + m_L + m_R] \qquad \text{(D-26)}$$

$$\text{and } I_2 = I_2' + I_L + m_L (x_2 + \frac{4}{3} \frac{\sin \theta_L/2}{\theta_L})^2 + I_R + m_R [x_2 - (l_2 + \frac{4}{3} \frac{\sin \theta_R/2}{\theta_R} R_R)]^2 \qquad \text{(D-27)}$$

where R_L and R_R are the sector radii of the left and right end counterweights, respectively.

APPENDIX E

SUMMARY OF COMPUTER PROGRAMS

A number of computer programs in FORTRAN IV have been written which are used to solve the numerical examples in Chapter V. Most of the programs are general and can be used in applications similar to the ones discussed in the present study for any planar mechanism. These programs are described below.

Program I (STRLIN)

This program determines the deflection and stresses in any planar mechanism having one or more number of degrees of freedom. It also makes dynamic force analysis. The input data required is the link lengths and cross-sections, input crank speed of the mechanism and material properties of the links. This program consists of the following subroutines.

(i) EKEM : It determines the mass matrix and stiffness matrix of the element (link) in element oriented coordinates.

(ii) KINANA : This program determines the angular position, absolute angular velocity and absolute angular acceleration of the various links for a given constant input crank speed.

(iii) ELOAD : It finds the element inertia load vector due to rigid body inertia of the links and their counterweights (if any) and the inertia load vector due to KED inertia of the counterweights only in element oriented coordinates.

(iv) SKMPDV : This program transforms the element oriented element matrices into system oriented element matrices and then assembles the element matrices into system matrices.

(v) EIGSOL: This program solve the eigenvalue problem and can supply the eigenvalues and modal matrix for the case when the rigid body degree of freedom is eliminated according to the procedure given in Chapter II and also when the crank input end is assumed instantaneously fixed as cantilever beam. This program requires a subroutine for the determination of eigenvalues and eigenvectors of the dynamical matrix which is discussed in Appendix C.

(vi) DEFAN: This program finds the displacement, velocity and acceleration vectors of the system at the end of a certain chosen interval by solving the equations of motion when initial displacement and velocity vectors are given.

(v) PROMAT: It is required to multiply matrices frequently during the above process. This program is used for multiplication of matrices.

Program II (OPTIMM)

The program minimizes any function using DFP method of minimization. The input data is the initial design vector. It consists of the following subroutines.

(i) DELFN: This program is used to determine gradients of any function. In the present work it determines the gradient of the minimizing function, the maximum link stresses and the maximum shaking force. The former gradient is used in optimization process, whereas the latter ones are used to predict the values of latter mentioned functions during one dimensional minimization.

(ii) FUN: This is a program in which the objective function and the various constraints are determined with the help of other subroutines. It also formulates the penalty function which is to be minimized.

(iii) MINGOL: This program finds the optimum step length in a certain move direction. It first brackets the minimum within a certain interval and then the interval is reduced using Golden-section method to obtain the optimum step length.

Program III (DYNAN)

This program makes the dynamic force analysis using the explicit equations given in Appendix D. The input data is the length, mass, moment of inertia, polar coordinates of

of the centroid of each link. The input crank speed and the density of the material of the links.

Program IV (KINSYN)

It is used to synthesize a planar four bar mechanism for rigid body guidance. The input data is the two angular relative positions of the coupler and two that of the follower. The rigid body positions and the corresponding crank rotations are already furnished to the program.

Program V (ELPERI)

This program determines the mass, moment of inertia, position of the centroid of the links when counterweights are attached to them. The input data is the length, width and thickness of each link and the radii of counterweights and their angular positions. The density of the material is also supplied.

A 67013

Date Slip

This book is to be returned on the date last stamped.

.....	.....
.....	.....
.....	.....
.....	.....
.....	.....
.....	.....
.....	.....
.....	.....
.....	.....
.....	.....
.....	.....

CD 6.72.9